Εθνικό Μετσόβιο Πολυτεχνείο

Σχολή Αγρονόμων Τοπογράφων Μηχανικών

Τομέας Τοπογραφίας

Διερεύνηση Οντολογιών, Μηχανικής Μάθησης, Μορφομετρίας, και Αντικειμενοστρεφούς Ανάλυσης Εικόνας για την Αναγνώριση Γεωμορφών, Κτιρίων, και Μεταβολών Κτιρίων

Διδακτορική Διατριβή

του

ΑΡΓΥΡΟΥ Κ. ΑΡΓΥΡΙΔΗ

Επιβλέπων: Δημήτριος Π. Αργιαλάς

Καθηγητής Ε.Μ.Π.

Εργαστήριο Τηλεπισκόπησης

19 ΙΟΥΝΙΟΥ, 2017

Εθνικό Μετσόβιο Πολυτεχνείο

Σχολή Αγρονόμων και Τοπογράφων Μηχανικών

Εργαστήριο Τηλεπισκόπησης

Διδακτορική Διατριβή

Διερεύνηση Οντολογιών, Μηχανικής Μάθησης, Μορφομετρίας, και Αντικειμενοστρεφούς Ανάλυσης Εικόνας για την Αναγνώριση Γεωμορφών, Κτιρίων, και Μεταβολών Κτιρίων

Αργυρός Αργυρίδης

Συμβουλευτική Επιτροπή: Δημήτριος Π. Αργιαλάς, Καθηγητής Ε.Μ.Π. (Επιβλέπων)
Μαρίνος Κάβουρας Καθηγητής Ε.Μ.Π.
Βασιλεία Καραθανάση Καθηγήτρια Ε.Μ.Π.

Επταμελής Εξεταστική Επιτροπή:

………………….
Δημήτριος Π. Αργιαλάς
Καθηγητής Ε.Μ.Π.

…………………
Μαρίνος Κάβουρας
Καθηγητής Ε.Μ.Π.

…………………
Βασιλεία Καραθανάση
Καθηγήτρια Ε.Μ.Π.

…………………
Κωνσταντίνος Καράντζαλος
Επ. Καθηγητής Ε.Μ.Π.

…………………
Γεώργιος Στάμου
Επ. Καθηγητής Ε.Μ.Π.

…………………
Ιωάννης Γήτας
Αν. Καθηγητής Α.Π.Θ.

…………………
Γεώργιος Μαλλίνης
Επ. Καθηγητής Α.Π.Θ.

Αθήνα, Ιούνιος 2017

NATIONAL TECHNICAL UNIVERSITY OF ATHENS

SCHOOL OF RURAL AND SURVEYING ENGINEERING

DEPARTMENT OF TOPOGRAPHY

Investigation of Ontologies, Machine Learning, and Object-based Image Analysis for the Identification of Landforms, Buildings, and Building Change Detection

Argyros K. Argyridis

Dissertation for the degree of

Doctor of Philosophy

Advisor: Demetre P. Argialas

Professor at NTUA

National Technical University of Athens

School of Rural and Surveying Engineering

Remote Sensing Laboratory

Dissertation Thesis

Investigation of Ontologies, Machine Learning, and Object-based Image Analysis for the Identification of Landforms, Buildings, and Building Change Detection

Argyros Argyridis

Dissertation Comitee: Demetre P. Argialas, N.T.U.A. Professor (Supervisor)
Marinos Kavouras, N.T.U.A. Professor
Vasilia Karathanassi, N.T.U.A. Professor

Examination Committee:

………………
Demetre P. Argialas
N.T.U.A. Professor

………………
Marinos Kavouras
N.T.U.A. Professor

………………
Vasilia Karathanassi
N.T.U.A. Professor

………………
Konstantinos Karantzalos
N.T.U.A. Assistant Professor

………………
Giorgos Stamou
N.T.U.A. Assistant Professor

………………
Ioannis Gitas
A.U.TH Associate Professor

………………
Giorgos Mallinis
A.U.TH Assistant Professor

Athens, June 2017

Acknowledgements

I would like to thank my advisor, Professor Demetre P. Argialas for his guidance and support through the years.

I would also like to thank all the members of the dissertation committee and my colleagues at Remote Sensing Laboratory for their useful comments and corrections.

Finally, I would like to thank the Free and Open Source Software community for providing the background, frameworks, and tools to implement my research.

Table of Contents

Table of Figures

Table of Tables

Major Acronyms Table

AML	Advanced Morphological Leveling
CD	Contrastive Divergence
DBN	Deep Belief Network
DEM	Digital Elevation Model
DSM	Digital Surface Model
DTM	Digital Terrain Model
FN	False Negative
FP	False Positive
GEOBIA	GEographic Object-Based Image Analysis
GPL	General Public License
LS	Left Shoulder Fuzzy Membership Function
ME	Mean Error
MLD	Machine Learning Datatype
MRVBF	Multi-Resolution index of Valley Bottom Flatness
MV	Membership Value
NDVI	Normalized Difference Vegetation Index
NDWI	Normalized Difference Water Index
OWL	Web Ontology Language
PCD	Persistent Contrastive Divergence
RBM	Restricted Boltzmann Machine
RS	Right Shoulder Fuzzy Membership Function
RSME	Root Square Mean Error
SPOR	SPatial Ontology Reasoner
TP	True Positive
TR	Triangular Fuzzy Membership Function
TRP	Trapezoidal Fuzzy Membership Function
W3C	World Wide Web Consortium

Extended Abstract

The objective of this research was the investigation, design, implementation, and enhancement of state-of-the-art computer vision and artificial intelligence approaches within the framework of GEographic Object-Based Image Analysis (GEOBIA) and their employment in specific remote sensing problems such as building extraction, foreshore mapping, building change detection and alluvial fan and bajada identification.

The first objective of this dissertation was the design and implementation of an ontological reasoner allowing to design ontologies based on fuzzy spectral, geometric, and spatial relationships through multi-scale GEOBIA analysis, named SPatial Ontology Reasoner (SPOR). Identification of complex landscape components in terms of spectral, geometric, and rich spatial relationships, requires the representation of expert knowledge into a problem-solving strategy through an establish-and-refine-paradigm, within the environment of a knowledge representation system. To take advantage of this expert knowledge within an automated image analysis system it is required to be formalized into a computer-conceivable form. Thus, a semantic gap arises between the high-level semantics employed by the experts to describe the phenomenon and the numerical low – level information extracted from data. To this end ontologies offer potential for knowledge formalization. Previous studies depicted the applicability of ontologies in GEOBIA. However, still remained the need to incorporate fuzzy reasoning in an ontology-based GEOBIA approach. Furthermore, the importance of spatial relationships and multi-scale analysis has already been stated in earlier GEOBIA studies. Although, spatial reasoning with ontologies for image analysis has been examined, still remained the need for spatial reasoning in a multi-scale GEOBIA approach. Finally a limitation was stated for current Description Logic (DL) – based ontology reasoners, concerning the required processing time, when dealing with large number of classes and objects, which is very common in GEOBIA studies. Thus to address these needs in SPOR, OWL 2 was selected to formalize the ontology, which is latest version of this W3C standard. OWL 2 ensures the integration and exchange of GEOBIA ontologies with current semantic web technologies. Since GEOBIA frameworks should be compatible with Open GIS Standards, and it was also required computation of spatial relationships during the reasoning process, SPOR integrated PostgreSQL which supported such functionality.

The second objective was the integration of advanced machine learning techniques within the ontological-based reasoning. In the literature machine learning techniques have been employed as a classification step before the ontology-based refinement in medical and scene analysis studies. However, still remains the need to examine the applicability of such approach in GEOBIA. To address this issue, it was decided to examine Deep Learning methods, which are machine learning algorithms aiming to model high-level abstractions in data by using model architectures composed of multiple non-linear transformations. Such algorithm is the

Deep Belief Network. DBN training is performed in two phases. At first unsupervised training is performed by stacking multiple layers of simple unsupervised networks such as the Restricted Boltzmann machines (RBM) which were trained by the contrastive divergence algorithm. Unsupervised training output is provided as input to Logistic Regression supervised algorithm which provides the final DBN output. To perform integrated reasoning with DBN and fuzzy ontologies, OWL 2 was enhanced with proper restrictions which allowed class definitions through the combination of DBN and fuzzy expressions. SPOR was also enhanced to be able to perform reasoning with such ontologies.

The third objective was the investigation and addressing of specific remote sensing problems through GEOBIA multiscale analysis. To evaluate SPOR a building extraction approach through multi-scale analysis from QuickBird imagery was designed. Three segmentation and classification levels were designed and implemented. Aim of level 1 was the extraction of spectral categories with spectral properties similar to the present buildings. Aim of level 3 was the elimination of the road network. The final buildings were extracted on level 2. Evaluation with photo-interpretation data was satisfactory since 75% of the total rooftop area was extracted while the commission error was around 20%.

Afterwards, an ontology-based multi-scale GEOBIA approach based on anisotropic diffusion and fuzzy ontologies for foreshore automatic identification was designed and implemented. The identification was based on the foreshore interpretation criteria provided by the Greek Cadastral Office, from multispectral and Digital Terrain Model (DTM) data. Management of the coastal zone is now recognized as an issue of importance due to the growing social and demographic pressures that threaten its sustainability. More than half of the world's population lives within 60 km of the coast. Specifically, foreshore mapping is important as the processes that take place in the foreshore affect the nearby water quality. Proper management of the foreshore will improve property values and provide recreational amenity. Foreshore mapping in Greece will contribute to the completion of the National Cadastre. Although in Greece this mapping was performed manually, it was decided to investigate methods for the formalization of the foreshore interpretation criteria provided by the Greek Cadastral Office towards the automation of the process. Due to the expression of the spatial organization of the foreshore within the interpretation criteria (e.g. present vegetation, slopes, present infrastructure etc.) it was decided to formalize the criteria through an Ontology-Based GEOBIA approach. Due to the number and complexity of these criteria, the two most commonly appearing criteria in Greece were investigated, the vegetation border and the topographic crown border. To reduce undesired spectral and spatial detail, the imagery was filtered through morphological leveling which smoothed small spectral differences while major edges of the original image objects were preserved. A three level segmentation and classification hierarchy was developed were smaller objects were created

8

on the lower levels, while larger objects where created on the higher levels. Level creation sequence was 1-2-3. On Level 1, general thematic categories were extracted (e.g. vegetation, water, low sloping areas). Through the interpretation rules derived from foreshore criteria these areas were refined on Level 2 and the final foreshore area was determined on Level 3. Evaluation with image interpreted reference data was satisfactory since 89% of the total foreshore area was identified while commission errors was around 14%.

A building change detection scenario was investigated in suburban areas of Greece. The developed multi-scale GEOBIA approach integrated Deep Learning classification with ontological reasoning. A three level segmentation hierarchy was designed and implemented. Level creation order was 1-2-3. On the lowest level an estimation of areas of possible change was performed through fuzzy properties and multiple DBN classifications. Through interpretation rules related to the geometry of the buildings, employed on Level 2 and level 3 the final changes were derived. Results were satisfactory since 73 out of 87 changes were successfully identified, while having small omission and commission errors (10 and 14 changes respectively).

To perform alluvial fan and bajada mapping, state-of-the-art DEM processing and multi-scale GEOBIA analysis approaches were investigated, extended, and implemented. Mapping of alluvial fans and bajadas is important for practical and economic importance to society, particularly in arid and semiarid climates where they may be the principal groundwater source for irrigation farming and the sustenance of life. In this study, advanced image processing and knowledge representation methods were investigated and enhanced, towards the automatic identification of alluvial fans and bajadas. The developed method was based on the landform-pattern element approach which identifies landforms based on pattern-elements such as topography, drainage pattern and texture, soil spectral signature, spatial relationships, and other characteristics. Data used included the 10m spatial resolution National Elevation Dataset, provided by USGS and a pan-sharpened Landsat OLi imagery. The study area was located in the Death Valley, Nevada, USA. DTM processing included noise-removal filtering and depression treatment. A two-phase GEographic Object-Based Image Analysis (GEOBIA) approach involving multi-scale segmentation and fuzzy ontology-based reasoning was designed. Aim of the first phase was the identification of topographic forms such as the basin, mountain-range, and piedmont. Piedmont is the area where alluvial fans and bajadas reside. A four level segmentation hierarchy, accompanied by a four level ontological hierarchy, were developed. The identification was based on topography attributes such as slope gradient and curvature, and spatial reasoning. Aim of the second phase was the identification of alluvial fans and bajadas based on drainage pattern texture and topographic features such as landform shape. Thus a two-level segmentation and ontological hierarchy were developed. Due to a systematic omission on the fan toe, each fan and bajada soil spectral signature was

taken into account to determine the omitted areas through region growing on the multispectral imagery. Accuracy assessment indicated satisfactory results, since a 90% completeness and 89% quality was achieved for both alluvial fans and bajadas.

Finally, the fourth objective of this dissertation was the development and release of all the developed methods as Free and Open Source Software.

Keywords: GEOBIA, ontologies, image analysis, buildings, change detection, foreshore, alluvial fan

Εκτενής Περίληψη

Στόχος της παρούσας διατριβής ήταν η διερεύνηση, ο σχεδιασμός, η επέκταση, και η υλοποίηση καινοτόμων μεθόδων Όρασης Υπολογιστών και Τεχνητής Ευφυΐας μέσα στα πλαίσια της Γεωγραφικής Αντικειμενοστρεφούς Ανάλυσης Εικόνας (GEographic Object-Based Image Analysis – GEOBIA) όπως εξαγωγή κτιρίων, οριοθέτηση αιγιαλού, ανίχνευση μεταβολών κτιρίων, και χαρτογράφηση αλουβιακών ριπιδίων.

Ο πρώτος στόχος αυτής της διατριβής αφορούσε την ανάπτυξη μιας μηχανής συλλογιστικής η οποία θα επέτρεπε την τυποποίηση της φωτοερμηνευτικής γνώσης των εμπείρων φωτοερμηνευτών σε μέσα από την υλοποίηση ασαφών φασματικών, χωρικών, γεωμετρικών και τοπολογικών σχέσεων στα πλαίσια της πολυκλιμακωτής ανάλυσης εικόνας, το οποίο ονομάστηκε SPOR (SPatial Ontology Reasoner). Καθώς η αναγνώριση θεματικών κατηγοριών οι οποίες έχουν πολύπλοκες φασματικές, γεωμετρικές και χωρικές ιδιότητες, απαιτεί την αναπαράσταση και δόμηση της φωτοερμηνευτικής γνώσης για την παρατηρούμενη κατηγορία σε μια διαδικασία επίλυσης προβλήματος, απαιτούνται μέθοδοι αναπαράστασης της ανθρώπινης γνώσης σε μορφή κατανοητή από τον υπολογιστή. Λόγω του ότι οι φωτοερμηνευτές χρησιμοποιούν "υψηλού επιπέδου" αναπαράσταση γνώσης για να περιγράψουν μια θεματική κατηγορία, ενώ ο υπολογιστής μπορεί να εξάγει "χαμηλού επιπέδου" αριθμητική πληροφορία από τα δεδομένα, παρουσιάζεται η ανάγκη να γεφυρωθεί το υπάρχον σημασιολογικό κενό (Semantic gap). Η τυποποίηση και αξιοποίηση αυτής της γνώσης σε μορφή "κατανοητή" από τον υπολογιστή επιτυγχάνεται με την χρήση μεθόδων όπως οι οντολογίες. Οι οντολογίες μπορούν να χρησιμοποιηθούν για να γεφυρώσουν το σημασιολογικό κενό και να αποτελέσουν τμήμα της υλοποίησης ενός αυτόματου συστήματος ανάλυσης εικόνας με βάση την GEOBIA. Η δυνατότητα που έχουν οι οντολογίες να τυποποιήσουν την φωτοερμηνευτική γνώση έχει ήδη αποδειχθεί από προηγούμενες μελέτες. Παρόλα αυτά, δεν είχε γίνει διερεύνηση των οντολογιών με ταυτόχρονη χρήση ασαφούς λογικής, χωρικών συσχετίσεων και πολυκλιμακωτής χωρικής ανάλυσης μέσα στο πλαίσιο της GEOBIA. Τέλος, έχει αναφερθεί στη βιβλιογραφία πως οι υπάρχουσες μηχανές συλλογιστικής για οντολογίες που στηρίζονται σε περιγραφικές λογικές χρειάζονται μεγάλο χρόνο για την περάτωση της συλλογιστικής διαδικασίας, όταν η βάση γνώσης περιέχει πολλές κατηγορίες ή/και αντικείμενα, όπως είναι οι μελέτες που στηρίζονται στην GEOBIA. Για να αντιμετωπισθούν αυτές οι ανάγκες, στην την ανάπτυξη και υλοποίηση του SPOR ως γλώσσα τυποποίησης της οντολογίας χρησιμοποιήθηκε η OWL 2 η οποία αποτελεί σήμερα το τελευταίο επίσημο πρότυπο της γλώσσας OWL για τον Σημασιολογικό Ιστό (ΣΙ). Έτσι διασφαλίζεται η συμβατότητα με τις τεχνολογίες του ΣΙ αλλά και την ανταλλαγή GEOBIA οντολογιών με χρήση των τεχνολογιών του. Καθώς τα συστήματα που στηρίζονται στην GEOBIA πρέπει να είναι συμβατά με τα ανοικτά γεωχωρικά πρότυπα (Open GIS Standards) και καθώς απαιτούνταν ο υπολογισμός χωρικών συσχετίσεων κατά τη

διάρκεια της συλλογιστικής διαδικασίας, στο SPOR χρησιμοποιήθηκε η PostgreSQL η οποία ενσωματώνει τέτοιες δυνατότητες.

Ο δεύτερος στόχος αυτής της διατριβής αφορά την διερεύνηση και ενσωμάτωση μεθόδων μηχανικής μάθησης μέσα στη συλλογιστική διαδικασία των οντολογιών. Στη βιβλιογραφία έχει ήδη διερευνηθεί ο συνδυασμός μεθόδων μηχανικής μάθησης με οντολογίες για την ταξινόμηση επίγειων λήψεων ή ιατρικών δεδομένων με ικανοποιητικά αποτελέσματα, αλλά κάτι τέτοιο δεν είχε διερευνηθεί στα πλαίσια της GEOBIA. Αποφασίστηκε η διερεύνηση μεθόδων Deep Learning, οι οποίες τυποποιούν πληροφορία υψηλής αφαιρετικότητας από τα δεδομένα, μέσω της υλοποίησης μη γραμμικών μετασχηματισμών. Σε αυτή την οικογένεια αλγορίθμων ανήκει και ο Deep Belief Network (DBN). Ένα DBN εκπαιδεύεται σε δύο φάσεις. Αρχικά γίνεται μη επιβλεπόμενη εκπαίδευση όπου χρησιμοποιούνται πολλαπλά επίπεδα από Restricted Boltzmann Machines (RBM) τα οποία εκπαιδεύονται μέσω του αλγορίθμου contrastive divergence. Η τελική έξοδος των RBM δίνεται ως είσοδο στον αλγόριθμο επιβλεπόμενης μάθησης Logistic Regression, ο οποίος εκπαιδεύεται μέσω του stohastic gradient decent. Η έξοδος της επιβλεπόμενης εκπαίδευσης αποτελεί το τελικό αποτέλεσμα της ταξινόμησης του DBN. Για να μπορέσει να γίνει συνδυαστική συλλογιστική DBN και ασαφών περιορισμών, επαυξήθηκε η τυποποίηση των οντολογιών με κατάλληλες δηλώσεις – περιορισμούς οι οποίοι επέτρεψαν τον ορισμό κατηγοριών με συνδυασμό ασαφών περιορισμών αλλά και μηχανική μάθηση. Επίσης επεκτάθηκε κατάλληλα η συλλογιστική διαδικασία του SPOR ώστε να συμπεριλάβει τον αλγόριθμο DBN.

Ο τρίτος στόχος αυτής της διατριβής ήταν η διερεύνηση συγκεκριμένων προβλημάτων της τηλεπισκόπησης και υλοποίηση μεθοδολογιών για την αντιμετώπισή τους μέσα από την υλοποίηση μεθοδολογιών πολυκλιμακωτής ανάλυσης εικόνας.

Ο SPOR δοκιμάστηκε σε ένα σενάριο εξαγωγής κτιρίων από εικόνες QuickBird στο οποίο σχεδιάστηκε και υλοποιήθηκε πολυκλιμακωτή ανάλυση εικόνας για την εξαγωγή τους. Υλοποιήθηκαν τρία (3) επίπεδα κατάτμησης. Για κάθε επίπεδο κατάτμησης υλοποιήθηκε ιεραρχία θεματικών κατηγοριών σε μια οντολογία. Στο επίπεδο 1 έγινε εντοπισμός κατηγοριών οι οποίες είχαν φασματικές ιδιότητες παρόμοιες με τα κτίρια. Στο επίπεδο 3, έγινε εξαγωγή των δρόμων ώστε να αφαιρεθούν από το τελικό αποτέλεσμα. Ο τελικός εντοπισμός των κτιρίων έγινε στο επίπεδο 2. Τα αποτελέσματα κρίθηκαν ικανοποιητικά μετά από σύγκρισή τους με φωτοερμηνευτικά δεδομένα αναφοράς, καθώς από τη συνολική επιφάνεια των κτιρίων, εντοπίστηκε επιτυχώς το 75%, ενώ υπήρχε σφάλμα συμπερίληψης της τάξης του 20%.

Στη συνέχεια διερευνήθηκε η δυνατότητα εξαγωγής του αιγιαλού μέσω της υλοποίησης πολυκλιμακωτής ανάλυσης εικόνας και ασαφούς οντολογικής συλλογιστικής. Η διαχείριση των παράκτιων ζωνών είναι πολύ σημαντική σε παγκόσμιο επίπεδο καθώς πάνω από 50%

του πληθυσμού του πλανήτη ζει σε απόσταση έως 60 Km από τις ακτές. Επίσης, η χαρτογράφηση του αιγιαλού είναι σημαντική λόγω των φυσικών διεργασιών που λαμβάνουν χώρα στη ζώνη αυτή, καθώς επηρεάζουν την ποιότητα του νερού. Στην Ελλάδα, η χαρτογράφηση της ζώνης του αιγιαλού θα συμβάλει και στην ολοκλήρωση του Εθνικού Κτηματολογίου. Παρόλο που η χαρτογράφηση αυτή έχει ήδη γίνει με φωτοερμηνεία, αποφασίστηκε η διερεύνηση μεθοδολογιών για την τυποποίηση των κριτηρίων της ΚΤΗΜΑΤΟΛΟΓΙΟ Α.Ε. με στόχο την αυτόματη χαρτογράφηση του αιγιαλού. Οι περιγραφές των κριτηρίων περιλαμβάνουν συσχετίσεις του αιγιαλού με γειτνιάζουσες χρήσεις γης (πχ βλάστηση, κλίσεις, τυχόν έργα υποδομής κτλ). Έτσι αποφασίστηκε η διερεύνηση της τυποποίησης των κριτηρίων με την υλοποίηση κατάλληλης οντολογίας στα πλαίσια της GEOBIA. Λόγω του πλήθους και της πολυπλοκότητας των κριτηρίων διερευνήθηκαν τα πιο κοινά εμφανιζόμενα στον ελλαδικό χώρο, το κριτήριο της βλάστησης και το κριτήριο της στέψης πρανούς. Για την αφαίρεση ανεπιθύμητης φασματικής και χωρικής πολυπλοκότητας από τις εικόνες, εφαρμόστηκε φίλτρο ανισοτροπικής διάχυσης στα δεδομένα. Τα φίλτρα αυτά εξομαλύνουν μικρές διαφορές φωτεινότητας, ενώ παράλληλα διατηρούν τις κύριες ακμές των αντικειμένων. Υλοποιήθηκε μια ιεραρχία τριών επιπέδων κατάτμησης όπου μικρότερα αντικείμενα σχεδιάστηκαν στα χαμηλότερα επίπεδα και μεγαλύτερα στα υψηλότερα. Για κάθε επίπεδο κατάτμησης υλοποιήθηκε στην οντολογία ιεραρχία θεματικών κατηγοριών στις οποίες ταξινομήθηκαν τα αντικείμενα. Η σειρά υλοποίησης των επιπέδων ήταν 1-2-3. Στο επίπεδο 1 αναγνωρίστηκαν γενικές θεματικές κατηγορίες (πχ βλάστηση, νερό, επιφάνειες με χαμηλή κλίση). Στη συνέχεια μέσω ερμηνευτικών κανόνων που προέκυψαν από τα κριτήρια χάραξης του αιγιαλού δημιουργήθηκαν ενδιάμεσες οντότητες συσχετιζόμενες με τα υποαντικείμενα του αιγιαλού, ο οποίος αιγιαλός αναγνωρίστηκε τελικά στο 3ο και τελευταίο επίπεδο. Η αξιολόγηση έγινε με φωτοερμηνευτικά δεδομένα αναφοράς και κρίθηκε ικανοποιητική καθώς αναγνωρίστηκε επιτυχώς περίπου το 89% της συνολικής έκτασης του αιγιαλού, ενώ τα σφάλματα συμπερίληψης δεν ξεπέρασαν το 14%.

Επίσης, ένα σενάριο ανίχνευσης μεταβολών σε περιαστικό περιβάλλον σχεδιάστηκε και υλοποιήθηκε. Μια ιεραρχία τριών επιπέδων σχηματίστηκε για την αναγνώριση των αλλαγών. Η σειρά δημιουργίας των επιπέδων ήταν 1-2-3. Στο χαμηλότερο επίπεδο με χρήση ασαφών κανόνων και πολλαπλών DBN ταξινομήσεων έγινε μια πρώτη εκτίμηση των περιοχών όπου έγιναν αλλαγές. Στη συνέχεια με χρήση ερμηνευτικών κανόνων στα επίπεδα 2 και 3 προσδιορίστηκαν οι τελικές αλλαγές. Τα αποτελέσματα έπειτα από σύγκριση με φωτοερμηνευτικά δεδομένα αναφοράς κρίθηκαν ικανοποιητικά, καθώς 73 από συνολικά 87 αλλαγές εντοπίστηκαν επιτυχώς, με μικρά σφάλματα παράλειψης (10) και συμπερίληψης (14).

Τέλος έγινε διερεύνηση, υλοποίηση και επέκταση προχωρημένων τεχνικών επεξεργασίας ψηφιακών μοντέλων αναγλύφων και την αξιοποίησή τους μέσα στο πλαίσιο της GEOBIA με

στόχο την αναγνώριση αλουβιακών ριπιδίων και Bajadas. Η αναγνώριση στηρίχθηκε στην προσέγγιση της αναγνώρισης προτύπων γεωμορφών το οποίο έχει αναπτυχθεί στις ΗΠΑ και ευρέως χρησιμοποιηθεί διεθνώς για την χαρτογράφηση γεωμορφών. Η χαρτογράφηση αυτών των σχηματισμών είναι πολύ σημαντική ειδικά σε ερημικές και ημιερημικές περιοχές όπου πιθανότατα οι σχηματισμοί αυτοί είναι η κύρια πηγή επιφανειακού νερού για χρήση σε ύδρευση και άρδευση. Έχοντας αυτό ως κίνητρο, διερευνήθηκαν και αναπτύχθηκαν προχωρημένες τεχνικές ανάλυσης εικόνας, ψηφιακών μοντέλων αναγλύφου και αναπαράστασης γνώσης με απώτερο στόχο την αυτόματη αναγνώριση αυτών των γεωμορφών. Στα πλαίσια αυτής της διερεύνησης η αναγνώριση αυτών των γεωμορφών έγινε αρχικά από ψηφιακά μοντέλα εδάφους (ΨΜΕ) και στη συνέχεια το αποτέλεσμα βελτιώθηκε με χρήση πολυφασματικών δορυφορικών δεδομένων. Για την απομάκρυνση του θορύβου το ΨΜΕ φιλτραρίστηκε με βέλτιστο φίλτρο Weiner. Στη συνέχεια, καθώς ένα από τα απαραίτητα στοιχεία για τον εντοπισμό αυτών των μορφών είναι το υδρογραφικό δίκτυο, σύγχρονες τεχνικές σχετιζόμενες με τη διαχείριση βυθισμάτων και επίπεδων περιοχών, καθώς και εξαγωγής του υδρογραφικού δικτύου από ΨΜΕ διερευνήθηκαν, επεκτάθηκαν, υλοποιήθηκαν. Τα αποτελέσματα της εξαγωγής του δικτύου ήταν ικανοποιητικά όσον αφορά το δίκτυο των υπερκείμενων λεκανών, αλλά όχι τόσο ικανοποιητικά για την εξαγωγή του διχοτομικού υδρογραφικού προτύπου. Έτσι αποφασίστηκε πως στη μέθοδο αναγνώρισης θα γίνει προσέγγιση του προτύπου μέσω ευρετικών κανόνων οι οποίοι θα χαρακτήριζαν τις ιδιότητες του. Επίσης, λόγω του ιδιαίτερου ημικυκλικού σχήματος του αλουβιακού ριπιδίου, σχεδιάστηκε και υλοποιήθηκε ένας δείκτης ο οποίος λαμβάνει υπόψη το υδρογραφικό δίκτυο της υπερκείμενης κοιλάδας, τη θέση, τον προσανατολισμό, και το μέγεθος της κάθε υποψήφιας για αλουβιακό ριπίδιο μορφής. Ο δείκτης συνέκρινε την υποψήφια μορφή με ισεμβαδικό κυκλικό τομέα και υπολόγιζε ένα ποσοστό ταύτισης. Η τελική διαδικασία εξαγωγής έγινε μέσω της GEOBIA με την υλοποίηση δύο ιεραρχιών κατάτμησης και ταξινόμησης των αντικειμένων μέσω οντολογιών. Η πρώτη ιεραρχία περιείχε 4 επίπεδα με σειρά δημιουργίας 4-1-2-3. Στο επίπεδο 4 αναγνωρίστηκαν οι κοιλάδες που υπήρχαν στην περιοχή. Στο 1ο επίπεδο έγινε αναγνώριση των ζωνών στις οποίες πιθανώς να υπάρχουν αλλουβιακά ριπίδια ή/και bajadas. Στο αποτέλεσμα της ταξινόμησης του επιπέδου 1 έγινε διόρθωση και πλήρωση κενών στα επίπεδα 2 και 3. Στο αποτέλεσμα της ταξινόμησης του επιπέδου 3 έγινε μορφολογικό άνοιγμα ώστε να μπορέσουν να διαχωριστούν οι αλλουβιακοί σχηματισμοί από άλλες περιοχές, και στο αποτέλεσμα αυτό έγινε κατάτμηση για τον υπολογισμό νέων αντικειμένων που θα αναπαριστούσαν τις επιθυμητές γεωμορφές, σχηματίζονται το επίπεδο 2b. Για να εντοπισθούν υποψήφια τμήματα του υδρογραφικού δικτύου σχετιζόμενα με τη μεταφορά φερτών υλικών για το σχηματισμό των αλουβιακών ριπιδίων, το επίπεδο 1b δημιουργήθηκε κάτω από το επίπεδο 2b. Η τελική αναγνώριση των μορφών έγινε στο επίπεδο 2b. Τα αποτελέσματα της αναγνώρισης μετά από αξιολόγηση με φωτοερμηνευτικά δεδομένα αναφοράς κρίθηκαν ικανοποιητικά, καθώς για όλες τις μορφές

εντοπίστηκε επιτυχώς το 90% των εκτάσεών τους, ενώ ο δείκτης ποιότητας του τελικού αποτελέσματος ήταν της τάξης του 89%.

Ο τελευταίος στόχος της παρούσας διατριβής ήταν η υλοποίηση και δημοσίευση των αλγορίθμων οι οποίοι υλοποιήθηκαν ως ελεύθερο λογισμικό.

Λέξεις κλειδιά: Αντικειμενοστρεφής ανάλυση εικόνας, ανίχνευση μεταβολών, κτίρια, εξαγωγή αιγιαλού, αλλουβιακά ριπίδια.

1 Introduction

1.1 Recent Advancements in Remote Sensing: From Pixels to Objects

Aerial photography has a long tradition dating back to Nadar's balloon-based images of Paris, France in 1858, while civilian space-borne remote sensing (RS) began in 1972 with Landsat-1. This sensor set the standards and foundation for future multi-spectral scanner technologies and its corresponding pixel-based image analysis (Blaschke et al. 2014). Towards the development of automatic image analysis tools, it is required a processing scheme able to encapsulate effectively the content of remote sensing data. Due to landscape complexity, the provided remotely sensed data represent a large variety of thematic categories, such as man-made infrastructure, various types of vegetation and water bodies etc. Furthermore, the scale of the represented categories differs in terms of their size and range.

In very high resolution imagery such as IKONOS and QuickBird, traditional classification methods which are tailored for lower resolution imagery have become less effective given the magnitude of heterogeneity appearing in the spectral feature space of such imagery. Classification results of such approaches exhibit the "salt and pepper" phenomenon in their classification results. Such problems occur also to medium resolution satellite data, such as Landsat TM, SPOT etc. Moreover the fact that pixels do not come isolated but are knitted into an image full of spatial patterns was left out of the early per-pixel investigation. Consequently, the full structural parameters of the image (i.e., color, tone, texture, pattern, shape, shadow, context, etc.) could only be exploited manually by human interpreters. However, around the year 2000, the first software appeared specifically for the delineation and analysis of image-objects (rather than individual pixels) from remotely sensed imagery. The subsequent area of research was referred to as object-based image analysis (OBIA). Since geographic space is intrinsic to this analysis, and as such, should be included in the name of the concept and, consequently, in the abbreviation: Geographic Object-Based Image Analysis (GEOBIA- Hay and Castilla 2008; Blaschke et al. 2014).

1.2 Geographic Object-Based Image Analysis

Unlike the georelational data model (such as the one employed in relational spatial databases), which separates spatial and attribute data and links them by using a common identifier, the object-oriented data model views the real world as a set of individual objects that may have spatial and non-spatial interrelationships among each other. Thus, an object has a set of properties and can perform operations on requests (Blaschke et al. 2014). To better understand and develop an explicit specification for a GEOBIA framework, Hay and Castilla (2008) provided a number of requirements for such frameworks:

- *Earth centric* – its data sources originate from the surface of this planet.

- *Multi-source capable* – its methods provide for the inclusion of multiple different digital data types/sources within a common geographic referent and for the flow of information and intelligence from pixel-based RS data to GIS ready polygons.

- *Object-based* – meaningful image-object delineation is a prerequisite of this approach, from which relevant intelligence can be generated.

- *Multiscale* – a scene is often composed of objects of different size, shape and spatial location, thus multiscale analysis both within a hierarchical level and between levels is essential. Because GEOBIA is multiscale, potential exists to model alternative 'multiscale' realities based on selective user defined aggregations of fine scale segments and/or their attributes.

- *Contextual* – it has the ability to incorporate or integrate surrounding information and attributes. When processing RS data, this includes mechanisms to quantify an object's photointerpretive elements i.e., color (hyperspectral), tone, size, shape, pattern, location, and texture. By adding time (multitemporal imagery), as well as other attributes such as height (Lidar) and heat (Thermal) into the 'contextual pool', there will be a greater information potential for each image-object than ever possible for individual pixels.

- *Adaptive* – it allows for the inclusion of human semantics and hierarchical networks – whether through experts systems, or expert interpreters, so that analysis may be tailored to specific user needs. However, to be fully adaptive, GEOBIA tools need to build on existing Open GIS standards and provide mechanisms to integrate user and domain specific ontologies into a semantic web so as to globally facilitate improved sharing, integration and generation of new synergistic geographic information and the development of their associated markets.

Thus, to determine the objects belonging to a thematic category one can employ Standard Nearest Neighbor or advanced Machine Learning techniques such as the Support Vector Machine (SVM), Relevance Vector Machine (RVM), Random Forest, Convolutional Neural Networks etc. (Baatz and Schäpe 2000; Tzotsos and Argialas 2008; Blaschke and Strobl 2010). Such methods can take advantage of the spectral, textural, and geometric properties of the objects and statistically determine the class they belong. However, the representation of contextual information within this multiscale requires the expression of human-derived interrelationships between the objects allowing the delineation of complex thematic categories. Since thematic delineation is often related to a certain field and application within this field (e.g. urban planning, geology etc.), different thematic maps can be derived from the same data. Thus, thematic delineation requires the application of field-expert knowledge into a problem-solving strategy through an establish-and-refine-paradigm, within the environment

of a knowledge representation system. Thus interpretation rules derived from knowledge stored in books, photo-interpretation manuals, certain specifications, relative work on the field, and personal experience of the phenomenon needs to be explicitly formalized and represented within an automated image analysis system (Argialas and Harlow 1990, Arvor et al. 2013, Blaschke et al. 2014).

1.3   Ontologies in GIS, Remote Sensing, and GEOBIA

Knowledge formalization into a computer-conceivable form creates a semantic gap between the complex high-level semantics employed by experts to describe a phenomenon (e.g. water absorbs infrared radiation) and the low-level data-derived numerical information extracted from the provided data (ndwi values larger than 0.25). To this end, rule-based systems and ontologies offer potential for knowledge formalization (Argialas and Harlow 1990, Argialas et al. 2013, Arvor et al. 2013, Blaschke et al. 2014).

Gruber (1995) defines the ontology as a formal, explicit specification of a shared conceptualization. An ontology is usually composed of two parts: A Terminological component (TBox) were the properties and the concept definitions are represented, and an Assertion Component (ABox) where the objects of the domain along with their properties are stored. Due to the Semantic Web movement, ontologies became a requirement to represent machine-readable knowledge. They support (Ding et al. 2007):

- *Extensibility*, as ontologies can be built in an incremental manner, by taking advantage of concepts declared in other ontologies.

- *Visibility*, as ontologies are shared through web publishing mechanisms and employ proper Syntax and semantics (URI based vocabulary, XML Syntax, RDF graph data model).

- *Inferenceability*, as ontologies are not only employed to represent knowledge but also infer knowledge based on the defined axioms.

Thus, ontologies can be employed when data, information, or services from different disciplines should be integrated, exchanged, or queried. Furthermore, ontologies enable semantic interoperability (Grubber 1995, Janowicz 2010).

Ontologies can help solve the semantic gap issue towards the implementation of an automatic image recognition system based on GEOBIA that is able to bridge the expert derived symbolic information and the numerical information extracted from the image (Arvor et al. 2013). Ontology-based recognition consists of classifying an image object as an instance of a specific type if it satisfies all of the constraints defined in the ontology for that object type (Arvor et al. 2013). The development of ontology-based recognition requires (i) formalizing the symbolic knowledge of an expert, of a specific image object type in an ontology, and (ii)

associating this knowledge with image segments described through annotations that are based on the same ontology.

Ontology studies have already been conducted in GIS, scene analysis, remote sensing, and GEOBIA. In GIS, ontologies have been successfully applied to perform knowledge representation. Torres et al. (2005) employed ontologies to describe the semantic content of topographic and thematic maps. Lutz and Klien (2006) used an ontology to explicitly specify and formalize the meaning of the domain concepts into a machine-readable language that enabled spatial information retrieval on a semantic level. Zhan et al. (2008) developed a framework to retrieve spatial information, based on spatial relation and geometric relation ontologies. Lüscher et al. (2009) developed an ontology-driven approach for cartographic pattern recognition in support of map generalization.

In the field of scene analysis, ontologies have been also employed to extract scene content. Wang et al. (2006) established a method for retrieving scene imagery, by developing ontologies which combined text annotation and image features. Hudelot et al. (2008) organized spatial relationships in an ontology representing topological relations (adjacency, inclusion etc.) and metric relations which further contained distance relations (far/close distance etc.), and directional relations (right to, left to, etc.). This ontology was linked with an upper ontology, describing brain entities, and spatial reasoning was performed to recognize various elements of the brain. In Bannour and Hudelot (2014) a multi-stage reasoning approach was developed, to perform semantic annotation/tagging on a target dataset containing ground scenes. An ontology was developed based on the imagery annotations and a common sense ontology was employed to extract additional concepts that linked the concepts defined by the annotations. A multi stage reasoning approach was developed to extract the annotations for each scene.

In the field of remote sensing, ontologies have been employed to represent expert knowledge for the representation of the properties and relations of objects in an image. Kohli et al. (2012) developed a generic slum ontology based on input from 50 experts, covering 16 countries. Bertrand et al. (2013) developed an ontology framework based on OWL 2 and the Semantic Web Rule Language (SWRL) employing expert knowledge, to describe urban elements and their spatial organization.

Ontologies have been also applied in the field of GEOBIA. Durand et al. (2007) developed a methodology for object recognition, from very high resolution imagery, based on an ontology developed by machine learning techniques and experts. The ontology was based on spectral and geometric properties of the objects. In Forestier et al. (2012) the matching algorithm introduced by Durand et al. (2007) was employed to map the observations extracted from the image with the domain nomenclature (linguistic notions). The method was employed to

extract image domain elements from QuickBird Imagery. In Belgiu and Lapoltshammer (2013), information contained in visual interpretation keys was modelled into an ontology to perform extraction from Very High Resolution imagery. An ontology was designed, defining a class – subclass hierarchy based on the United Nations Land Cover Classification System. Each class was defined by employing spectral and geometric features existing in visual interpretation keys. Belgiu et al. (2014) employed random forest and ontologies to extract buildings from ALS data by employing topographic and geometric features.

1.4   Research Objectives and Contributions

The objective of this research was the investigation and implementation of state-of-the-art computer vision and artificial intelligence approaches within the framework of GEographic Object-Based Image Analysis (GEOBIA). More specifically, the motivation was the investigation of the potential of ontologies as a knowledge formalization method in GEOBIA through multiscale analysis to improve the knowledge representation for the GEOBIA classification task. A second objective was the integration of ontologies with advanced machine learning methods towards the automation of the recognition process. A third objective was the employment of these algorithms in specific image analysis problems such as building extraction, building change detection, foreshore, alluvial fan, and bajada identification. Finally the fourth objective was the development of these image analysis frameworks in the form of Free and Open-Source Software (FOSS).

More specifically, the first objective was the design and implementation of a SPatial Ontology Reasoner (SPOR) to allow the development of GEOBIA ontologies by employing fuzzy, spatial and multiscale representations, with time efficiency (Argyridis and Argialas 2015). An enhanced version of the Web Ontology Language 2 (OWL 2) with fuzzy representations was adopted and expanded to represent fuzzy spatial relationships within the framework of GEOBIA. Segmentation results are stored within PostgreSQL. An ontology described the class/subclass hierarchy and class definitions. SPOR integrated PostgreSQL and the ontology, to store the objects, compute spatial relationships during the reasoning process, and store the classification results.

The second objective was the integration of advanced machine learning approaches with ontological reasoning in GEOBIA. To address this, the OWL 2 syntax was enhanced to allow the declaration of machine learning restrictions within class definitions. To define the machine learning method and its parameters, a machine learning datatype was designed and implemented. The information related with to machine learning method properties was encoded within proper OWL 2 metadata. To denote which classes should be involved in the same machine-learning classification, the machine-learning restriction should be included in their definition. Training samples were created as OWL 2 individuals. The machine learning method which was integrated with SPOR was the Deep Belief Network (DBN).

The third objective was the investigation and addressing of specific image analysis problems. Four remote sensing cases were investigated: building extraction, foreshore extraction, building change detection, and alluvial fan and bajada identification.

To evaluate SPOR a building extraction approach through multi-scale analysis from QuickBird imagery was designed. Three segmentation and classification levels were designed and implemented. Aim of level 1 was the extraction of spectral categories with spectral properties similar to the present buildings. Aim of level 3 was the elimination of the road network. The final buildings were extracted on level 2 with satisfactory results, since 75% of the total building rooftop area was correctly identified.

To investigate foreshore mapping from single-date very high resolution imagery and DTM, a multi-scale GEOBIA approach, employing anisotropic filtering and fuzzy ontologies was designed and implemented. At first the imagery was filtered through anisotropic morphological levelings. A three level segmentation approach was investigated, to design proper objects. Ontological reasoning was employed to formalize symbolic expert knowledge describing the spectral and spatial organization of the foreshore to classify the objects into semantic categories. Accuracy assessment with reference data provided satisfactory results, as for the identified foreshore border a mean error of 2.4m was scored.

To investigate building change detection, a GEOBIA approach integrating Deep Learning classification and Fuzzy ontologies was designed and implemented. The method was tested in building monitoring in suburban areas of Greece. Three suburban areas of east Attica, Greece were selected as representative to test the methodology. For each area one QuickBird and one WorldView 2 image, taken in 2006 and 2011 respectively were employed. Three segmentation levels and a three level class hierarchy were developed for the extraction process. Deep Belief Networks and fuzzy reasoning were employed on the lowest level of the segmentation hierarchy (Level 1) for an initial detection of areas of possible change. To detect the changes in building infrastructure, the classification result of Level 1 was refined based on interpretation rules, developed on the upper levels of the hierarchy (Level 2 and Level 3). Classification evaluation showed satisfactory results since 93.5% of the total number of changes were successfully detected, while the commission error was less than 20%.

Finally, to investigate alluvial fan and bajada mapping, a GEOBIA approach, following the landform-pattern element approach was designed and implemented. Alluvial fan and bajada mapping is important for practical and economic importance to society. Thus, state-of-the-art geomorphometric, image processing, and knowledge representation methods were investigated, enhanced, and developed, towards the simultaneous identification of alluvial fans and bajadas. Data used included the 10m spatial resolution National Elevation Dataset, provided by USGS and a pan-sharpened 15m Landsat OLi imagery. The study area was located

in the Death Valley, Nevada, USA. DTM processing included noise-removal filtering and depression treatment. A two phase GEographic Object-Based Image Analysis approach involving multi-scale segmentation and fuzzy ontology-based reasoning was designed. On the first phase, topographic-forms were identified, by examining their morphometry and spatial relationships. On the second phase, the alluvial fans and bajadas were identified based on drainage pattern texture and topographic features such as landform shape. Due to a systematic omission on the fan toe outline, each fan and bajada spectral signature was taken into account to determine the omitted areas through region growing on the multispectral imagery. Accuracy assessment indicated satisfactory results, since a 90.2% completeness and 88.8% quality was achieved for both alluvial fans and bajadas.

In terms of the algorithms developed in this dissertation, this research introduced five (5) contributions. One (1) fuzzy ontology reasoner optimized for GEOBIA studies which integrates fuzzy rule-based reasoning and deep learning classification, four (4) ontologies developed for GEOBIA studies compatible with the developed reasoner, one (1) improved version of a depression treatment algorithm, and one (1) algorithm for drainage network extraction, and one fan-shape index. The last three aided in alluvial fan and bajada mapping.

Finally, this dissertation had the following publication contributions:

- Two publications in highly rated Remote Sensing Journals (Argyridis and Argialas 2015; Argyridis and Argialas 2016).

- One submitted manuscript in a highly rated Remote Sensing Journal, accepted with minor revision (Argyridis and Argialas 2017a).

- One submitted publication in a highly rated Remote Sensing Journal pending review (Argyridis and Argialas 2017b).

- One publication submitted in conference proceedings (Argyridis and Argialas 2014).

1.5   Overview

The presented contributions are presented in detail in the following chapters. In Chapter 2, the development of SPOR is presented. Chapter 3 discusses the development of the foreshore extraction algorithm. Chapter 4 concerns the enhancement of SPOR with Deep Learning classification and the development of a change-detection method based on this improvement. Chapter 5 presents the development of a GEOBIA method towards the automatic identification of alluvial fans and bajadas and Chapter 6 presents the overall conclusions along with the prospects for future research.

2 Development of a Generic Spatial Ontology Reasoner for Multi-scale GEOBIA ontologies

2.1 Introduction

In GEographic Object-Based Image Analysis (GEOBIA) an image is partitioned into primitives (segments), which are classified into semantic categories by employing Standard Nearest Neighbor, fuzzy inferencing or advanced machine learning techniques (Baatz and Schäpe 2000; Blaschke et al. 2008; Hay and Castilla 2008; Tzotsos and Argialas 2008; Blaschke and Strobl 2010; Mallinis et al. 2011; Blaschke et al. 2014). However, to extract complex landscape components in terms of spectral, geometric, and rich spatial relationships, it is required the representation of expert knowledge into a problem-solving strategy through an establish-and-refine-paradigm, within the environment of a knowledge representation system (Argialas and Harlow 1990; Argialas et al. 2013). This requires the application of heuristic rules derived from knowledge stored in books, photo-interpretation manuals, relative work on the field and personal experience of the phenomenon (Argialas and Harlow 1990; Arvor et al. 2013). To take advantage of this symbolic knowledge within an automated image analysis system it is required to be formalized into a computer-conceivable form. Thus, a semantic gap arises between the high-level semantics employed by the experts to describe the phenomenon (Vegetation has high infrared reflectance values) and the numerical low – level information extracted from data (NDVI values greater than 0.25). To address this problem, methods are required to identify optimal features to discriminate between evaluated classes and to explicitly specify the knowledge of the experts on the evaluated classes (Belgiu et al. 2014). To this end, rule-based systems and ontologies offer potential for knowledge formalization (Argialas and Harlow 1990; Lüscher et al. 2009; Belgiu et al. 2014).

In recent years, ontologies have become popular as a means of representing machine-readable knowledge. An ontology is defined as a formal, explicit specification of a shared conceptualization (Gruber 1995). Ontologies allow to capture the semantics of the domain concepts into knowledge organization systems that can be easily reused and extended (Belgiu and Lampoltshammer 2013). In Guarino (1997), ontologies were classified based on their detail as top-level (describing generic concepts), domain (describing the knowledge of a certain field), task (describing generic tasks) and application ontologies (describing concepts related to a certain field and related tasks). Domain, task and application ontologies need to be aligned with the top-level ontology to ensure collaboration with other domain applications.

Ontologies can help solve the semantic gap problem towards the implementation of an automatic image recognition system based on GEOBIA that is able to bridge the symbolic information derived from the experts and the numerical information extracted from the data (Blaschke et al. 2014). Ontology-based recognition consists of classifying an image object as

an instance of a specific type if it satisfies all of the constraints defined in the ontology for that object type (Arvor et al. 2013). The development of ontology-based recognition requires (i) formalizing the symbolic knowledge of an expert, of a specific image object type in an ontology, and (ii) associating this knowledge with image segments described through annotations that are based on the same ontology.

The applicability of ontologies in GEOBIA has already been depicted in the literature (e.g. Durand et al. 2007, Forestier et al. 2012, Belgiu et al. 2014). However, still remains the need to integrate fuzzy reasoning with spatial relationships and multiscale analysis in an ontology-based GEOBIA approach. Indeed, Belgiu et al. (2013) stated the need for fuzzy reasoning in GEOBIA ontologies. Furthermore, the importance of spatial relationships has already been stated in early GEOBIA studies (Baatz and Schäpe 2000; Burnett and Blaschke 2003). Although, spatial reasoning with ontologies for image analysis has been examined (Hudelot et al. 2008; Forestier et al. 2012; Bannour and Hudelot 2014), still remains the need of spatial reasoning for multiscale analysis in GEOBIA ontologies. Arvor et al. (2013) and Belgiu et al. (2014) stated a limitation of current Description Logic (DL) – based ontology reasoners, concerning the required processing time when dealing with a large number of classes and objects, which is very common in GEOBIA studies.

To address the above stated needs, this research aided in the development of an ontological reasoner for GEOBIA, named SPatial Ontology Reasoner (SPOR). SPOR was developed to provide representation of fuzzy spectral, geometric, and spatial relationships for the development of a GEOBIA ontology. Spatial relationships were designed to express relationships between single or multiple levels of analysis. Considering the language employed to represent ontologies, OWL 2 was selected, which is a World Wide Web Consortium (W3C) recommendation (W3C 2012). OWL 2 ensures the integration and exchange of GEOBIA ontologies with current semantic web technologies. Hay and Castilla (2008) stated the need to incorporate Open GIS Standards (Open Geospatial Consortium 2014) in GEOBIA applications to ensure collaboration with current remote sensing and GIS software. Thus, SPOR was designed to incorporate technologies which already adopted these standards (notably PostgreSQL) and also provide for time efficiency in processing large amount of data.

2.2   Methodology and Implementation
2.2.1   Fuzzy OWL 2 Ontologies for GEOBIA
Based on the OWL 2 specification, OWL 2 ontologies enable the design of classes, individuals, properties, datatypes, and annotations (W3C 2012). In the following the main expressions along with their employment in SPOR is presented. It is noted that all OWL 2 expressions will be presented in Manchester OWL 2 Syntax which is a user-friendly syntax for OWL 2 descriptions (W3C 2012). Thus of OWL 2 supports:

- *Classes* to represent groups of things, thus they were employed to represent thematic categories.

- *Individuals* to represent actual objects of the domain, thus they could be employed to represent the segments from the segmentation process. However, since spatial reasoning was required, and also to ensure collaboration with current GIS software, it was determined to store the segments in PostgreSQL.

- *Data properties* to represent relationships between an individual and data values, thus they were employed to represent quantitative properties of the objects.

- *Object properties* to connect pairs of individuals, thus they were employed to represent spatial relationships between objects. Spatial relationships were interpreted as topologic links between two segments.

- *Datatypes* to refer to sets of data values, which are used in *expressions* to restrict *Data properties*.

- *Annotation properties* to encode metadata of the ontology itself or the declarations within the ontology.

- *Axioms* which are statements asserted to be true in the described domain.

- *Expressions* to represent complex notions in the described domain, employed mostly in class definitions.

Bobillo and Straccia (2011) enhanced OWL 2 with fuzzy representations encoded as OWL 2 metadata (*Annotation properties*). This allowed the development of class definitions with fuzzy representations. To restrict *Data properties*, *fuzzy datatypes* were employed (Bobillo and Straccia 2011). As an example, the partial definition of Vegetation class is presented as follows:

ndvi some mediumToLargeValuesOfNDVI

The mediumToLargeValuesOfNDVI is a *fuzzy datatype*. The fuzzy information, regarding the membership function and its borders is encoded, within an *annotation property* called *fuzzyLabel*, as follows:

<Datatype type="rightshoulder" a="0.2" b="0.4" />

To design *fuzzy object properties* capable of defining topologic/spatial relationships, the relative annotation should include information regarding the type of the spatial relationship, the membership function, and its borders. Thus, in the restriction *isSurroundedBy some Water*, the *isSurroundedBy* notion was designed to be the *fuzzy object property* representing the spatial relationship of the segments with the ones belonging to the *Water* class. Thus, the *fuzzy object property* was designed to have an annotation property as it follows:

<Role datatype="highRelBrdr" spatial_relationship="relative_border" />

The highRelBrdr is a *fuzzy datatype* with similar definition to the one presented earlier. The *spatial_relationship* attribute describes the type of the spatial relationship represented by the *fuzzy object property*. The developed spatial relationships express relationships between objects belonging at the same level (relative border, length of common border, distance of centroids, and distance from the outer border of a class), between an object and objects of lower levels (relative area and overlaps) and between an object and objects of higher levels (overlapped by). In Table 1, the expressions supported by SPOR are presented.

2.2.2   Design and Implementation of SPOR for GEOBIA

To gain in terms of computation performance, SPOR was developed in C++. Integration of SPOR with PostgreSQL was achieved through PostgreSQL C++ interface. SPOR performs the following actions (Figure 1).

- Parsing of the ontology.

- Connection to PostgreSQL and retrieval of the stored segments attribute table.

- Computation of topologic tables (if not present).

- Reasoning/classification process based on the axioms defined in the ontology.

- Labeling of segments.

Initially the ontology is parsed by SPOR. Afterwards the attribute table of the segments is retrieved from PostgreSQL. For multiscale segmentation analysis (Baatz and Schäpe 2000; Tzotsos and Argialas 2006), two topologic relationships were considered to represent the hierarchical and spatial relationships of the segments. Each segment requires knowledge of its neighbors at the same level, its sub-objects at lower levels and its super objects at higher levels. Before the reasoning process, if these relationships have not been computed by the segmentation algorithm, SPOR carries out the required computations through SQL queries.

Table 1: Expressions supported by SPOR and MV computation.

Constructor	Manchester OWL 2 Syntax	Explanation/Information
Class	VegetationL1, WaterL1	Image thematic categories
Individual	id100	Samples required in cases where DBN classification is involved. Segments are stored in PostgreSQL
Top	Thing	All classes are subclasses of Thing
Fuzzy Datatype	fuzzy_RS_0.2_0.3	Fuzzy function and borders
Datatype Property	ndvi, msavi2, machineLearningFeature	Segment quantitative properties
Object Property	has_Fuzzy_RS_0.3_0.5_RelativeBorder	Spatial relationships
Existential fuzzy data property restriction	ndvi some fuzzy_RS_0.2_0.3	Each segment MV is determined based on its feature value and Fuzzy Datatype information.
Conjunction	WaterL1 and VegetationL1 (msavi2 some fuzzy_RS_0.5_0.6) and (ndvi some fuzzy_RS_0.2_0.3)	For each segment the MV is computed as the minimum MV computed from the two involved expressions.
Fuzzy Existential Object Property restriction	has_Fuzzy_RS_0.3_0.5_RelativeBorder some WaterL1	Spatial relationship with a class. At first the value of the spatial relationship is computed for each segment. Afterwards the MV is computed based on the feature value and the fuzzy information.
Disjunction	VegetationL1 or WaterL1 (msavi2 some fuzzy_RS_0.5_0.6) or (ndvi some fuzzy_RS_0.2_0.3)	For each segment the MV is computed as the maximum MV computed from the two involved expressions.
Negation	not (VegetationL1) not (msavi2 some fuzzy_RS_0.5_0.6)	Negation. For each segment the MV is computed by subtracting the MV determined by the involved expression from 1.
Concept Definition	not (WaterL1) and ((msavi2 some fuzzy_RS_0.5_0.6) or (ndvi some fuzzy_RS_0.2_0.3))	A complex expression that defines a class.
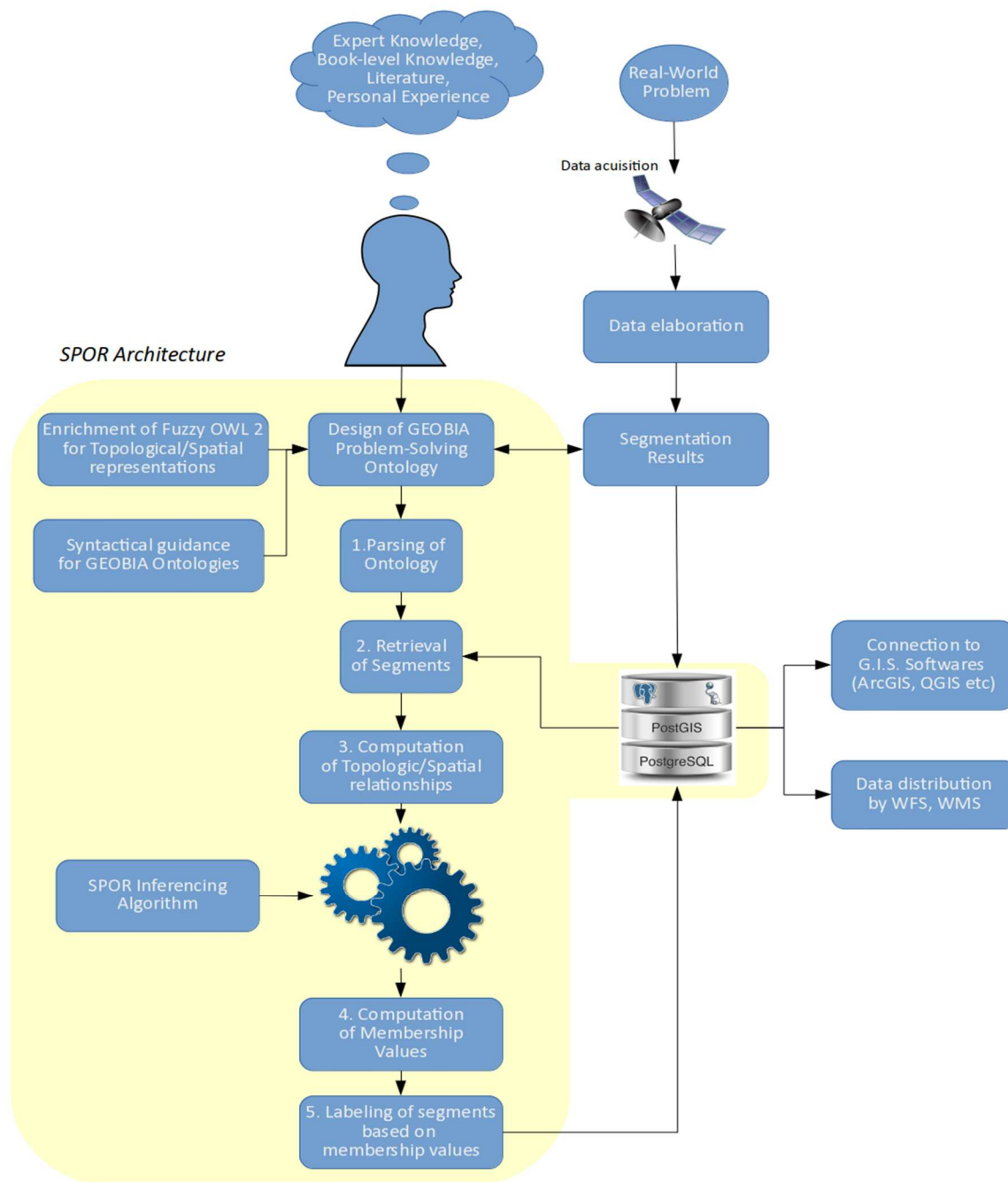
Figure 1: Overview of SPOR architecture

To determine the MV of each segment with all classes, SPOR iterates over the classes defined in the ontology (Figure 2). As OWL 2 does not provide information regarding the hierarchy depth of the examined class, the classes are examined in alphabetical order. At first the reasoner iterates over the referenced classes in class definition (e.g. parent, spatially-related, or appearing in a logical operation). If MVs of the segments for these classes have not as yet been computed, then the reasoner tries to compute their MVs. To consider objects with adequate MVs for all parent classes, as candidate segments for the currently examined class,

are considered objects having MV greater than 0.5 for all parent classes (*computeCandidates()*). Afterwards the spatial relationships are computed (*computeSpatialRelationship()*). If the class has a spatial relationship with herself, then multiple classification iterations are performed. In the first iteration the spatial relationship is ignored. In the next iteration, the objects belonging to the examined class are considered to compute the spatial relationship. This is repeated until the classification result is not altered between two iterations.

From the examined-class definition, a node graph is created (*computeMembership()*). Each node can represent a class, a feature node (fuzzy *Data* or *Object property restriction*) or a logical operator (*and*, *or*, *not*). For each candidate-segment the MV is computed. The node is scanned in depth-first order and the membership value for each node is computed. If it is a class node, then the MV of the current candidate with the referenced class is set as node value. If it is a feature node, then the MV of the current candidate is computed, based on its feature value and the fuzzy operator determined by the ontology. If it is a logical operator node, then at first the MVs of the sub-nodes are computed. Afterwards, based on Zadeh semantics (Zadeh 1965) the logical node MV is computed. Computation stops when the MV of the top node is computed. If the final MV is greater than 0.5, then the class name of the currently examined class is assigned as label to the candidate. SPOR is a Free and Open Source Software under the terms of GPLv3 (or later) and the source code can be downloaded from the following url:

https://github.com/ArArgyridis/SPOR
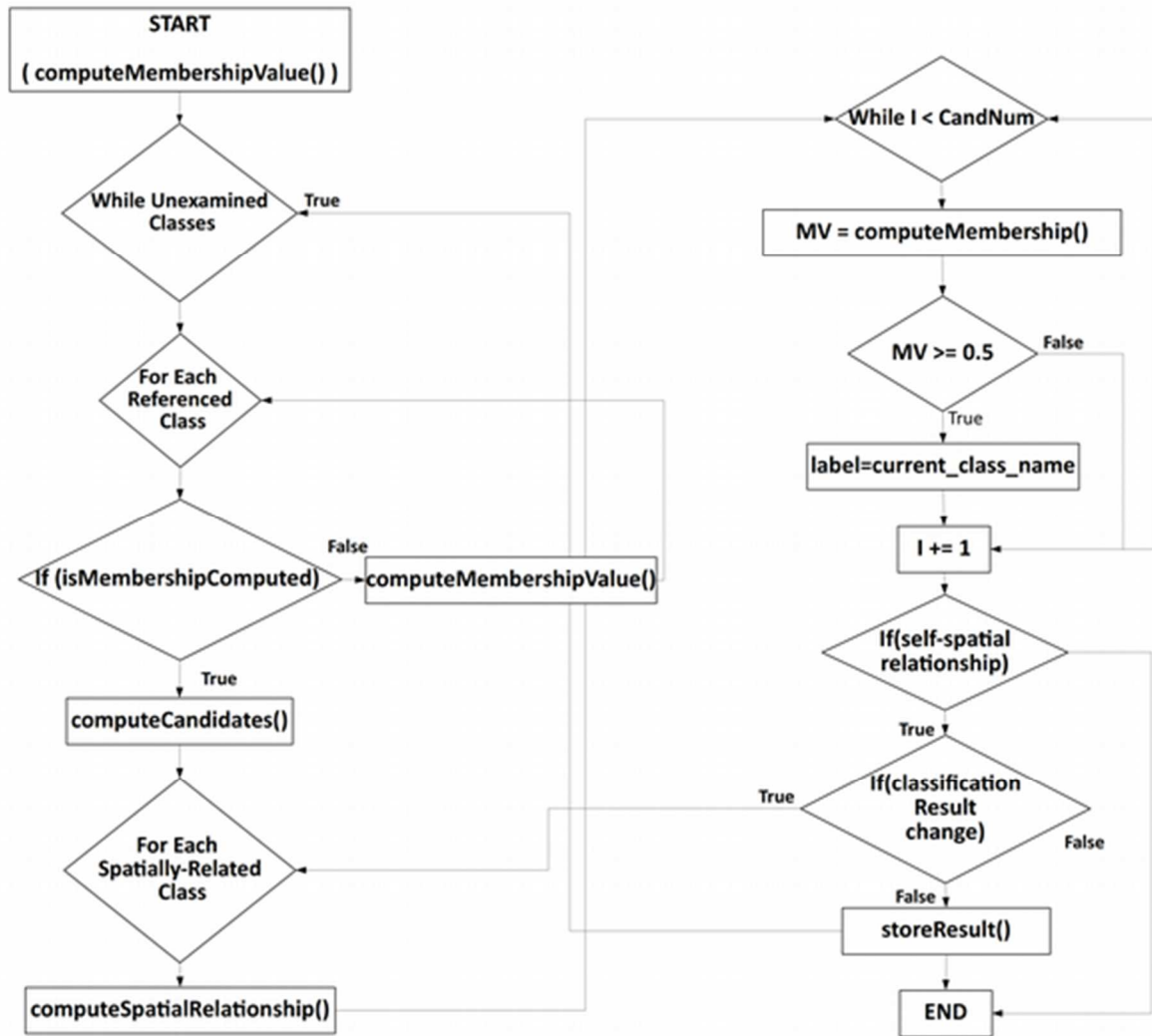
Figure 2: SPOR reasoning process that determines the membership value of each segment with a class.

2.3 Building Extraction through GEOBIA and SPOR

In this section building extraction from remotely sensed imagery is presented. The aim was to develop a problem solving strategy to represent the implicit relationships of image elements with an ontology. Data used included one fused QuickBird image of a sub-urban residential area of east Attica, Greece, taken in 2006. Before the extraction analysis, the image was georeferenced.

2.3.1 Design of the ontology

The aim was to represent domain knowledge (such as land cover classes) and remote sensing knowledge (such as the required indices for the definition of land cover classes) within a GEOBIA ontology. The development began with the specification phase (Paslaru et al. 2006; Brusa et al. 2006), where the general concepts that were going to be described by the ontology were determined. These concepts correspond to the land use / land cover classes, present in the imagery (Figure 3). Given that only spectral information was available for building extraction and the majority of the rooftops appeared relatively spectrally

homogeneous and rectangular, it was decided to extract the rooftops based on their spectral and geometric signature.
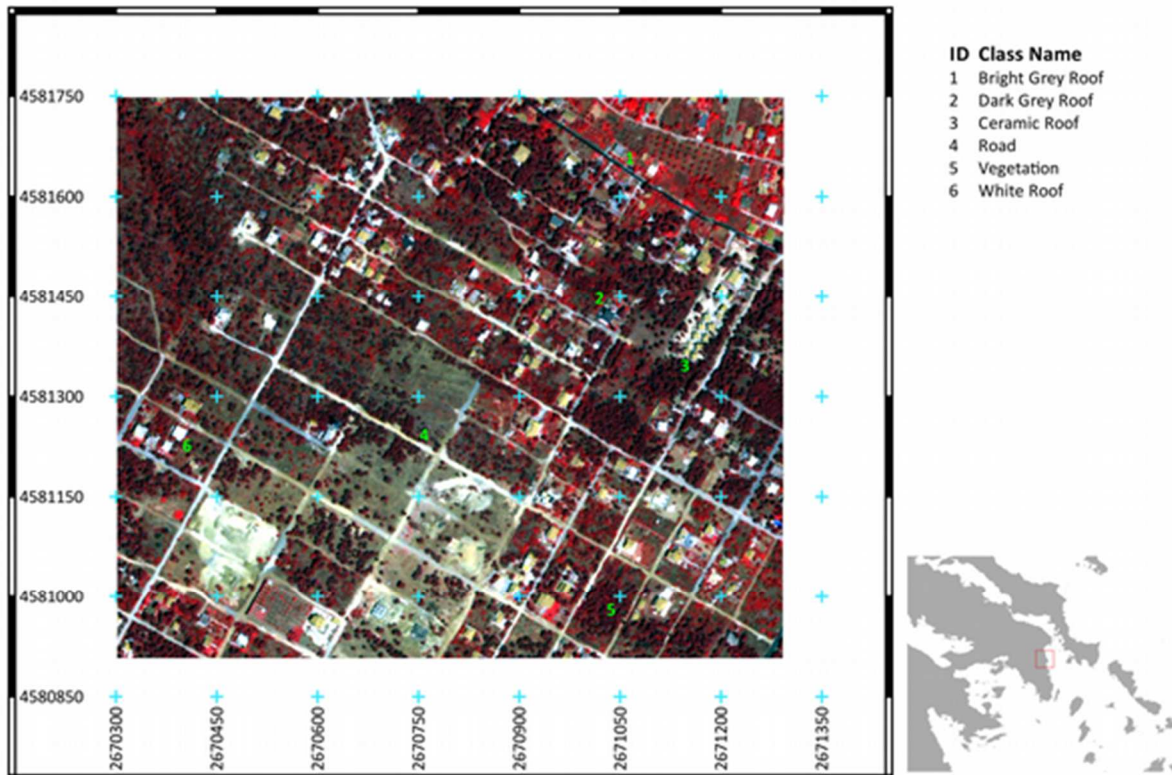
Figure 3: Overview of the examined area. The coordinates are presented in Greek National Grid 87 (EPSG: 2100).

In the conceptualization phase, the main concepts were formalized in an initial taxonomy, independently of any software or language implementation along with the properties required to define each class. As the taxonomy was related with the levels of analysis, the number and parameters of the segmentation levels were also approximately determined. The lower level properties were determined based on remote sensing knowledge, literature survey, and personal experimentation. Knowledge formalization, the final step, involved the development of a fuzzy OWL 2 ontology, based on the conceptual scheme. Through the formalization step, the ontological conceptual scheme was refined, by a repeated trial and error process. In the following, the extraction strategy is presented.

For the segmentation process the multiresolution segmentation algorithm included in Definiens eCognition 8.6 (Trimble 2011) was employed. Any single or hierarchical segmentation algorithm could be employed along with SPOR. Segmentation results were exported from eCognition and imported into PostgreSQL. To visualize extraction results, the Quantum GIS environment was employed (QGIS Development Team 2014). The aim was to

extract rooftops based on their spectral and geometric properties; thus spectrally-homogeneous areas should at first be detected, which could later be refined into rooftops considering their geometry as well. It was determined that three segmentation levels were required for the extraction of buildings. Each level aimed to represent different scale objects. In implementing a mixed bottom-up and top-down approach, larger objects were created in higher levels of the hierarchy and finer scale objects were created in the lower levels. Details concerning the classes, properties and class definitions developed, can be found in the uploaded ontology in the following link, while an overview of the developed classes is presented in Figure 4.

https://github.com/ArArgyridis/GEOBIA-Ontologies/blob/master/GEOBIA_Ontology_Quickbird_2006.owl
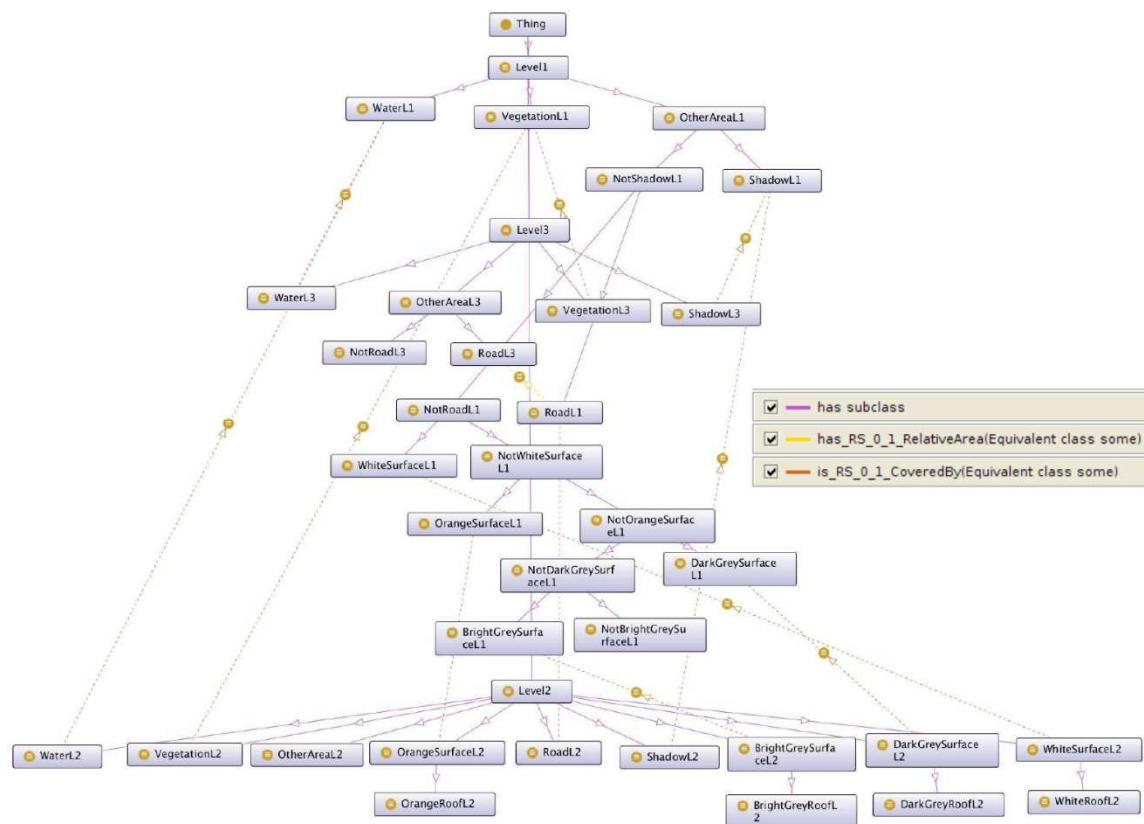
Figure 4: Classes developed in building extraction from QuickBird 2006.

Given that vegetated, shadowed, and water areas (e.g. pools) can be detected based on their spectral properties, a small scale should be employed for proper extraction. Thus, *Level 1* was designed on the lower level of the multiresolution analysis (Scale=5, Shape = 0.5 and Compactness = 0.5). For the segmentation process all the available bands were employed. First, the classes *VegetationL1* and *WaterL1* were created and defined by large values of the Normalized Difference Vegetation Index (*NDVI*) and Normalized Difference Water Index (*NDWI*), respectively. The rest of the areas were classified as *OtherAreaL1* (Figure 4). *ShadowL1* was created as subclass of *OtherAreaL1*, defined by low intensity values of Hue

Saturation Intensity (*HSI*) transform of infrared, red, and green bands. All other areas were classified as *NotShadowL1* (Figure 4). As buildings and roads have similar spectral signatures, roads were also extracted to avoid confusion with the buildings. As roads are elongated objects, the small objects of *Level 1* were not appropriate for their extraction.

Thus, a coarser level (*Level 3*) (Scale = 45, Shape = 0.8, Compactness = 0.0) was created above *Level 1*. Again, all bands were included in the segmentation process. Classification results from *Level 1* were projected onto *Level 3*, and the classes *VegetationL3*, *WaterL3,* and *ShadowL3* were developed and defined (Figure 4). To demonstrate the projection from lower to upper levels the definition of class *VegetationL3* is presented in Equation (1):

  VegetationL3 EquivalentTo:

$$\text{Level3 and (has\_RS\_0\_1\_RelativeAreaToSubObjects some VegetationL1)} \qquad (1)$$

This definition reads as follows: *Objects were assigned to class VegetationL3 if they were belonging to Level3 class and had relative area with the objects classified as VegetationL1, greater than 50%.* All other areas were classified as *OtherAreaL3*. *RoadL3* was created as subclass of *OtherAreaL3*, defined by large values of the *asymmetry*, low values of the *density* and relatively large values of the *length* properties. The results from the classification process of *Level 3* were projected onto *Level 1*. Thus, the class *RoadL1* was defined as subclass of *NotShadowL1* (Figure 4). To demonstrate the projection from upper to lower levels, the definition of class *RoadL1* is presented in Equation (2):

  RoadL1 EquivalentTo:

$$\text{NotShadowL1 and (is\_RS\_0\_1\_OverlappedBy some RoadL3)} \qquad (2)$$

This definition reads as follows: *objects were assigned to class RoadL1 if they were classified as NotShadowL1 and they were overlapped by objects of class RoadL3.* As *NotRoadL1* were classified *NotShadowL1* segments which were not classified as *RoadL1*. Four classes (*WhiteSurfaceL1*, *OrangeSurfaceL1*, *DarkGreySurfaceL1* and *BrightGreySurfaceL1*) were designed to represent objects with spectral properties similar to those of the rooftops. After defining each class (e.g. *WhiteSurfaceL1*) a complement class was defined (e.g. *NotWhiteSurfaceL1*). The next class (e.g. *OrangeSurfaceL1*) and its complement (*NotOrangeSurfaceL1*) were defined as subclasses of the aforementioned class (Figure 4). This approach was applied to all four spectral classes related to rooftop areas. A set of spectral indices were employed, to describe the spectral properties of each of these classes.

The objects, classified as *WhiteSurfaceL1*, *OrangeSurfaceL1*, *DarkGreySurfaceL1*, and *BrightGreySurfaceL1* were spatially merged and a new level, *Level 2* was created between *Level 1* and *Level 3*. Classification results from *Level 1* were projected onto *Level 2*, thus the classes *BrightGreySurfaceL2*, *DarkGreySurfaceL2*, *OrangeSurfaceL2*, *RoadL2*, *ShadowL2*,

33

VegetationL2, *WaterL2* and *WhiteSurfaceL2* were defined through a set of proper topologic/spatial properties (Figure 4). Misclassified *Level 1* areas were excluded by applying additional spectral and texture properties.

Based on geometric properties (such as the rectangular fit, length/width ratio and the area) the classes *BrightGreySurfaceL2*, *DarkGreySurfaceL2*, *OrangeSurfaceL2* and *WhiteSurfaceL2* were refined into the final classes representing building roofs: *BrightGreyRoofL2*, *DarkGreyRoofL2*, *OrangeRoofL2* and *WhiteRoofL2*. To demonstrate the geometric refinement, the definition of the class *WhiteRoofL2* is presented in Equation (3):

   WhiteRoofL2 EquivalentTo:

        WhiteSurfaceL2

        and (areaM2 some fuzzy_TRP_20_40_360_380)

        and (rectangularFit some fuzzy_RS_0.6_0.7)   (3)

This definition reads as follows: *Objects were assigned to class WhiteRoofL2 if they were classified as WhiteSurfaceL2, and had area between 30m² and 370m², and had rectangular fit greater than 0.65*. In Figure 5 the results of the building extraction process are presented. Some omission errors are shown in ellipsis, while some commission errors are shown in rectangles. A visual examination showed satisfactory results, since few areas were misclassified as rooftops, while the majority of the rooftops were correctly classified.

2.3.2   Accuracy assessment

Classification results were compared with human interpreted ground truth and were evaluated with two methods. At first, the number of ground truth rooftops was compared to the number of extracted building rooftops. From the total of 191 rooftops, 166 (87%) were detected, 25 (13%) were omitted and 16 (8%) were committed. On a second step, the areas correctly detected (True Positive - TP), omitted (False Negative – FN) or committed (False Positive – FP) were computed by comparison to the ground truth. Thus, the *Completeness*, *Correctness*, and *Quality* indices were computed as shown in Equations (4)-(6) (Agouris et al. 2004).

$$\text{Completeness} = \frac{TP}{TP+FN} = 75.0\%$$
                                                                                   (4)

$$\text{Correctness} = \frac{TP}{TP+FP} = 79.4\%$$
                                                                                   (5)

$$\text{Quality} = \frac{TP}{TP+FP+FN} = 62.8\%$$
                                                                                   (6)

Evaluation based on fuzzy logic was performed by computing the classification stability index which is the difference between the two largest membership values for each segment (Trimble 2011). Table 2 contains the results of this index, for each of the building classes of Level 2.

Table 2: Evaluation based on fuzzy logic index (classification stability).

Class Name	Number of Classified Objects	Mean	St. dev	Min	Max
BrightGreyRoofL2	22	0.85	0.18	0.52	1
DarkGreyRoofL2	26	0.88	0.18	0.53	1
OrangeRoofL2	89	0.97	0.08	0.57	1
WhiteRoofL2	45	0.94	0.13	0.55	1

2.4   Discussion of Results

A fuzzy reasoner, SPOR, was designed and implemented in C++ for OWL 2, by integrating PostgreSQL with a fuzzy OWL 2 ontology. This enabled the definition of classes with fuzzy data properties and the expression of spatial relationships though properly designed fuzzy object properties. The design of the reasoner enabled handling of spatial relationships of objects belonging to a single or multiple levels of analysis. Adoption of fuzzy logic enabled the evaluation of the knowledge base through stability measures. The integration with PostgreSQL allowed computation of spatial relationships during the reasoning process and ensured collaboration with current GIS and remote sensing technologies.
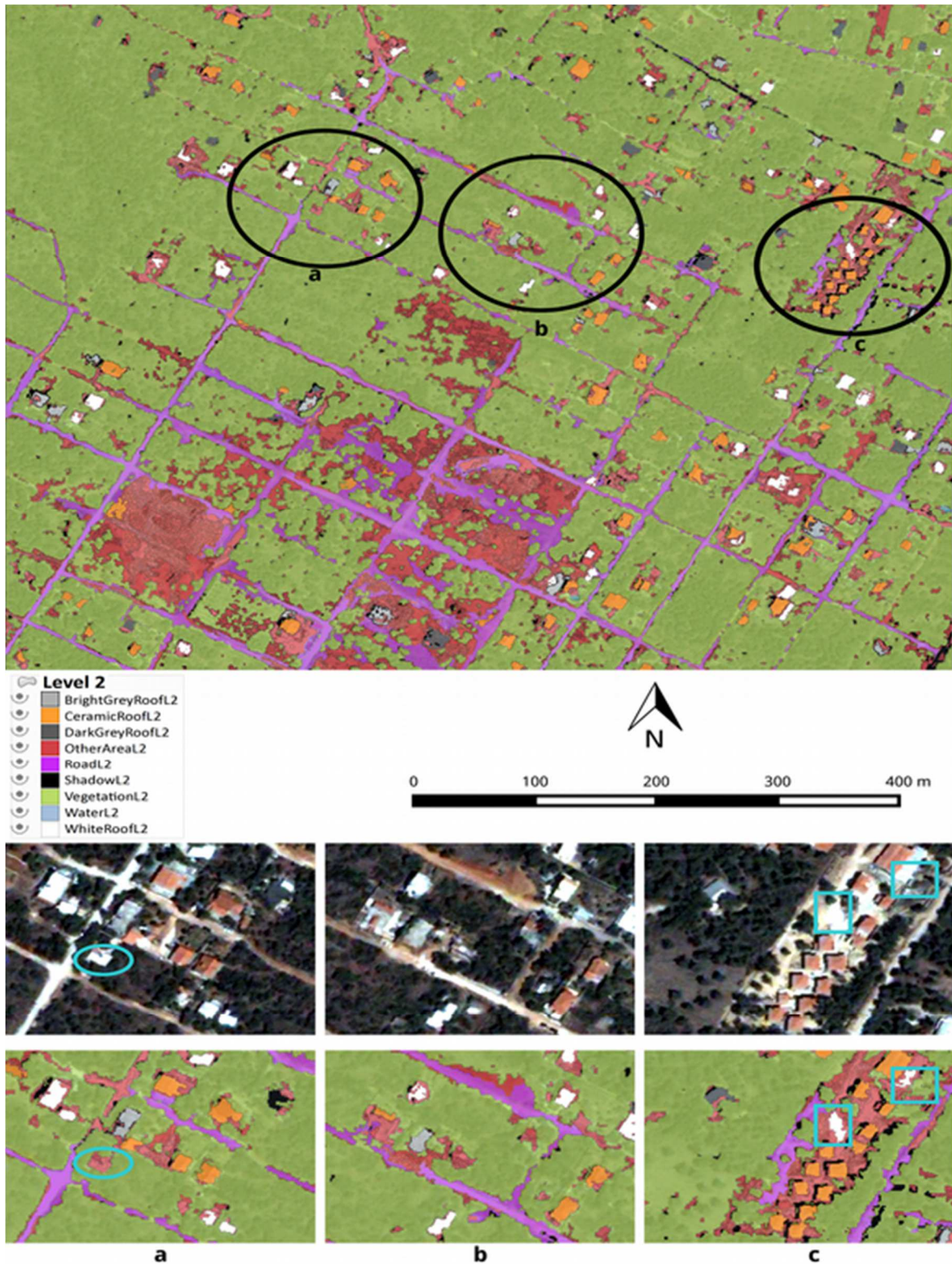
Figure 5: Result of building extraction from QuickBird 2006 imagery. Omission errors appear in ellipses while commission errors appear in rectangles.

Development of GEOBIA ontologies provides for critical review and correction of the represented knowledge. It can also be directly employed in a GEOBIA process to extract landscape components. The adoption of OWL 2 for ontology formalization ensures the integration of GEOBIA ontologies between them or with others from different disciplines through Semantic Web ontologies. Towards the exchange of knowledge with other domains, it can be examined the integration of the developed ontology with top level ontologies, such as DOLCE or SWEET (Belgiu et al. 2014). To experiment with and evaluate SPOR, a case study regarding building extraction was designed. Classification stability results indicated that the segments were classified with high confidence in their respected classes, since the lowest average stability was 0.8503. Accuracy assessment showed that 87% of the total number of buildings and 75.0% of the total rooftop area was correctly classified. Most of the omission error, was due to the heterogeneity of spectral and geometric signature of some rooftops. Most of the commission error was due to the spectral similarities of various bare ground areas with rooftops. Elimination of such commission error could be achieved if DSM data were available, such as in Belgiu et al. (2014). The above observations indicate the difficulty of completely reducing the semantic gap.

Possible extensions of SPOR might include some of the following. An earlier approach, developed by Hudelot et al. (2008), aimed at the development of a generic spatial relations ontology. It can be examined the extension and integration of their approach within SPOR, to take advantage of the representation of spatial relationships from a generic ontology. Furthermore, approaches have been developed aiming to automatically create an ontology from given data by employing machine learning techniques (Durand et al. 2007; Forestier et al. 2012; Bannour and Hudelot 2014; Belgiu et al. 2014). Such approaches might be employed for the automatic design of the ontology hierarchy and the determination of the required features that define each class. Another consideration could be the extension of the reasoner with additional fuzzy membership functions and spatial properties.

Despite the rather large size of the knowledge base (37 classes, 300.000 segments) the reasoning process required satisfactory time to complete (around 31s, on an Intel i7 3770K). This addressed the issues reported by previous studies (Arvor et al. 2013; Belgiu et al. 2014), regarding the extended time required by current reasoners to perform the classification process, on large knowledge bases.

2.5   Conclusions and Future Perspectives

Already, a lot of effort has already been developed within the GEOBIA community to extract semantic information from images. The results of these efforts (knowledge bases, employed strategies, extraction process) today exist only on paper or isolated and unrelated implementations. Thus, the generic knowledge base is available only to a strict number of individuals. Ontologies, on the other hand, have been developed for knowledge exchange

within the Semantic Web. Therefore, such efforts provide an opportunity for the development of a collaboration tool to allow exchanging and enhancing of the developed ontologies for image extraction by all GEOBIA community.

SPOR is as Free and Open Source Software, under the terms of GNU GPL v3 (Free Software Foundation, 2007). The purpose is to integrate SPOR with other open source GEOBIA environments, such as GNORASI (Doulaverakis et al. 2014). This would allow to take advantage of the capabilities of an integrated environment and to enhance the design of such ontologies with the development of additional tools such as an appropriate ontological editor.

3 Fuzzy Ontology-Based Foreshore Identification from Digital Terrain Model and Very High Resolution Airborne Imagery through GEOBIA Multi-Scale Analysis

3.1 Introduction

Coastal zone management is important due to the growing social and demographic pressures that threaten its sustainability. More than half of the world's population lives within 60 km of the coast. Almost 70% of the world's beaches are under coastal erosion (Moore et al. 1999; Ghosh et al. 2015).

Coastal mapping from remotely sensed data has already been achieved from multispectral/hyperspectral, Digital Elevation Model (DEM) data or their combination. Pixel-based, GIS, and object-based approaches have been developed for coastline extraction and change detection (e.g. Liu et al. 2007, Urbanski 2010, Braga et al. 2013, Hannv et al. 2013, Niya et al. 2013, Gong et al. 2014, Ghosh et al. 2015), as well as coastal habitat mapping such as the beach, foreshore, backshore, and dunes (e.g. Bertels et al. 2012, Baptist 2009, Urbanski 2010, Forestier et al. 2013).

Foreshore mapping specifically is important, since the processes that take place in the foreshore affect the nearby water quality. Proper management of the foreshore will improve property values and provide recreational amenity (Water and Rivers Commission 2001). Furthermore foreshore mapping assists on the definition of the zone of entry (ZOE), delineating coastal landing zones, coastal obstacle mapping, and other terrain analysis operations (FM 5-33, 1992). Foreshore is the land between the mean high water limit and the mean low water limit (Baptist 2009). Foreshore is the land that adjoins or directly influences a waterway. It is the area of transition between the edge of the waterway and the furthest extent of riparian vegetation, flood prone land, and riverine landforms or simply the adjacent upland. Thus, the morphology of the foreshore is affected by the presence of various elements, such as the present vegetation, slopes, etc. (Water and Rivers Commission 2001, Department of Water 2012). Since the foreshore is related with land management and property, its delineation can be also affected by the relevant law.

Foreshore definition involves foreshore spatial relationships with the nearby land cover. To standardize foreshore mapping, the Greek Cadastral office (Ktimatologio S.A.) published a set of foreshore interpretation criteria as guidance to photo – interpreters. Ktimatologio S.A. (2006) provided multiple criteria to determine the foreshore position, which consider present nearby land cover and terrain features such as vegetation, slope, infrastructure etc. In this study, the two most commonly occurring interpretation criteria were examined, the *vegetation border* and the *topographic crown border*, defined as follows (Ktimatologio S.A., 2006):

The *vegetation border* criterion defines the foreshore as the land between the sea and last vegetation line towards the land. It is applied in cases where vegetation is present, the shore has small slope gradients and the various types of vegetation are clearly the limit of the foreshore. The last line of vegetation towards the sea is taken into account. The exact border should coincide with the tree trunk position (Figure 6.a).

The *topographic crown border* criterion is applied in cases where there is significant height difference in the foreshore area (Figure 6.b). The delineation is performed on a Digital Terrain Model (DTM). The borderline is placed on the topographic crown.

(a)   (b)
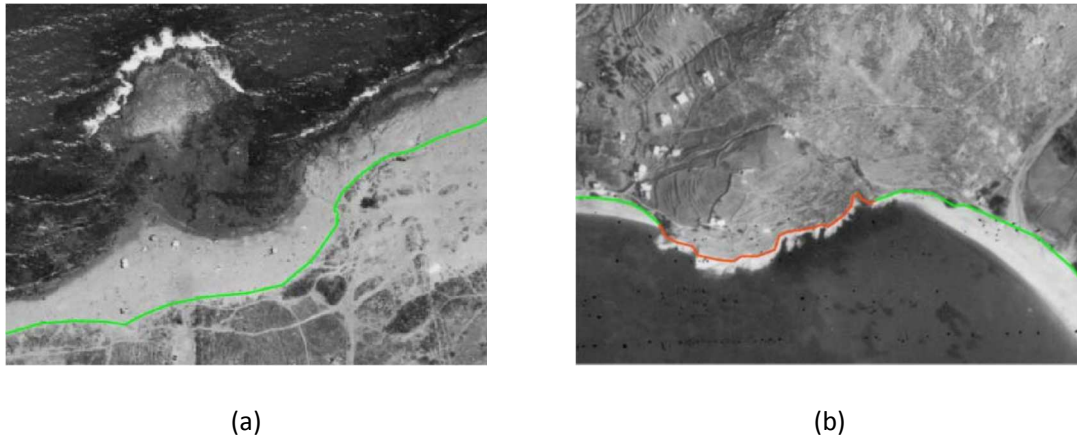
Figure 6: Foreshore Interpretation examples, provided by Ktimatologio S.A, (2006) a. The vegetation border criterion presented with green line. b. Vegetation border (green line) and topographic crown border criteria (orange line).

Since the spatial organization of the foreshore is important in foreshore definition and delineation, a Geographic Object-Based Image Analysis (GEOBIA) approach was investigated. GEOBIA partitions the imagery into primitives (segments) representing thematic objects. These objects can be assigned into thematic categories through machine learning. However, mapping of thematic categories having complex spectral, geometric and spatial relationships, requires the formalization of expert knowledge into a problem-solving strategy through an establish-and-refine-paradigm, within the environment of a knowledge representation system (Argialas and Harlow 1990, Baptist 2009, Arvor et al. 2013, Forestier et al. 2013). The expert knowledge acquired from books, photo-interpretation manuals, relative work on foreshore, and personal experience of the phenomenon needs to be formalized into a computer-conceivable form to be employed in image analysis approaches. This leads to a semantic gap, between the expert high-level semantics employed for the interpretation of the phenomenon and the data-derived low-level information. To this end, ontologies offer potential for knowledge formalization (Arvor et al. 2013, Blaschke et al. 2014).

Gruber (1995) defines the ontology as a formal, explicit specification of a shared conceptualization. The Semantic Web movement made ontologies a requirement for

knowledge representation. Thus, they were built to be extensible (created in an incremental manner), visible (shared through web publishing mechanisms) and support inference. Furthermore, ontologies enable semantic interoperability (Grubber 1995, Janowicz 2010). Ontologies can help to address the semantic gap issue towards the implementation of an automatic image recognition system based on GEOBIA that is able to bridge the symbolic information derived from the experts and the numerical information extracted from the image (Blaschke et al. 2014). Their applicability in GEOBIA has already been depicted in previous studies (e.g. Forestier et al. 2013, Argyridis and Argialas 2015).

Aim of this chapter was the extraction of the foreshore border towards the land by making explicit and by formalizing the interpretation rules related to foreshore delineation (Ktimatologio S.A. 2006) through a GEOBIA approach. Objects representing thematic categories were extracted in a multi-scale approach. Image interpretation knowledge required for object classification into semantic categories, was formalized through the development of an ontology, which represented the explicit and/or implicit relationships of each category.

3.2 Materials and Methods

3.2.1 Preprocessing: Morphological Levelings

Aim of the preprocessing was the reduction of noise and undesired spatial detail by preserving the borders of the main thematic categories of the imagery. Thus morphological leveling filtering was performed (Meyer and Maragos 2000, Meyer 2004, Karantzalos and Argialas 2006). A leveling $\Lambda(F, H)$ transforms a marker H, into an image G, which is a leveling of image F as follows. If {H < F}, H is increased as little as possible. If {H > F}, H is decreased as little as possible. This process continues until a flat zone is created or G reaches the borders of F. Thus G is flat when {G < F} and {G > F} and the procedure continues until convergence. Leveling markers can be sampled from Gaussian scale-space. Employment of different scaled markers, can create a multiscale representation of F. In this study, the Anisotropic Morphological Leveling (AML) similar to Karantzalos and Argialas (2006) was employed. AML was designed to smooth small differences in reflectance values in a direction parallel to image object edges, while preserving major edges.

3.2.2 GEOBIA Ontologies

OWL 2 ontologies allow the design of *Classes*, *Individuals*, *Properties*, *Datatypes* and *Annotations*. In the following, all OWL 2 restrictions will be presented in Manchester OWL Syntax (W3C 2012). The reasoning process was performed by SPOR (Argyridis and Argialas 2015). *Classes* represent groups of things (image categories), while *Individuals* represent actual objects of the domain (segments). *Data properties* represent relationships between an *individual* and data values (e.g. spectral or geometric properties). *Object properties* express relationships between pairs of *Individuals*. *Datatypes* refer to sets of data values. *Annotation*

properties (AP) encode metadata related to the ontology or its entities. *Axioms* or *Expressions* are statements that are asserted to be true in the described domain.

Fuzzy datatypes were employed to encode fuzzy information for *Data property restriction*. Membership functions were represented through the left shoulder (LS) right shoulder (RS), triangular (TR) and trapezoidal (TRP) functions (Bobillo and Straccia 2011). Thus the expression mNDWI some fuzzy_RS_0.05_0.15 restricts the NDWI (Normalized Difference Water Index) property with a fuzzy right shoulder function (greater than) with its left border equal to 0.05 and its right border equal to 0.15. Respectively, fuzzy objects properties were employed to restrict fuzzy spatial relationships (Argyridis and Argialas 2015). Thus the expression *has_Fuzzy_RS_0.15_0.40_RelativeBorderTo some SeaL2*, denotes all the objects, having relative border with objects classified as *SeaL2*, restricted by a right shoulder function with borders 0.15 and 0.40. Interweaving of such expressions through the and, or, and not operators were employed as class definitions.

3.3 Foreshore identification through ontologies and GEOBIA

3.3.1 Data used and foreshore interpretation

The study area was the coastal zone of Preveza Prefecture, Greece. A total length of 5 Km of coastline was investigated, divided into seven representative areas (Figure 7). In areas *a-d* the foreshore is interpreted based on the *vegetation border* criterion. In areas *e-f* the foreshore is interpreted by both the *vegetation* and *topographic crown* border criteria. In area *a* the foreshore area is composed mostly by vegetation with relative border with the sea, while a small part of it is bare ground. Areas *b – d* have variations related to their slopes and elevations. Area *e had* minor slopes. Area *f* had both major and minor slopes. In area *g* the foreshore has been affected by human intervention. For each area, the dataset, included a georeferenced multispectral image taken by the airborne DMC sensor, having four bands (blue, green, red, and infrared) with spatial resolution of 0.25m and a Digital Terrain Model (DTM) of 1m spatial resolution. The data were also accompanied by foreshore reference data, derived by manual photo – interpretation including coastline and the foreshore border towards the land (Figure 7).
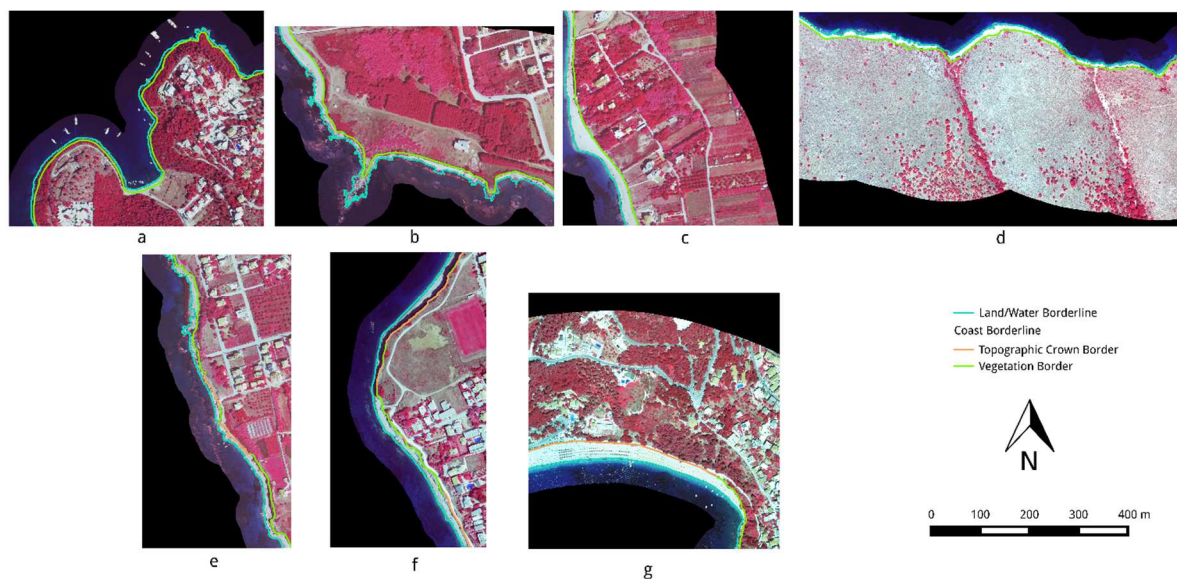
Figure 7: Overview of the examined areas. Foreshore in areas a – d is interpreted based on vegetation border criterion, while in areas e-g is interpreted based on vegetation and topographic crown border criteria.

3.3.2   Foreshore identification and evaluation of results

Due to the different spatial resolution of the multispectral imagery and the DTM, to eliminate possible noise, and compute larger homogeneous objects during the segmentation process (due to the local increase of pixel homogeneity), the multispectral imagery was smoothed by the AML algorithm. After extensive trial and error experimentation a 2000 scale was found appropriate for the AML.

To design an ontology-based identification strategy, two types of knowledge were investigated and represented: domain knowledge (such as land cover classes) and remote sensing knowledge (such as the indices required for class definitions). The exact classes, properties, and their interweaving in the ontology, were determined after three phases: the *specification*, *conceptualization*, and *knowledge formalization* (Paslaru et al. 2006, Brusa et al. 2006) as shown in the following sections.

3.3.3   Ontology Specification and Conceptualization

In the *specification phase* the main thematic categories required to be represented by the ontology were determined. Foreshore border delineation required the extraction of the area between the coastline and the foreshore border towards the land, a unified polygon called from now on *foreshore-area*. The foreshore border will be derived by intersecting the foreshore-area with the inland areas. Coastline identification required the determination of land and sea (e.g. Hannv et al. 2013). Identification of the Foreshore land-border based on the provided interpretation rules (Ktimatologio S.A. 2006) requires the following. From the *vegetation border criterion* definition, two components should be identified: the foreshore vegetation, and small sloped areas, close to the sea. From the definition of the *topographic*

43

crown border criterion, areas with large slopes, close to the sea should be identified as part of the foreshore.

In the *conceptualization phase*, the main classes were represented in an initial taxonomy. For each class a number of properties which could be employed in their definition were also examined. The classes within the taxonomy were organized to eliminate areas of no interest, leading to the desired thematic categories (Figure 8). The *Sea* and *Land* areas should be firstly identified. Afterwards, the vegetated areas (*Vegetation*) should be identified from the other (*Impervious*) areas. Given that the foreshore is composed by land and vegetated areas, the foreshore components should be derived as sub-classes of the *Vegetation* and *Impervious* classes. Thus, the *VegetationOfForeshore* and *InlandVegetation* should be defined as sub – classes/objects of *Vegetation.* Furthermore, the impervious land composing the foreshore-area can be separated into two types: areas with small slopes (*Vegetation Border* criterion) and areas with large slopes (*Topographic crown border* criterion). Thus, three classes, the *LandWithLowSlopeNearTheSea*, the *LandWithHighSlopeNearTheSea*, and *InlandImpervious* should be defined as sub – classes/objects of *Impervious* (Figure 8). The *Inland* areas should be composed by the areas classified as *InlandVegetation* and *InlandImpervious,* while the *ForeshoreArea* should be composed by the areas classified as *VegetationOfForeshore*, *LandWithHighSlopeNearTheSea*, and *LandWithLowSlopeNearTheSea*.

Land, Sea and *Vegetation* class definitions should involve spectral indices (e.g. NDWI and NDVI). *LandWithLowSlopeNearTheSea* and the *LandWithHighSlopeNearTheSea* definitions should involve the expression of slope gradient values and neighborhood relationships with the *Sea* or other *foreshore-area* components. Determination of the last line of vegetation towards the land, expressed in *VegetationOfForeshore* definition, should involve neighborhood relationships with the *LandWithLowSlopeNearTheSea* (Figure 8).
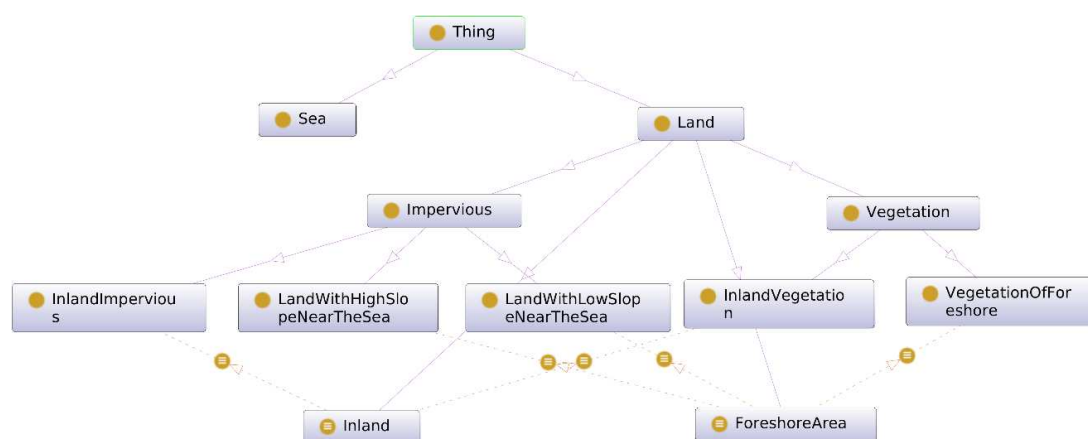
Figure 8: Conceptualization taxonomy indicating the part-whole hierarchy of the main components related to the foreshore extraction.

3.3.4 Formalization of the conceptual scheme

In the *knowledge formalization* stage, the abstract taxonomy developed in the *conceptualization phase* was transformed into a fuzzy OWL 2 ontology. While the taxonomy initially thought to specify the profound categories required for foreshore-area identification (Figure 8), a great number of additional classes needed to be invented and defined as intermediate concepts for knowledge representation in order to fill the semantic gaps intrinsic to the GEOBIA approach (Arvor et al. 2013, Blaschke et al. 2014). The semantic gap issue was taken care by an establish-and-refine-paradigm, and classes were conceived, represented, and formalized through a trial – and – error procedure where proper heuristics were developed for class definitions. Since class definitions in GEOBIA are derived as a result of hierarchical multiresolution segmentation and repeated classification based segmentations, they constitute an additional procedural semantic gap. During this process multiple segmentation levels were developed and tested, along with correlation plots of the feature values to determine proper features for the taxonomy.

Since a unique scale could not be determined to extract each foreshore component as a single object, the dataset was initially oversegmented to extract sub-objects of the foreshore components. Through proper classification-based fusions and classification refinement of the resulting fused objects through spatial reasoning the final foreshore components were derived. Thus, a multi – scale segmentation approach was investigated. In a bottom – up approach, finer objects were created on the lower levels while larger objects were created on the higher levels of the segmentation hierarchy. Segmentation was performed by the multi – resolution segmentation algorithm included in Trimble eCognition (Baatz and Schäpe, 2000). Segmentation results were exported from eCognition and imported into PostgreSQL to perform reasoning with SPOR (Argyridis and Argialas 2015). The segmentation hierarchy was represented within the ontology by developing a class representing the objects of each segmentation level. For example, the class *Level1* represented *Level 1* segmentation objects. To ease the reading of the ontology a notation was appended to the names of the thematic classes indicating the segmentation level of the class members. For example, the class *VegetationL2* represented *Level 2* objects, classified as vegetation. Details concerning the exact classes, properties, property formulas, and ranges of values employed in this study can be found in the following URL:

https://github.com/ArArgyridis/GEOBIA-Ontologies/blob/master/GEOBIA_foreshore.owl

Level 1 aimed to represent sub-objects of the spectral and topologic categories, related to foreshore-area components (sea, vegetation, and low/high sloping areas) on the lowest level of the hierarchy. Thus it was created with a small *scale* (*Scale = 5, Shape = 0.1, Compactness = 0.1*). Segmentation was performed on the four multispectral bands and the slope gradient.

45

Due to the orthorectification procedure, the imagery contained blank (empty) areas. Thus, classification began with the elimination of these areas and the classes *BlankSpaceL1* and *ImageSpaceL1* were developed. Initially the land and sea should be determined to identify the coastline. However, the *Sea* could not be determined only by spectral information since the water areas did not have adequate depth near the coast to absorb infrared radiation, allowing the extraction of sea-like areas only and later refine them as *Sea*. Thus, as sub-classes of *ImageSpaceL1* the classes *SeaLikeAreaL1* and *NotSeaLikeAreaL1* were defined (Figure 9.a). To avoid omission of sea areas, small values of the *slope* and *elevation* parameters were included in *SeaLikeAreaL1 definition*. For the determination of vegetated areas, the classes *VegetationL1* and *NotVegetationL1* were developed as sub-classes of *NotSeaLikeAreaL1* (Figure 9a). Medium values of the *NDVI* feature were examined and employed in *VegetationL1* definition.

(a)   (b)   (c)
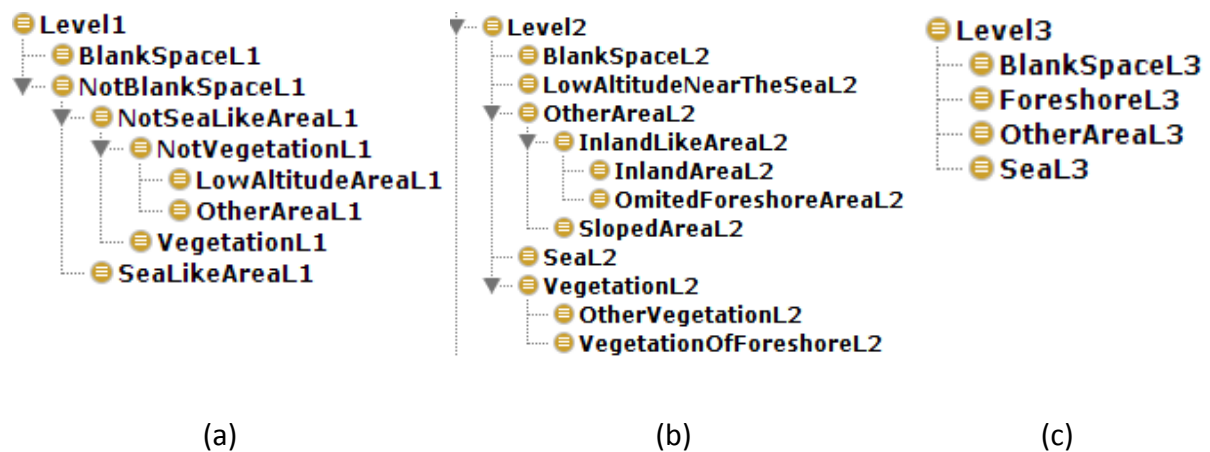
Figure 9. Final developed taxonomy for foreshore identification

Since the sea was not properly identified, *LandWithLowSlopeNearTheSea* (Figure 8) could not be properly identified as well. Thus, areas with smooth slopes were identified, which will be refined on an upper level. However, data examination showed that the *Vegetation border* criterion was not only applied in areas with small slopes, but in areas with larger slopes as well if the elevation was sufficient and the vegetation was the border between the foreshore and the main land. Thus, *NotVegetationL1* was refined into *LowAltitudeAreaL1* (determined by relative small values of the *mDem* property) and *OtherAreaL1* (Figure 9.a)*.

All imagery of the Hellenic foreshore mapping project, was acquired in a way to represent the sea as feature with large areal extents to properly determine the foreshore. Thus, to determine the *Sea* through GEOBIA, it was decided to take advantage of its spectral (e.g. absorption of infrared radiation) and geometric properties (large areal feature). Furthermore, refinement of *LowAltitudeAreaL1* into *LandWithLowSlopeNearTheSea* (Figure 8)*,* required the examination of these objects as a single unified object. To address these needs, *SeaLikeAreaL1*

46

and *LowAltitudeAreaL1* objects were spatially fused and a new level (*Level 2*) was created above *Level 1.*

The class *SeaL2* (Figure 9.b) was defined by projecting the objects classified as *SeaLikeAreaL1* on *Level* 2 and determining proper values for the *NDWI* and *area* features, as presented in Equation (7):

Class: SeaL2 EquivalentTo:

Level2

and (hasFuzzy_RS_0_1_RelativeAreaToSubObjects some SeaLikeAreaL1)

and (areaM2 some fuzzy_RS_800_1000)

and (mNdwi some fuzzy_RS_0.05_0.15)   (7)

This definition reads as follows: As SeaL2 were classified Level2 objects, covering SeaLikeAreaL1 objects by at least 50%, and had area greater than 900m^2, and had ndwi values greater than 0.1.

To separate the *LowAltitudeAreaL1* foreshore-area objects from other inland areas, since the foreshore has at the same time relative border with the sea, the inland areas, and the imagery borders, the relative border with the *SeaL2* can be no more than about 30%. This heuristic was represented with a left shoulder function having left border equal to 0.15 and a right border equal to 0.40. The final definition of the class *LowAltitudeAreaNearTheSeaL2* is presented as presented in Equation (8):

 Class: LowAltitudeAreaNearTheSeaL2 EquivalentTo:

Level2

and (hasFuzzy_RS_0_1_RelativeAreaToSubObjects some LowAltitudeAreaL1)

and (has_Fuzzy_RS_0.15_0.40_RelativeBorderTo some SeaL2)   (8)

This definition reads as follows: *As LowAltitudeAreaNearTheSeaL2 were classified Level2 objects, covering LowAltitudeAreaL1 objects by at least 50%, and having relative border with SeaL2 objects greater than 27.5%.*

Level2 vegetated areas were determined by projecting *VegetationL1* objects (*VegetationL2*). *Level2* objects not classified as either *LowAltitudeAreaNearTheSeaL2, SeaL2, or VegetationL2,* were classified as *OtherAreaL2*.

The foreshore-area defined by the *Topographic Crown border* criterion, consists on impervious areas with large slopes. To determine such areas, at first the classes *SlopedForeshoreLikeAreaL2* and *InlandLikeAreaL2* were defined as sub-classes of

OtherAreaL2. After experimentation, it was determined that *SlopedForeshoreLikeAreaL2* should be defined with the *mSlope* feature restricted by a right shoulder function with left border equal to 21.5 and right border equal to 23.5. All other areas were classified as *InlandLikeAreaL2*.

Due to the coastal configuration in some of the examined areas, objects of the foreshore, close to the sea, classified as *LowAltitudeAreaL1* at *Level 1*, were not classified as *LowAltitudeAreaNearTheSeaL2*. Thus, the classes *OmittedForeshoreAreaL2 and InlandAreaL2* were developed as subclasses of *InlandLikeAreaL2. OmittedForeshoreAreaL2* definition was determined to involve the spatial relationship with the *LowAltitudeAreaL1* and a search buffer beginning at the border of *SeaL2* objects. A search distance of 4 to 5 meters was found appropriate after experimentation. Thus, the class *OmittedForeshoreAreaL2* was developed as sub-class of *OtherAreaL2*, and defined as presented in Equation (9):

Class: OmittedForeshoreAreaL2 EquivalentTo:

    InlandLikeAreaL2

    and (hasFuzzy_RS_0_1_RelativeAreaToSubObjects some LowAltitudeAreaL1)

    and (has_Fuzzy_LS_4_5_DistanceToExterior some SeaL2)   (9)

This definition reads as follows: *As OmittedForeshoreAreaL2 were classified InlandLikeAreaL2 objects covering LowAltitudeAreaL1 objects by at least 50%, with less than 4.5m distance from SeaL2 objects*. All other objects were classified as *InlandAreaL2*.

Foreshore-area vegetation (*VegetationOfForeshore* – Figure 8) had two components: the vegetation having relative border with (i) the smooth sloped area of the foreshore and (ii) the sea (*Vegetation border criterion*). The tree trunk position was estimated by an ideal tree with a 5.5m crown diameter. The tree trunk should reside near the center of the tree. These heuristics were included in the definition of the class *VegetationOfForeshoreL2*, as presented in Equation (10):

Class: VegetationOfForeshoreL2 EquivalentTo:

    VegetationL2

    ((has_Fuzzy_TRP_0_0.01_2.5_3.0_DistanceToExterior   some LowAltitudeNearTheSeaL2)

    or   (has_Fuzzy_TRP_0_0.01_2.5_3.0_DistanceToExterior   some OmittedForeshoreAreaL2)

    or (has_Fuzzy_TRP_0_0.01_2.5_3.0_DistanceToExterior some SeaL2))   (10)

This definition reads as follows: *As VegetationOfForeshoreL2 were classified the objects having a distance between 0 and 2.75m from the areas classified as LowAltitudeNearTheSeaL2, or OmittedForeshoreAreaL2, or SeaL2.*

To define the final foreshore-area components the expression of spatial relationships of unified objects was required. Thus, the objects classified as *OmittedForeshoreAreaL2*, *InlandAreaL2*, *OtherVegetationL2*, *SlopedAreaL2* and *VegetationOfForeshoreL2* were spatially merged and a new level (*Level 3*) was created above *Level 2*. On *Level 3* the classes *ForeshoreL3, InlandAreaL3* and *SeaL3* (Figure 9.c) were created.

SeaL3 objects were determined by projecting *SeaL2* objects onto *Level 3*. For *ForeshoreL3* class definition the spatial relations between all the candidate components were examined as shown in the definition presented in Equation (11). The fuzzy function borders were determined after sufficient experimentation.

Class: ForeshoreL3 EquivalentTo:

Level3

    and (((hasFuzzy_RS_0_1_RelativeAreaToSubObjects some SlopedAreaL2)

       and (has_Fuzzy_RS_0.09_0.11_RelativeBorderTo some ForeshoreL3))

       or ((has_Fuzzy_LS_0_0.2_RelativeBorder some BlankSpaceL3)

        and (has_Fuzzy_RS_0.7_0.8_RelativeBorder some ForeshoreL3))

       or   (hasFuzzy_RS_0_1_RelativeAreaToSubObjects   some OmittedForeshoreAreaL2)

       or   (hasFuzzy_RS_0_1_RelativeAreaToSubObjects   some VegetationOfForeshoreL2)

       or (has_Fuzzy_RS_0.7_0.8_RelativeBorder some ForeshoreL3))

    and (has_Fuzzy_LS_0.90_0.95_RelativeBorder some SeaL3)   (11)

Determination of *ForeshoreL3* objects required multiple classification iterations. In each iteration additional *Level3* objects were classified as *ForeshoreL3*. Classification stopped when no other objects could be added in the current iteration step. Thus, in the first classification step, as *ForeshoreL3* were assigned objects:

- Having at most 92.5% relative border with *SeaL3* objects since the foreshore-area has a large relative border with the sea, or

- Objects classified as *OmittedForeshoreAreaL2* or

- Objects classified as *VegetationOfForeshoreL2*.

- In the following classification steps, an object was classified as foreshore if:

- It had large slopes (classified as *SlopedAreaL2*) and relative border (which after experimentation was determined to be more than 10%) with areas previously classified as *ForeshoreL3*, or

- It was mostly surrounded by other *ForeshoreL3* objects, thus it had greater than 75% relative border with objects previously classified as *ForeshoreL3*, or

- To eliminate a commission error, created by some objects existing between the sea and the imagery blank-space, an object was classified as *ForeshoreL3* if it had less than 10% relative border with *BlankSpaceL3* objects (thus avoiding omitting objects which touched on a small percentage the imagery blank-space) and also had greater than 75% border with objects previously classified as *ForeshoreL3*.

3.4   Evaluation of results

Figure 10 presents the results of *Level 3* classification for all areas of interest, accompanied by the reference data. It is observed that both the foreshore border and the coastline is satisfactory determined by the developed method. Omissions were related with the determination of the coastline, as in area b where part of the coastline is composed by rocks with low elevation, and were not identified as land by the ontology. Furthermore, omissions were observed and in the foreshore border towards the land, as in area d where bare ground belonging to the foreshore was not adequately identified. Furthermore, commission errors were observed due to the definition of the vegetation border criterion. In cases where the present vegetation had a smaller crown than the one considered, (as in areas *a* and *b*) part of the vegetation near the sea which should not be committed to the foreshore, was considered as such.
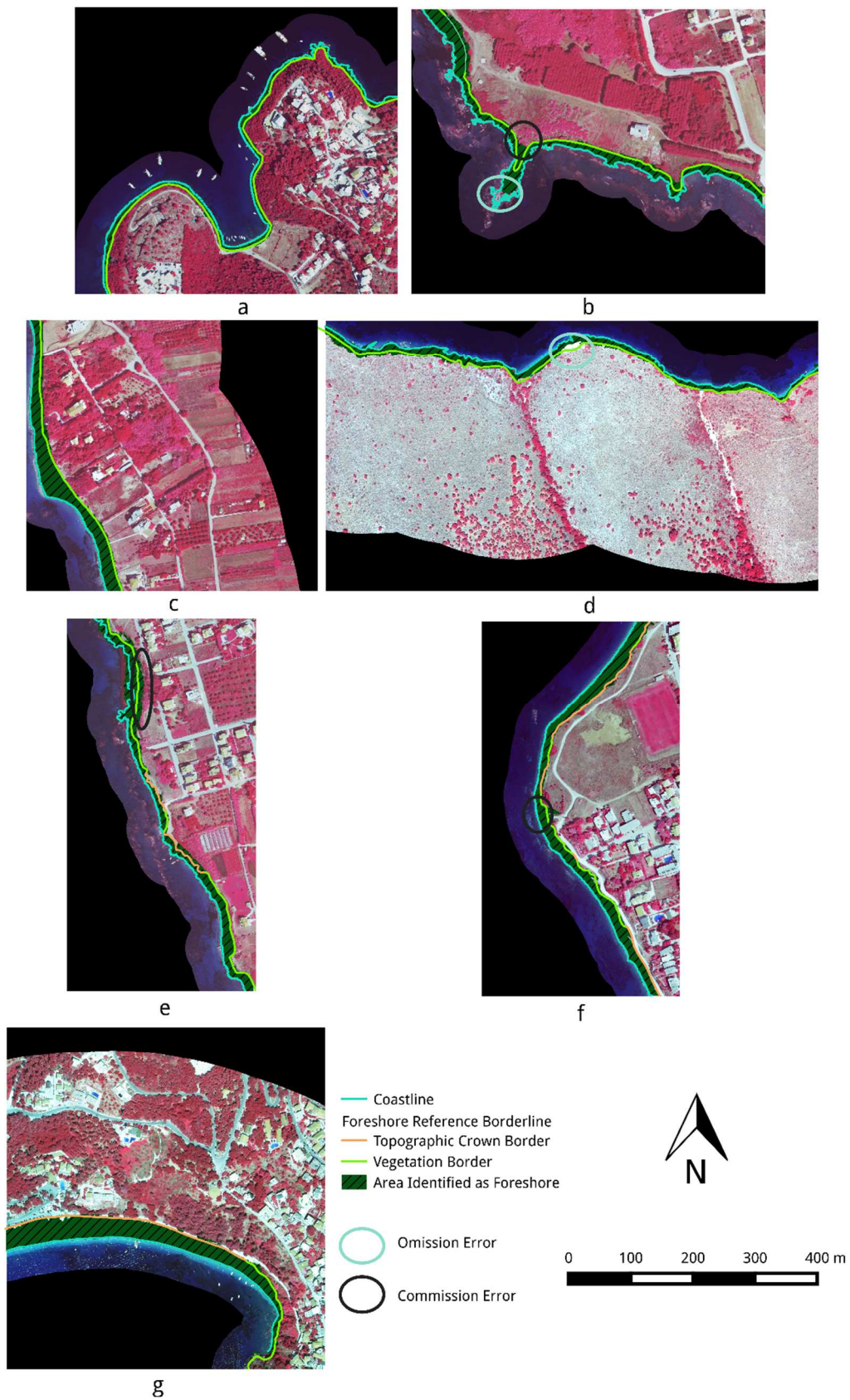
Figure 10: Final classification result for all test areas.

Classification results were compared with the reference data as follows. At first the entire foreshore-area was compared with the reference data which were converted into a unified polygon. Afterwards, the foreshore border was extracted as a line by intersecting *ForeshoreL3* with *InlandAreaL3* objects and was compared with the reference data.

To evaluate the *foreshore area* accuracy, the areas correctly detected (True Positive – TP), omitted (False Negative – FN) or committed (False Positive – FP) were computed. Afterwards, based on these areas the Completeness, Correctness and Quality indices (Equations (4)-(6)) were computed (Agouris et al. 2004), and the results are presented on Table 3. It is observed that large results were achieved for all measures. The lowest completeness and quality were scored for area *a* (80.6% and 67.6%) while the lowest correctness was scored for area *e* (75.1%), which was considered satisfactory.

Table 3: Area-based quantitative evaluation of the extracted foreshore-area and the reference data.

Area	Completeness (%)	Correctness (%)	Quality (%)
a	80.6	80.7	67.6
b	88.8	82.4	74.7
c	84.4	92.0	78.6
d	86.2	80.9	71.3
e	88.9	75.1	68.6
f	92.3	90.6	84.2
g	95.6	95.5	91.5
Overall	**88.9**	**86.4**	**77.9**

To assess the distance between the identified foreshore border and the reference data, the mean error (ME) and the root mean square error (RSME) were computed as shown in Equations (12) and (13), between each point of the extracted and the reference lines.

$$ME = \frac{\sum_{i=1}^{n} di}{n} \tag{12}$$

$$RMSE = \sqrt{\frac{\sum_{i=1}^{n}(d_i - ME)^2}{n-1}} \tag{13}$$

The results of this evaluation is presented in Table 4. It is observed that overall the extracted foreshore border falls within 2.4m from the interpreted foreshore borderline with a mean square error of 3.2m. This is considered satisfactory by considering the issues depicted previously, along with the fact that the foreshore does not have precise physical borders like man-made objects and its delineation is based on abstract interpretation criteria where the decision and experience of the interpreter affects the final result.

Table 4: Evaluation of the foreshore border, by computing the distance of the extracted foreshore border with the reference data.

Area	a	b	c	d	e	f	g	overall
ME (m)	1.34	3.28	2.40	2.32	4.40	2.25	2.02	**2.44**
RSME (m)	2.66	5.60	1.97	2.02	3.10	3.13	1.80	**3.17**

3.5 Discussion of Results

In this study an ontology – based, multi – scale GEOBIA approach was investigated and developed towards the automatic identification of the foreshore area. At first, the multispectral imagery was filtered by the AML, which smoothed the imagery and preserved the borders of the foreshore components at the same time. During experimentation an effort was attempted to filter the DTM with the AML, but the derived slopes from the filtered DEM were significantly affected and thus it was avoided. To identify foreshore components based on the *vegetation border* and *topographic crown border* criteria three segmentation levels of analysis were developed. Through the development of a three-level ontology hierarchy, the foreshore interpretation guidelines provided by Ktimatologio S.A. (2006) were explicitly represented, formalized, and employed in the GEOBIA identification process through the development of proper heuristics.

Sea identification (Figure 8), required the extraction of sea-like areas on *Level 1*, their spatial merging, and their spectral and geometric refinement on *Level 2*. The *LandWithLowSlopeNearTheSea* was determined by fusing objects with small elevation detected on *Level 1* and considering their spatial relationship (relative border) with the *Sea*. The controversy between the class name in the conceptualization phase (*LandWithLowSlopeNearTheSea*) and the properties involved in the final definition (*altitude / relative border with the sea*) is due to the semantic gap introduced by the interpretation criteria and specifically the *vegetation border* criterion. In its definition the *vegetation border criterion* is applied in areas with small slopes near the sea, however in practice it is applied in areas with low altitude near the sea.

As *VegetationOfForeshore* objects (Figure 8) were identified the vegetated areas having distance from the *Sea* or from the *LandWithLowSlopeNearTheSea* less than 2.75m. If Digital Surface Model data were available instead of DTM, in cases of trees or shrubs, one could determine the crown and estimate the tree trunk position by considering the medial axes of the crown which is parallel to the coastline. Finally, the *LandWithHighSlopeNearTheSea* (Figure 8) was determined by considering large values of the slope property derived from the *DTM*.

The final foreshore-area was determined on *Level 3,* through spatial merging and representation of foreshore spatial relationships with the remaining land cover. Visual examination of the results showed that the coastline and the foreshore border provided in

the reference data were close to those extracted by the developed method. Only in area *b* the extracted coastline was differentiated significantly from the reference coastline (Figure 9). Due to the existence of rocks near the sea with near to zero elevation and slope in the provided DTM this area was classified as sea by the developed method, however in the provided reference data it belonged to the land.

Omission and commission errors of the foreshore area were mostly related with the exact interpretation of the shoreline and the estimation of the tree trunk position (which also affected the identification of the foreshore border) by the interpreter. These differences however were generally acceptable. The largest commission error caused by this effect was observed in area *e*, where the foreshore was interpreted based on the *vegetation border* criterion on very sparse vegetation near the sea, which was not captured by the ontology, since the NDVI values of the representing objects were not adequate.

Evaluation of the foreshore area showed that, the lowest *completeness* was 80.6% in area *a*, while a total score of 88.9% was achieved for all areas (Table 3), thus the majority of the foreshore area was correctly determined. The lowest achieved *correctness* was 75.1% for area *e* with a total score of 86.4% for all areas (Table 3), indicating that the extracted foreshore area was satisfactorily not confused with other land cover. Finally, the lowest quality index was 67.6% for area *f* with a total of 77.9% for all areas, indicating that the result was overall satisfactory.

Evaluation of the distance of the foreshore border from the reference data (Table 4) showed that an overall ME of 2.4m and an overall RSME of 3.2 was achieved. Thus, the identified foreshore border by the algorithm was satisfactory close with the reference data. In area e the worst ME (4.4) and in area b the worst RSME (5.6) were scored. This can be correlated with the low quality values achieved from the foreshore area evaluation for these areas, due to the commission errors which were related with the exact position of the foreshore border.

3.6 Conclusions and Future Perspectives

Automatic foreshore delineation, by proper knowledge representation of interpretation criteria is feasible through a GEOBIA multi-scale approach and fuzzy ontology-based reasoning. GEOBIA offers the capability of expressing spatial relationships aiding in the identification process. Ontological formalization standardized the implicit interpretation knowledge into an explicit computer-conceivable form which can be at the same time interpreted and enhanced by humans. Thus, it contributed to reduce the semantic gap between the implicit interpretation knowledge and the developed formalization.

Evaluation of the developed approach was satisfactory, since the majority of the foreshore area was accurately mapped. Comparison of the automatically extracted foreshore border with the reference one was also satisfactory, since both fall within close distance. Apart from

the omission and commission errors which depend on the developed methodology, differences between the automatically extracted and the human interpreted borderlines are related with the fact that the foreshore does not have strong physical borders like man-made objects, making its border rather fuzzy and open to heuristic interpretation decisions.

Considering foreshore mapping, it would be desirable to examine and formalize additional criteria for foreshore interpretation which consider complex thematic categories such as building area density near the sea, present infrastructure such as breakwaters etc. Furthermore, towards the identification of the true foreshore area, one could examine tidal models to estimate the position of the *mean low water limit* as the borderline of the foreshore towards the sea. Finally machine learning approaches such as deep learning or the consideration of additional data such as those provided by crowdsourcing technologies could be also examined for foreshore mapping.

Acknowledgments

4 Integration of Deep Belief Networks with Fuzzy Ontologies to perform Building Change Detection through Multi-Scale GEOBIA Analysis

4.1 Introduction

Urban environments are dynamic and complex, evolve over time and constitute the key elements for currently emerging environmental and engineering applications in global, regional, and local spatial scales (Wurm et al. 2011). The necessity for monitoring urban growth is now more intense than ever, especially in developing countries such as Greece. The existence of informal settlements leads to lower revenues for the government, additional investments to create and develop the necessary infrastructure, high expenses to restrict and repair the environmental damage and lack of public acceptance (Ioannidis et al. 2009). Urban environment is covered with urban green, various types of buildings, roads and other settlements. Due to the complexity of the urban environment, mapping of urban elements and their changes can be tedious and time-consuming. To this end, automatic or computer-assisted methods are desirable in terms of economy and efficiency (Bouziani et al. 2010, Argialas et al. 2013, Karantzalos 2015).

To capture the spectral, geometric and spatial relationships of the urban elements, a pixel-based method is not promising; instead, it is required unfolding of the structure, of objects at various scales, involving properties of objects and spatial relations among them (Argialas and Harlow 1990, Blaschke et al. 2014). These capabilities are offered by frameworks based on GEographic Object-Based Image Analysis (GEOBIA), thus it was determined that a GEOBIA approach will be developed.

Urban mapping has been studied in remote sensing, computer vision, and geography scientific communities (Karantzalos 2015). Already GEOBIA change detection studies were conducted in the urban environment. Bouziani et al. (2010) detected changes by comparing a very high spatial resolution imagery with an existing urban geodatabase. Brunner et al. (2010) developed a methodology for building damage assessment after earthquakes. Doxani et al. (2012) detected urban changes based on the Multivariate Alteration Detector (MAD) from IKONOS and QuickBird imagery. Initially the images were filtered through scale-space filtering and MAD components were computed. Afterwards, the imagery was segmented, with chessboard segmentation and a rule-based classification was designed to compute a first estimation of the possible changes from the MAD components. Finally, another level was designed above Level 1 through multiresolution segmentation and a knowledge-based rule set was designed to detect the changes. Hebel et al. (2013) detected changes in urban areas from multi-view Advanced Laser Scanner data. In the work by Karantzalos (2015) a detailed review of the advances in urban change detection methodologies was presented.

Bannour and Hudelot (2014) interweaved machine learning, and specifically Support Vector Machine classification, with ontological refinement. However, there still remains the need to examine the applicability of such approach in GEOBIA and specifically in building change detection. Thus, state-of-the-art Deep Learning methods were examined, which are machine-learning algorithms aiming to model high-level abstractions in data by using model architectures composed of multiple non-linear transformations (Deng and Yu 2014). Such algorithm is the Deep Belief Network, (DBN) which was already applied in image analysis (Hinton and Salakhutdinov 2006, Mnih and Hinton 2010, Wang et al. 2014). Thus DBN was integrated with fuzzy ontologies. Fuzzy OWL 2 was enhanced to include machine learning algorithms within class restrictions. To perform the reasoning process the DBN algorithm was integrated with SPOR, enabling the assignment of objects to classes with fuzzy properties, DBN, or by their combination. This was tested by the development of a building change detection method through multi-scale analysis. Since auxiliary data such as building geodatabases or 3D information such as a Digital Surface Model (DSM) were unavailable, the developed approach was designed to detect changes in buildings by strictly employing multitemporal satellite imagery.

4.2 Methods

4.2.1 Morphological Levelings

Morphological levelings are employed to construct nonlinear scale space image representations (Meyer and Maragos 2000, Meyer 2004, Karantzalos et al. 2007). Levelings are transformations $\Lambda(f, h)$ where a marker h is transformed to an image g, which is a leveling of the reference image f (Karantzalos et al. 2007). In places where {h < f}, h is increased as little as possible until a flat zone is created or the image g reaches the reference image f. In places where {h > f}, h is decreased as little as possible until a flat zone is created or image g reaches the reference image f. This makes image g to be flat on {g < f} and {g > f} and the procedure continues until convergence. The markers employed in the transformation can be sampled by Gaussian scale-space. By performing the leveling transformation with multiple markers of different scales one can produce a multiscale representation. To preserve building edges, it was decided to smooth the imagery with the Anisotropic Morphological Leveling (AML) as stated by Karantzalos and Argialas (2006). AML was designed to smooth small differences in reflectance values in a direction parallel to image object edges, while preserving major edges.

4.2.2 Deep Belief Network

A DBN is a deep neural network composed of multiple layers of hidden units. When trained in an unsupervised way (by training multiple Restricted Boltzmann Machines – RBM) a DBN can learn to probabilistically reconstruct its inputs (generative model). Afterwards, the layers act as feature detectors on inputs, allowing to be further trained in a supervised way to perform classification (Hinton et al. 2006, Bengio et al. 2007).

An RBM is an undirected graphical model having a visible layer representing the observable data (V) and a hidden layer (H) that learn to represent features that capture higher-order correlations in the data, by modeling the distribution of the provided training set (P(v)). V can have Boolean or continuous values, while H are Boolean. A weight matrix (W) is associated with the connections between V and H, along with bias weights a, b for both V and H respectively. In RBM hidden to hidden or visible to visible connections are not permitted, allowing training with the gradient-based contrastive divergence algorithm. The training process maximizes the expected log probability presented in Equation (14) of the training set V, by optimizing the weight factor W (Bengio et al. 2007, Hinton 2009).

$$\arg\max_W E\left[\sum_{v\hat{I}V}\text{Log}P(v)\right]$$

(14)

with P(v) computed as in Equation (15):

$$P(v) = \exp(a^T v + \sum_{j=1}^{H_v}\log\left(1+\exp\left(b_j + W_j v\right)\right)/Z$$

(15)

Where Z is a normalization constant for this distribution. The following steps describe the contrastive divergence (CD) for Boolean V.

1. A number of training samples k is provided as input. Let the size of H be h, the size of V be v and i a training sample.

2. The conditional probability (mean activation) of H, given the values of V is computed (σ: logistic sigmoid function):

$$H[\ 1{:}h,\ i\hat{I}[1,k]\ ] = \sigma\left(b + P[1{:}h, i]\right), \text{ where } P = WV$$

(16)

3. A sample of the hidden units (H_s) is computed based on H from a binomial distribution.

4. The conditional probability of V given H (V') is computed:

$$V'[\ 1{:}v,\ i\hat{I}[1,k]\ ] = \sigma\left(a + L[1{:}v, i]\right), \text{ where } L = W^T H_s$$

(17)

5. A sample of the visible units (V'_s) is computed based on V' from a binomial distribution.

6. Steps 2-5 are repeated for k times (Gibbs sampling – Figure 11). In each iteration, V'_s is provided as input to compute H'.

7. The weight W along with the biases a, b are updated (e: learning rate) as in Equations (5-7):

$$W = W + e\left(H\,V^T - H'V'_s{}^T\right) \tag{18}$$

$$a = a + \frac{e}{k}\sum_{i=1}^{k} N[1{:}v,\,i],\ \text{where } N = V{-}V'_s \tag{19}$$

$$b = b + \frac{e}{k}\sum_{i=1}^{k} R[1{:}h,\,i],\ \text{where } R = H{-}H' \tag{20}$$

8. Steps 1-7 are repeated for a number of epochs. In each epoch the learning rate is underestimated by a coefficient c (e'=ec).
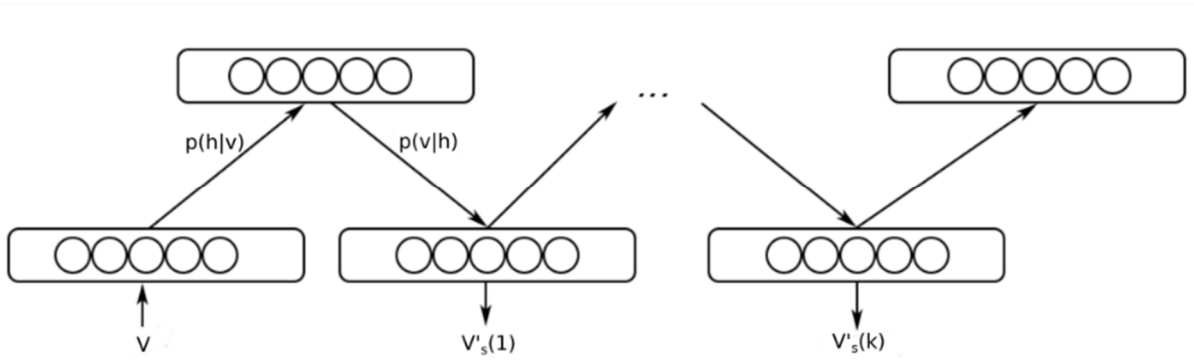
Figure 11. Gibbs sampling process (adopted from Hinton et al. 2006).

If the visible layer contains continuous values (Bengio et al. 2007) then the input values are scaled in the interval [0, 1]. Afterwards, in step 4, the conditional probability is computed as follows:

$$V'[\,1{:}v,\,\hat{\imath}[1,k]\,] = \frac{1}{1-\exp(-a-L[1{:}v,\,i])} - \frac{1}{\exp(a+L[1{:}v,\,i])} \tag{21}$$

In step 5, V'$_s$ is sampled from a uniform distribution.

To improve RBM training, Tieleman (2008) enhanced CD. In persistent contrastive divergence (PCD), the Gibbs sampling process is initiated from the sample (V's) computed in step 5 of the previous loop.

DBN training begins by treating the first two layers (v and h1) as an RBM (Figure 12). After training with PCD, from h1 a representation of the input is computed and is provided as input for the second layer which is also trained as an RBM. This process is repeated until all hidden layers are trained (Hinton et al. 2006, Bengio et al. 2007).
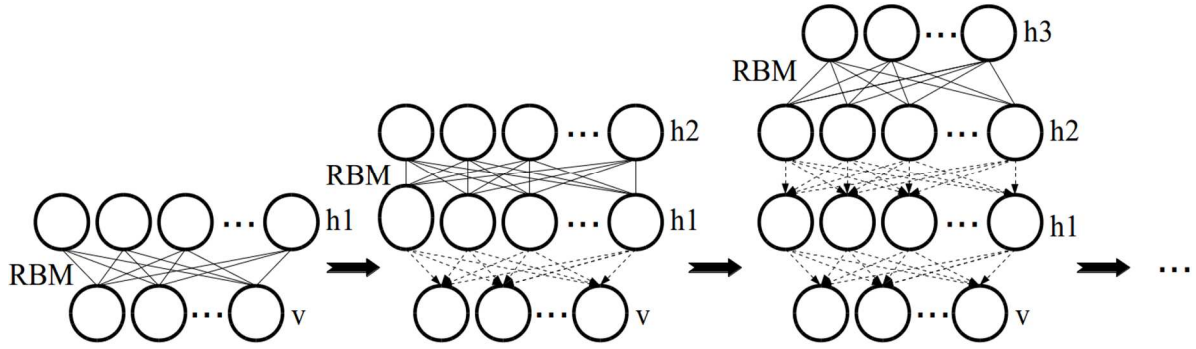
Figure 12. DBN layer-wise training process. v is the input vector, while hi are DBN hidden layers. In each training iteration one DBN layer is considered as a hidden RBM layer. DBN arrows indicate the direction of the generative model (adopted from Wang et al. 2014).

Supervised fine-tuning was performed by Logistic Regression, a probabilistic, statistical classifier. Its parameters are a weight matrix W and a bias vector b. Classification is performed by projecting an input vector onto a set of hyperplanes, each of which corresponds to a class. As input is provided the sample computed from the mean activation of the last DBN hidden layer. The distance of an input to a hyperplane reflects the probability to be member of the corresponding class (Bishop 2006). The probability being an input vector x a member of a class i is computed by Equation (22):

$$P\left(Y=i\middle|x,W,b\right)=\text{softmax}_i\left(Wx+b\right)=\frac{e^{w_i x+b_i}}{\sum e^{w_j x+b_j}} \tag{22}$$

Learning the parameters W, b involves the minimization of a cost function. For multi-class regression the negative log likelihood was chosen as a loss function. Cost minimization is achieved through stochastic gradient decent, thus W is computed through multiple iterations with respect to a learning rate.

4.3   Representation of DBN in ontologies and integration with SPOR

In the following the integration of DBN with SPOR will be presented. Classes involved in a DBN classification were declared by including proper restrictions in class definitions. Conceiving the result of the DBN classification as a table having the probability of each segment to be an object of each class, and considering that *datatypes* in OWL 2 define sets of data values, it was decided that such restrictions should be developed as *Data property restrictions*, called *Machine Learning Data Property Restrictions*. Thus, a proper *datatype* was designed, called *Machine Learning Datatype* (MLD). An AP attached to the MLD was designed to encode DBN training parameters, called *machineLearningLabel*. Training parameters were encoded through XML Syntax. Table 5 presents a summary of the parameters related to DBN training along with a brief description, and the values employed in this study which were derived after extensive experimentation. The size of a DBN visible layer is determined by the number of the input features, while the number of the classes involved in supervised training by the number

60

of the class definitions an MLD was included. In this study, in each DBN only the input features were modified to represent the desired properties of the involved classes.

To include certain classes in the same DBN classification the same machine learning restriction was added in their definition. Thus, Equations (23)-(25) involve the classes, *WhiteSurface20062011*, *CeramicSurface20062011*, and *PossibleChangeL1* in the same DBN. DBN parameters (Table 5) are encoded as in Equation (26). Thus dbn1 has four (4) input features and three (3) output classes.

Class: WhiteSurface20062011   EquivalentTo:

    OtherAreaL1

    and (machineLearningFeature some dbn1)   (23)

Class: CeramicSurface20062011 EquivalentTo:

    OtherAreaL1

    and (machineLearningFeature some dbn1)   (24)

Class: PossibleChangeL1   EquivalentTo:

    OtherAreaL1

    and (((not (CeramicSurface20062011))

    and (not (WhiteSurface20062011)))

    or (machineLearningFeature some dbn1))   (25)

Table 5. DBN training parameters.

Parameter Name (XML attribute name)	Description	Example value
Input features (feature_space)	Features employed in DBN training and classification process.	"whiteIndex2006,whiteIndex2011,ceramicIndex2006,ceramicIndex2011"
Number of layers and number of units per layer (network)	Number and size of the hidden layers of the DBN.	170-170
Unsupervised Learning rate (learning_rate)	learning rate employed for RBM training	0.0001
Unsupervised Learning coefficient (learning_coef)	Degree of underestimation of the RBM learning rate in each iteration	0.95
Unsupervised number of epochs (epochs)	Number of iterations of the contrastive divergence	2000
Number of Gibbs sampling iterations (k)	Number of Gibbs sampling iterations in each epoch	3
Supervised learning rate (supervised_lr)	Learning rate employed by logistic regression	0.7
Supervised learning rate coefficient (supervised_coef)	Degree of underestimation of the logistic regression learning rate in each iteration	0.95
Supervised number of epochs (supervised_epochs)	Number of iterations for logistic regression training	2000

```
<method type="DBN">
   <properties       feature_space       =       "whiteIndex2006,whiteIndex2011,
ceramicIndex2006,ceramicIndex2011"   network="170-170"   learning_rate   =
"0.0001" learning_coef = "0.95" epochs = "2000" k = "3" supervised_lr = "0.7"
supervised_coef = "0.95" supervised_epochs = "2000"/>
</method>
```
(26)

To classify groups of classes with different DBNs, multiple MLDs were designed and the proper machine learning restrictions were included within their definitions. Training samples were represented as *OWL 2 Individuals*. To match the sample-individual with the segment in PostgreSQL, each *Individual* contained an *id Data Property* representing the id of the segment in PostgreSQL table. The samples were collected through Quantum GIS (QGIS Development Team 2014).

To integrate DBN within SPOR, the reasoning process was performed as follows. To determine the MV of each segment with all the classes, SPOR iterates over the classes defined in the ontology (Figure 13). As OWL 2 does not provide information regarding the hierarchy depth of the examined class, the classes are examined in alphabetical order. At first the reasoner iterates over the referenced classes in class definition (e.g. parent, spatially-related, or

appearing in a logical operation). If MVs of the segments for these classes have not as yet been computed, then the reasoner tries to compute their MVs.
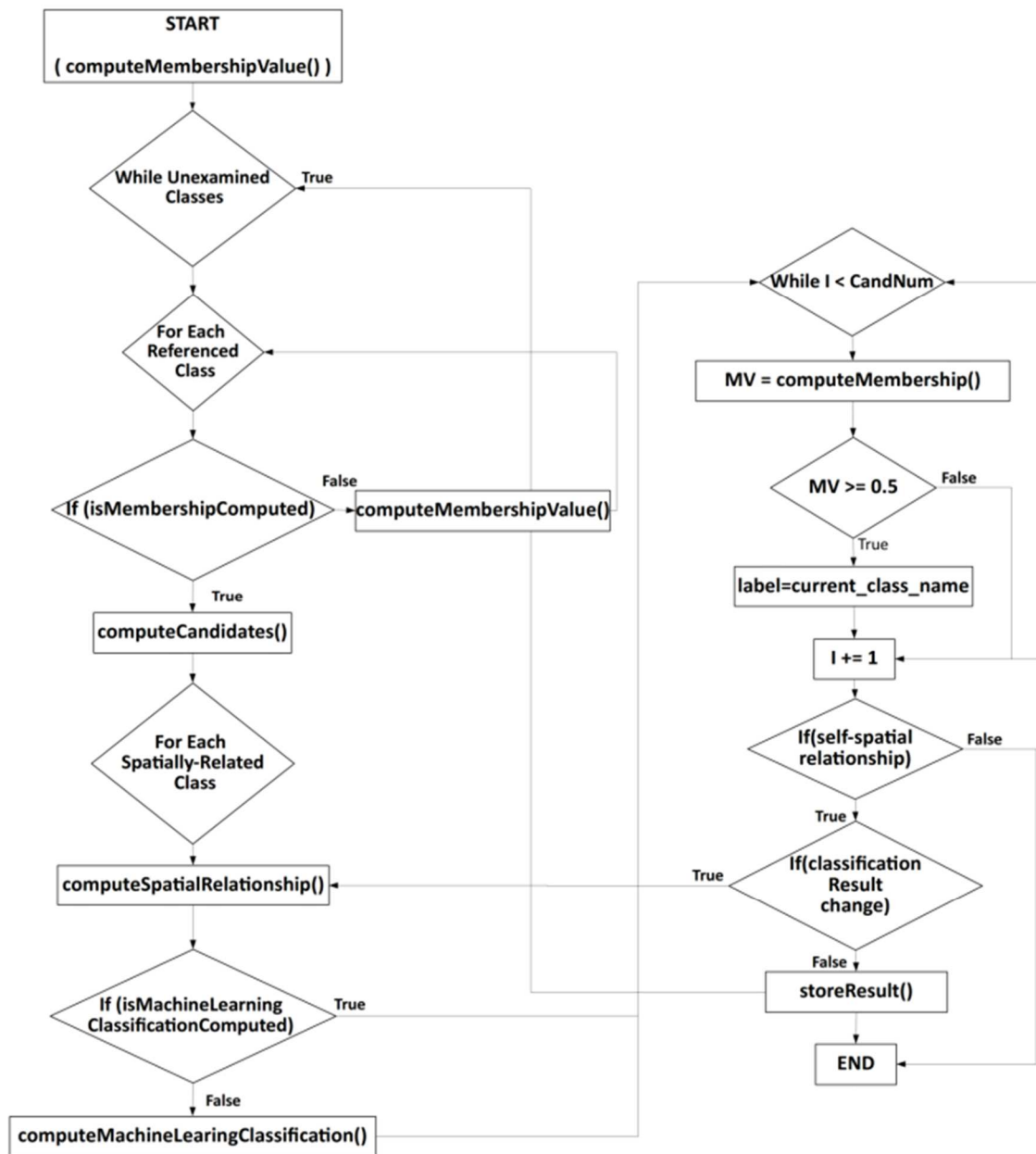
Figure 13. SPOR reasoning process after DBN integration

As candidates for the currently examined class, are considered objects having MV greater than 0.5 for all parent classes (*computeCandidates()*). Afterwards the spatial relationships are computed (*computeSpatialRelationship()*). If the class has a spatial relationship with herself, then multiple classification iterations are performed. In the first iteration the spatial relationship is ignored. In the next iteration, the objects classified in the examined class are considered to compute the spatial relationship. This is repeated until the classification result

is not altered between two iterations. If the class is involved in a DBN classification, the probability of each candidate segment to belong to the class is computed through DBN classification.

From the examined class definition, a node graph is created (*computeMembership()*). Each node can represent a class, a feature node (fuzzy *Data* or *Object property restriction*) or a logical operator (*and*, *or*, *not*). For each candidate segment the MV is computed (Figure 14).
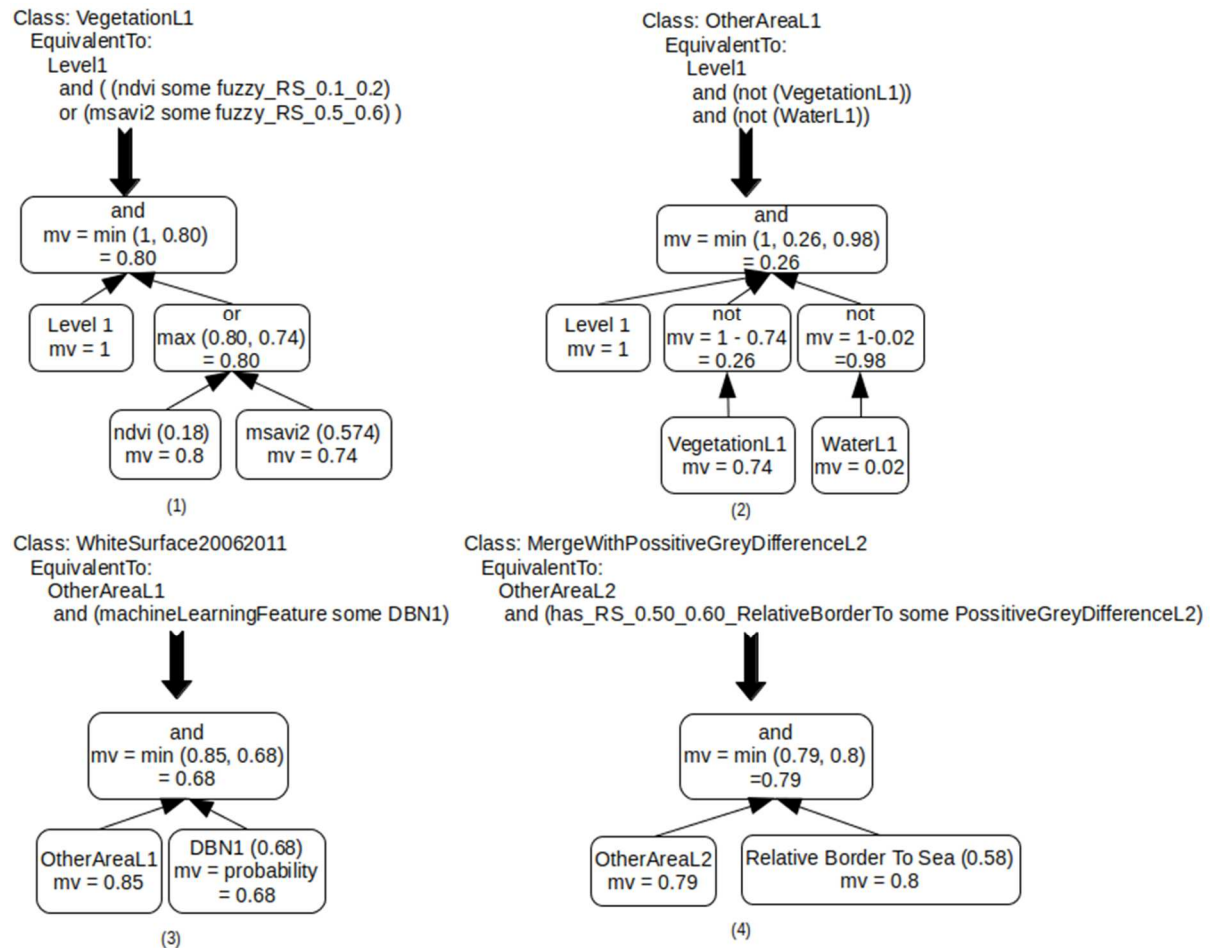
Figure 14. Examples of segment membership values computation based on OWL 2 fuzzy restrictions.

If it is a class node, then the MV of the current candidate with the referenced class is set as node value. If it is a feature node, then the MV of the current candidate is computed, based on its feature value and the fuzzy operator determined by the ontology. If the *data property restriction* refers to a DBN, then DBN probabilities are converted into MVs as in Equation (27) (Figure 14.3):

$$MV = x \text{ (x: DBN probability)} \qquad (27)$$

If it is a logical operator node, then at first the MVs of the sub-nodes are computed. Afterwards, based on Zadeh semantics (Zadeh 1965) the logical node MV is computed.

Computation stops when the MV of the top node is computed. If the final MV is greater than 0.5, then the class name of the currently examined class is assigned as label to the candidate.

4.4 Buildings change detection through DBN and ontologies

4.4.1 Study area and data used

To perform change detection in building infrastructure in the sub urban area of east Attica, Greece, between 2006 and 2011, three study areas were examined. For each area data included one QuickBird image taken in 2006 and one WorldView 2 (WV2) image taken in 2011. Figure 15 presents an overview of the three study areas. Prior to the extraction process the imagery was atmospherically corrected and georeferenced by rational functions.

4.5 Change detection and evaluation of results

To eliminate noise and lessen the undesired spatial detail, the imagery was filtered through the AML algorithm. After experimentation, a scale of 1000 was found appropriate to smooth the imagery. In the sub-images presented in Figure 16, it is observed that areas related to the building rooftops (denoted with B) and the vegetation (denoted with V) were smoothed, while their major edges were preserved.
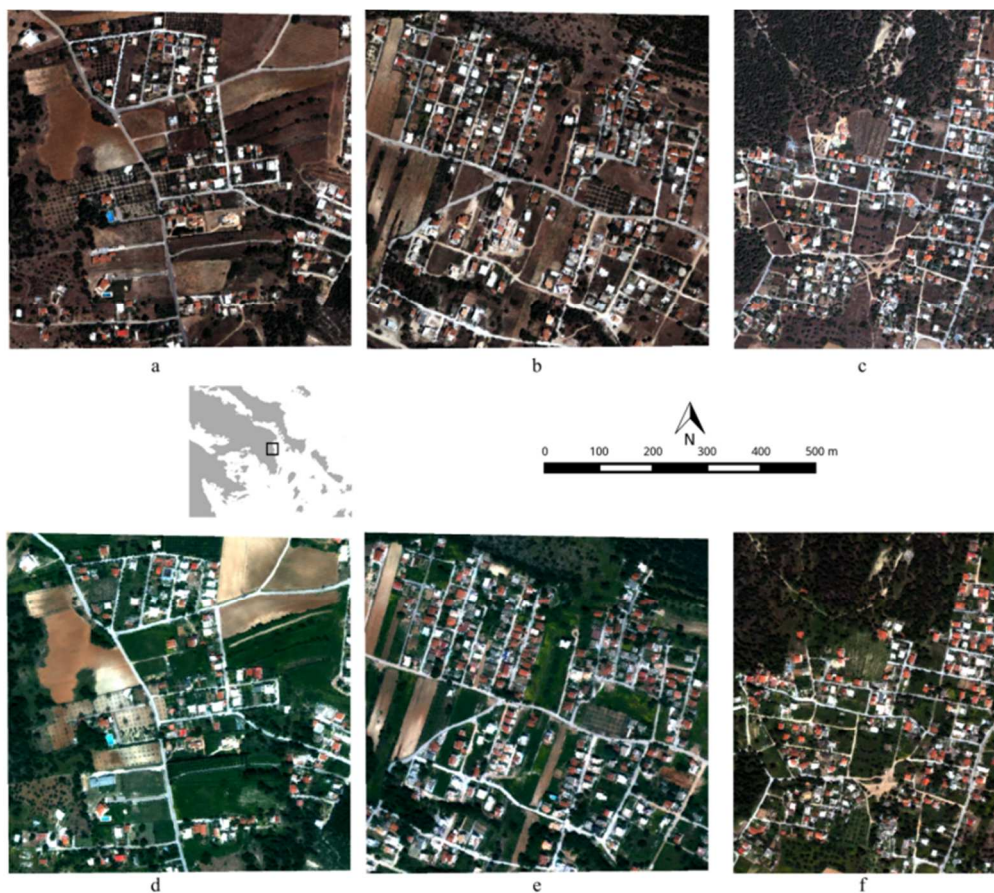
Figure 15. Overview of the study area. a-c: Quickbird imagery taken in 2006. d-f WV2 Imagery taken in 2011. Left: Imagery of area 1, middle: Imagery of area 2, right: Imagery of area 3.

To design an ontology-based change-detection strategy, domain knowledge (such as land cover classes) and remote sensing knowledge (such as the required indices for the definition of land cover classes) was collected. The exact classes, properties, and their interweaving in the ontology, were determined after three phases: the *specification*, *conceptualization*, and *knowledge formalization* (Paslaru et al. 2006, Brusa et al. 2006). In the *specification phase*, the general land cover classes that will be defined in the ontology were determined. Inspection of the imagery, showed that the area was covered by *vegetation*, *water* (mostly appearing in pools), *bare ground*, *roads*, and the *rooftops*. The rooftops were further divided into rooftops which remained unchanged between 2006 and 2011 and rooftops which were newly built or modified during the examined period.
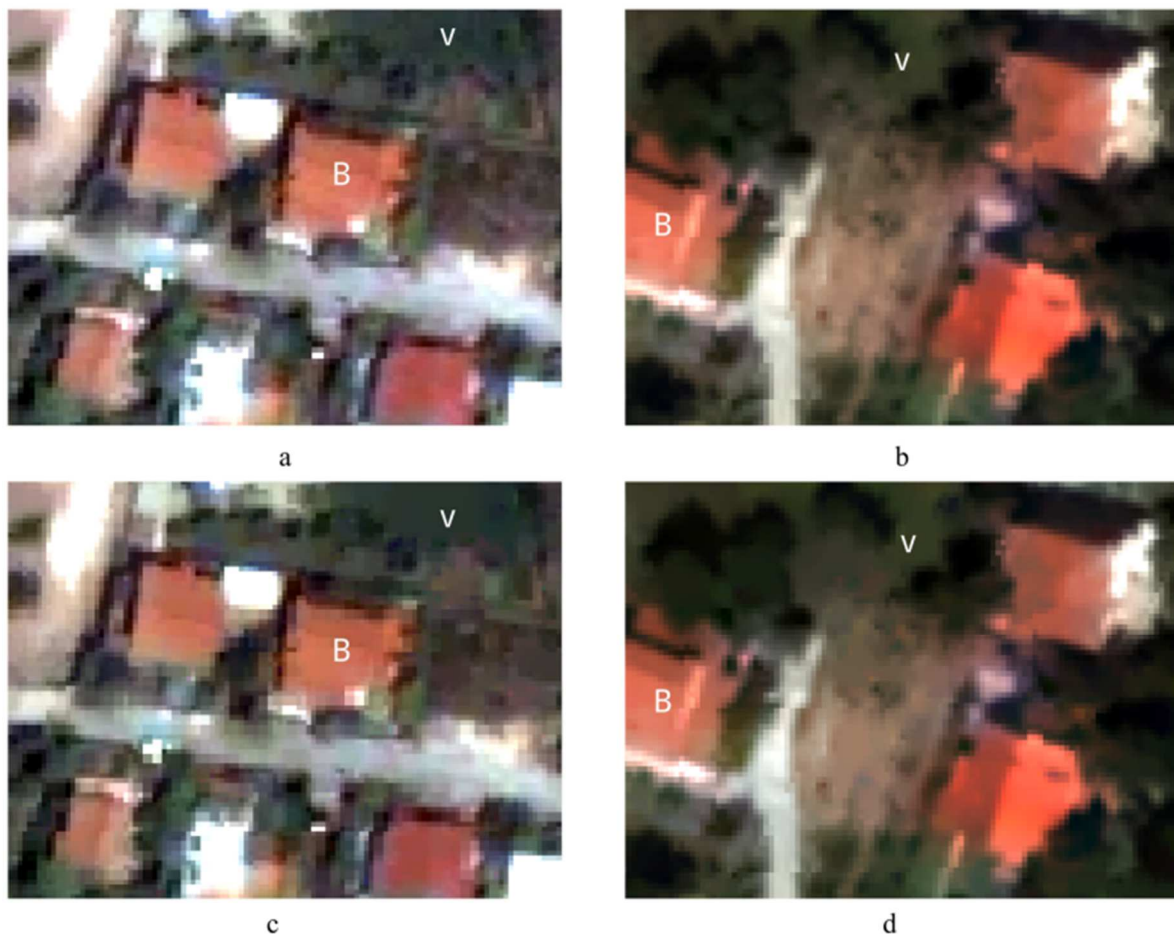
Figure 16. Magnifications of the original dataset. a-b. Original QuickBird and WV2 imagery. c-d. The same areas after morphological leveling. It is observed that vegetation and rooftop areas were smoothed from the filtering process.

In the *conceptualization phase*, the main classes were represented in an initial taxonomy. For each class a number of properties which could be employed in their definition were also examined. The classes within the taxonomy were organized to eliminate areas of no interest, resulting into the desired classes (i.e. rooftop changes). At first the *Vegetation*, *Water*, and

66

Impervious classes were defined. Since some buildings and roads were expected to be the same in both years, the impervious areas were refined into *PossibleChange* (areas where a change could take place), and *NoChange* (Figure 17). To define the *Vegetation* and *Water* classes the *ndvi* and *ndwi* indices were considered. *Impervious* can be defined as the intersection of the negation of the other two classes (*not (Vegetation)* and *not (Water))*.

Since each rooftop in the examined areas was relatively spectrally homogeneous, spectral indices were investigated to emphasize them and determine areas of possible change. The dominant rooftops in the area were white tiled and ceramic rooftops (Figure 15). After experimentation two indices were found appropriate to emphasize the rooftops, the *WhiteIndex* and the *CeramicIndex* (Figure 18), computed from Equations (28)-(29) as follows:

$$\text{WhiteIndex} = \frac{\text{RedBand} + \text{BlueBand} + \text{GreenBand}}{3} \tag{28}$$

$$\text{CeramicIndex} = \frac{\text{RedBand}^2}{\text{GreenBand}^3} \tag{29}$$
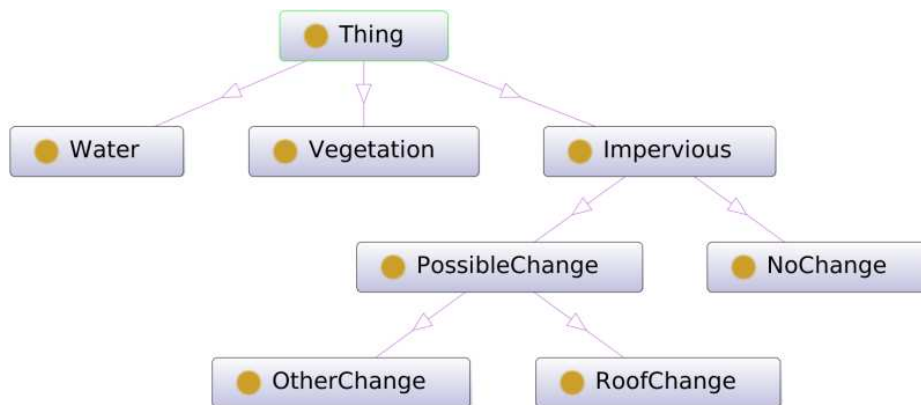
Figure 17. Conceptualization of the change detection process. The RoofChange class should contain the final changes in building rooftops.
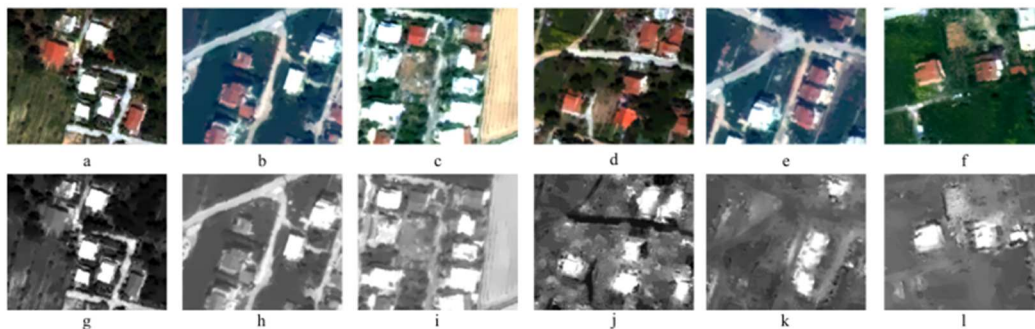
Figure 18. Examples of the white and ceramic indices. a-c: Areas with white tiled roofs. d-f: Areas with ceramic roofs. g-i: Results of the whiteIndex. The white areas are presented with high values of the index while other areas appear with lower values. j-l: Similarly the ceramicIndex emphasizes the ceramic roofs, while other areas have lower values.

Their differences (*difWhite* and *difCeramic*) should be considered to define the class *PossibleChange*. New white tiled and new ceramic rooftops should be detected with high values of the difWhite and the difCeramic index respectively. Likewise, demolished white and ceramic rooftops should be detected by low values of the *difWhite* and *difCeramic* index. A ceramic rooftop which was previously a white tiled rooftop should be detected by high values of the *difCeramic* index and low values of the *difWhite* index.

By considering the rectangular-like geometric signature of the rooftop, rooftop changes were expected to be rectangular also. Thus, *RoofChange* should be defined based on geometric indices (such as the *rectangular fit*), representing the rectangular shape of the objects.

In the *knowledge formalization* stage, the abstract taxonomy developed in the *conceptualization phase* was transformed into a fuzzy OWL 2 ontology. Thus, the actual taxonomy for the change detection process was developed after performing sufficient tests to determine the required number of segmentation levels, and the exact classes and properties through an iterative trial – and – error process.

To perform the segmentation process, the multiresolution segmentation algorithm, included in Definiens eCognition 8.6, was employed (Baatz and Shäpe 2000, Trimble 2011). Segmentation results were exported from eCognition and imported into PostgreSQL. Results were visualized through Quantum GIS.

Figure 19 presents an overview of the classes developed and their interweaving, derived from the *knowledge formalization* stage. Since multiple DBN classifications were defined in the ontology, the classes involved in each DBN classification are also highlighted. Details concerning the exact developed classes, properties, and class definitions, can be found in the uploaded ontology in the following url:

https://github.com/ArArgyridis/GEOBIA-Ontologies/blob/master/GEOBIA_Change_Detection_Quickbird_Worldview2.owl
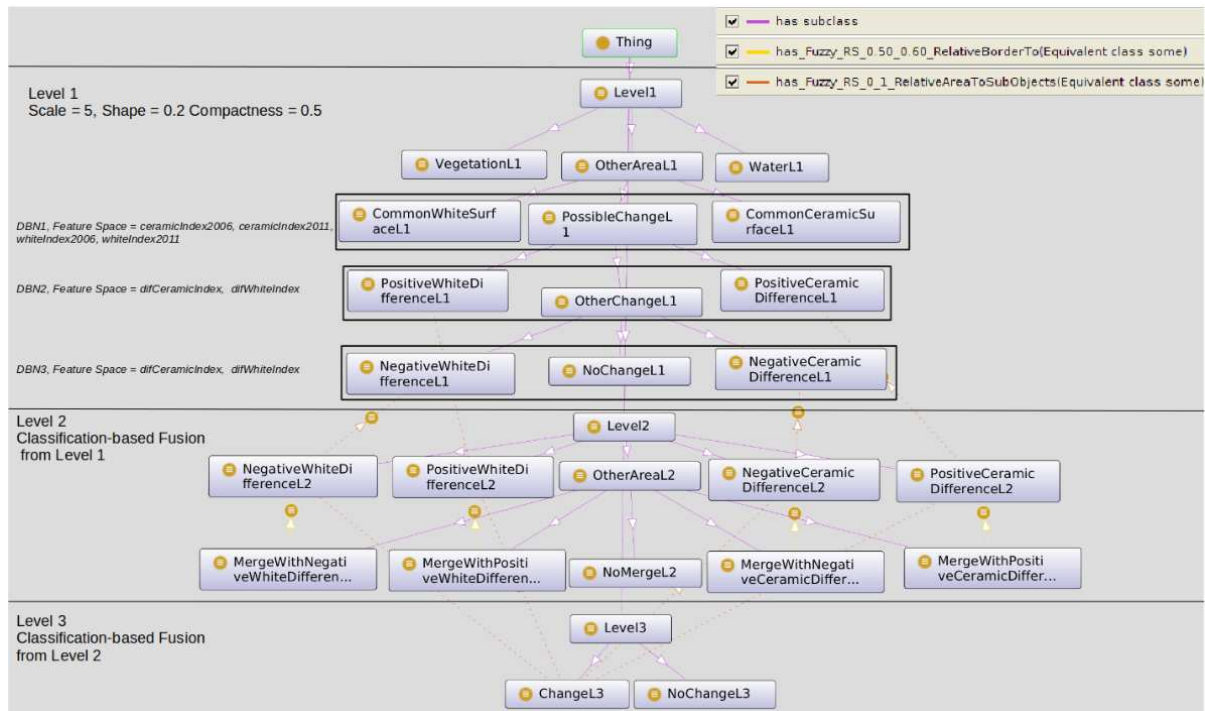
Figure 19. Overview of the developed change extraction strategy.

Aim of *Level 1* was to extract objects representing the rooftops. Since the rooftops were relatively spectrally homogeneous, due to the anisotropic diffusion the homogeneity within the rooftops was increased. Since the edges of the image objects were preserved from the filtering, a small segmentation parameter should compute objects representing parts of the rooftops (since the segmentation heterogeneity will be very small), and at the same time achieve minimum confusion with the surroundings. Thus, *Level 1* was designed on the lowest level of the segmentation hierarchy. After experimentation it was observed that a scale parameter equal to 5 (shape = 0.2, compactness = 0.5) was satisfactory.

In the ontology, each segmentation level was represented by a class, e.g. for segmentation *Level 1*, the class *Level1* was developed and defined as in Equation (30) (*level*: position of the segmentation level in the hierarchy):

Class: Level1 EquivalentTo:

level some fuzzy_TR_0_1_2   (30)

Based on the conceptualization scheme (Figure 17), classification of *Level 1* began with *VegetationL1* and *WaterL1* which were defined through medium to large values of the *NDVI* and *NDWI* respectively. All impervious areas were classified as *OtherAreaL1* (Figure 19). To reduce possible noise, it was determined to eliminate areas, with spectral profile similar to the white or ceramic rooftops, where no change occurred (*NoChange* – Figure 17). Thus, *OtherAreaL1* was refined, and the classes *CommonWhiteSurfaceL1*,

69

CommonCeramicSurfaceL1 and *PossibleChangeL1* were defined. A DBN was included in the definition of these classes (Figure 19). As input properties were given the *whiteIndex* and *ceramicIndex* of 2006 and 2011. Segments from representative areas were sampled, spread throughout the imagery. For each image 20 samples were collected for each class. The other training parameters were the same as in Table 5.

To detect areas of possible rooftop change, *PossibleChangeL1* was refined into *PositiveWhiteDifferenceL1* to represent areas with large values of the *diffWhite index, PositiveCeramicDifferenceL1* to represent areas with large positive values of the *diffCeramic index,* and *OtherDifferenceL1*. However, as areas existed having at the same time high values of the *diffCeramic index* and low values of the *diffWhite index,* it was decided to classify these areas as *PositiveCeramicDifferenceL1*. A second DBN restriction was created and included in the definition of these classes (Figure 19). As input features were set the *diffWhite index* and the *diffCeramic index*. The same sampling strategy and parameters for DBN were employed as in the previous case.

To detect areas with low values of the *diffWhite index* and the *diffCeramic index, OtherDifferenceL1* was further refined into *NegativeWhiteDifferenceL1*, *NegativeCeramicDifferenceL1* and *NoChangeL1*. A third DBN restriction was created and included in the definition of these classes (Figure 19). Its parameters were the same as with the second DBN. Figure 20 presents examples from the classification results of *Level 1*. Visual inspection shows that the combination of fuzzy rules with DBN classification captured satisfactorily the objects belonging to the developed classes.

Since building rooftops changes were expected to have rectangular-like shape, due to the rectangular shape of the roofs, *Level 1* classification should be refined based on geometric properties which express shape rectangularity. However, prior to this refinement, to optimize the shape of the possible roof changes, it was decided to create a new level above *Level 1*. Due to the small shape of the objects, it was assumed that objects that were surrounded by areas of possible change actually belong to the area that could be considered as change by a photo-interpreter. Thus, the areas classified as *PositiveWhiteDifferenceL1*, *PositiveCeramicDifferenceL1*, *NegativeWhiteDifferenceL1*, and *NegativeCeramicDifferenceL1* were merged, and *Level 2* was created above *Level 1.* The classes *PositiveWhiteDifferenceL2*, *PositiveCeramicDifferenceL2*, *NegativeWhiteDifferenceL2*, and *NegativeCeramicDifferenceL2* were created (Figure 19). To project classification results from *Level 1* to *Level 2* each of these classes were defined with the *has_Fuzzy_RS_0_1_RelativeAreaToSubObjects fuzzy object property*. In Equation (31) the definition of the class *PositiveWhiteDifferenceL2* is presented:

Class: PositiveWhiteDifferenceL2 EquivalentTo:

    Level2

        and   (has_Fuzzy_RS_0_1_RelativeAreaToSubObjects   some

  PositiveWhiteDifferenceL1)

(31)

This definition reads as follows: *Objects were assigned to class PositiveWhiteDifferenceL2 if they were belonging to class Level2 and had relative area with the objects classified as PositiveWhiteDifferenceL1 greater than 50%. All other areas were classified as OtherAreaL2.*

▢ CommonCeramicSurfaceL1	▢ CommonWhiteSurfaceL1	▢ NegativeCeramicDifferenceL1	▢ NegativeWhiteDifferenceL1
▢ NoChangeL1	▢ PositiveCeramicDifferenceL1	▢ PositiveWhiteDifferenceL1	▢ VegetationL1 ▢ WaterL1
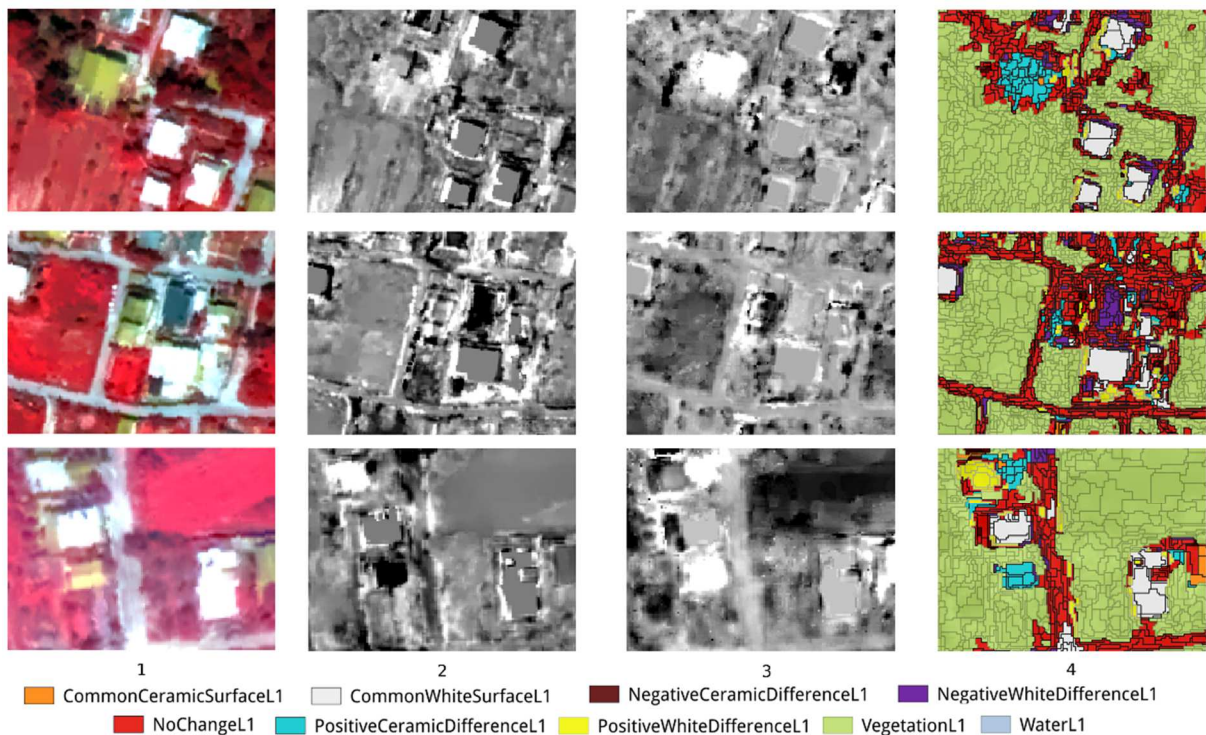
Figure 20. Examples from the classification of Level 1. (1): RGB 753 of WV2. (2): diff white index. (3): diff ceramic index. (4): Result of the classification process, derived through the interweaving of multiple DBNs and fuzzy ontologies.

Objects having relative border greater than 55% with areas of possible change, were considered appropriate to be merged with the areas of possible change. Thus, the class *OtherAreaL2* was refined into *MergeWithPositiveWhiteDifferenceL2*, *MergeWithPositiveCeramicDifferenceL2*, *MergeWithNegativeWhiteDifferenceL2*, and *MergeWithNegativeCeramicDifferenceL2*. To show how each of these classes were defined, in Equation (32) the definition of *MergeWithPositiveWhiteDifferenceL2* is presented:

71

Class: MergeWithPositiveWhiteDifferenceL2 EquivalentTo:

OtherAreaL2

and (has_Fuzzy_RS_0.50_0.60_RelativeBorderTo some PositiveWhiteDifferenceL2)   (32)

This definition reads as follows: *Objects were assigned to class MergeWithPositiveWhiteDifferenceL2 if they were belonging to class OtherAreaL2 and had relative border with objects classified as PositiveWhiteDifferenceL2 greater than 0.55. All other objects were classified as NoMergeL2.*

To extract the rooftop changes, the objects classified as PositiveWhiteDifferenceL2, PositiveCeramicDifferenceL2, NegativeWhiteDifferenceL2, and NegativeCeramicDifferenceL2 were spatially merged with the objects classified as MergeWithPositiveWhiteDifferenceL2, MergeWithPositiveCeramicDifferenceL2, MergeWithNegativeWhiteDifferenceL2, and MergeWithNegativeCeramicDifferenceL2 and a new level (Level 3) was created above Level 2. The classes ChangeL3 and NoChangeL3 were defined (Figure 19). To express the shape of the rooftops, ChangeL3 was defined based on geometric properties as shown in Equation (33):

Class: ChangeL3 EquivalentTo:

Level3

and   ((has_Fuzzy_RS_0_1_RelativeAreaToSubObjects   some NegativeCeramicDifferenceL2)

or   (has_Fuzzy_RS_0_1_RelativeAreaToSubObjects   some NegativeWhiteDifferenceL2)

or   (has_Fuzzy_RS_0_1_RelativeAreaToSubObjects   some PositiveCeramicDifferenceL2)

or   (has_Fuzzy_RS_0_1_RelativeAreaToSubObjects   some PositiveWhiteDifferenceL2))

and (areaM2 some fuzzy_TRP_50_55_360_380)

and (compactness some fuzzy_LS_2.2_2.4)

and (density some fuzzy_RS_1.75_1.80)

and (lengthM some fuzzy_TRP_8_9_30_35)

and (rectangularFit some fuzzy_RS_0.6_0.7)

and (widthM some fuzzy_RS_5_7)   (33)

This definition reads as follows: *Objects were assigned to class ChangeL3 if they were covering at least one of the classes PositiveWhiteDifferenceL2, PositiveCeramicDifferenceL2, NegativeWhiteDifferenceL2, and NegativeCeramicDifferenceL2 by at least 50%, and had area between 52.5m2 and 370m2 and had compactness smaller than 2.3, and had density larger than 1.775, and had length between 9m and 32.5m, and had rectangular fit larger than 0.65, and had width larger than 6m. All other objects were classified as NoChangeL3.* Figure 21 presents the objects classified as ChangeL3 in the examined areas. As changes were detected entirely new buildings and changes in existing building infrastructure (for example the creation of a ceramic roof on top of a white roof).

Classification results were compared with human interpreted reference data and evaluated with two methods. At first, the number of changes recorded in ground data was compared to the number of extracted changes (Table 6).

Table 6. Quantitative evaluation comparing the number of extracted changes with the reference data.

Area	Ground Truth Changes	Extracted changes	Correctly detected changes	Committed changes	Omitted changes	Commission (%)	Omission (%)
Area 1	19	23	19	4	0	21.1	0.0
Area 2	36	37	30	7	6	19.4	11.8
Area 3	28	27	24	3	4	10.7	14.3
Overall	**83**	**87**	**73**	**14**	**10**	**18.3**	**12.1**

area 1
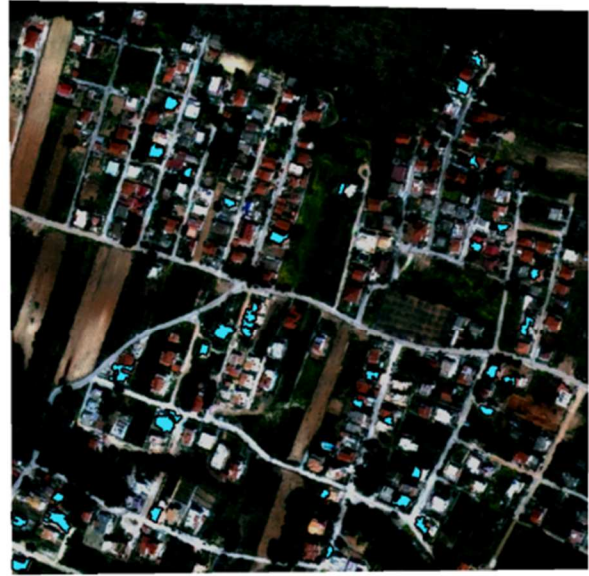
area 2
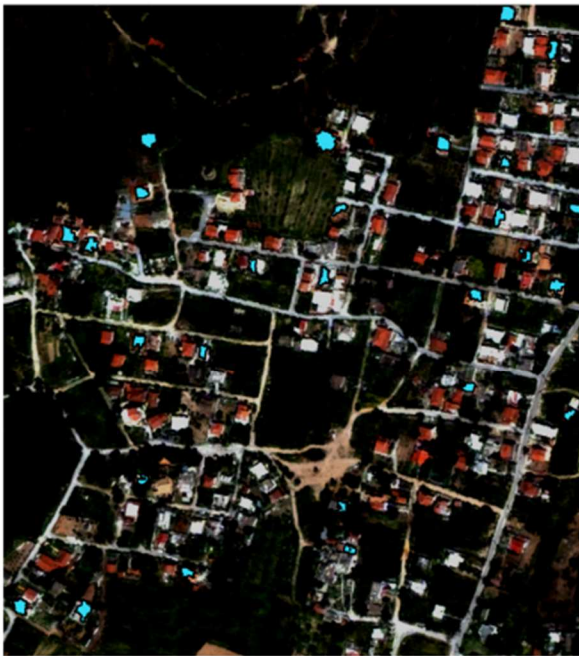
area 3

Building Changes

N

0   100   200   300   400 m

Figure 21. Final changes recorded in the three areas, shown in WV2 2011 (RGB 532).

Second, the areas correctly detected (True Positive – TP), omitted (True Negative – TN) or committed (False Positive – FP) were computed by comparison to the ground data. Based on these areas, the Completeness, Correctness and Quality indices (Table 7 - Agouris et al. 2004) were computed as presented in Equations (4)-(6).

Table 7. Quantitative evaluation based on the Completeness, Correctness, and Quality indices for each examined area.

	Ground Data (m²)	TP (m²)	FN (m²)	FP (m²)	Completeness (%)	Correctness (%)	Quality (%)
Area 1	2021.50	1634.91	386.59	468.84	80.9	77.7	65.7
Area 2	4038.82	2570.59	1468.23	1360.16	63.6	65.4	47.6
Area 3	3055.82	1779.21	1276.61	881.79	58.2	66.9	45.2
Overall	**9116.14**	**5984.71**	**3131.43**	**2710.79**	**65.6**	**68.8**	**50.6**

4.6   Discussion of results

In this chapter fuzzy ontologies were integrated with Deep Learning techniques, allowing the development of class definitions with fuzzy properties and machine learning. To perform the reasoning process with such ontologies, a reasoner developed for GEOBIA ontologies, SPOR, was enhanced through the integration of DBN algorithm. The approach was tested in building change detection.

Due to the relatively spectral homogeneity of the rooftops, the reduction of undesired spatial detail through the anisotropic filtering aided in the extraction of proper objects, similar to Doxani et al. (2012). Through multi-scale analysis objects representing properties of the present thematic categories were computed. The spectral properties of the rooftops were captured on the lowest level of the hierarchy by creating objects representing parts of the rooftops with a small scale parameter (5). Fuzzy rules and machine learning classification were combined to determine areas of possible rooftop change (Figure 19). *Level 2* was designed above *Level 1* by fusing the objects belonging to classes representing areas of possible rooftop change. Based on spatial rules, the shape of these objects was optimized to be closer to a rectangle, by considering areas partially or completely included within the rooftops as parts of possible change. This was achieved through the *relative border* spatial property. *Level 3* was designed at the top of the hierarchy, by fusing the areas of possible change with their respective contained areas. Spectral properties of the sub-objects along with the geometric properties of the rooftops were employed to discriminate the rooftop changes from the other areas.

Evaluation with ground data showed satisfactory results, since the majority of the changes were successfully detected (73 out of 83) and a relative small number of changes were omitted (9) and committed (15). Evaluation based on the extracted area showed that the overall result was around 68% complete and accurate (Completeness and Correctness indices), thus the omission and commission errors were around 30%.

A major issue was the acquisition angle of the imagery. For the QuickBird imagery it was 8.2°, and for the WV2 19.6°. The large acquisition angle of the WV2 imagery affected significantly the computation of the difference of the white and ceramic indices in areas with tall buildings and committed as part of the changed rooftop area parts of the building sides, or shifted parts of rooftops. In area 1, where the buildings were not as tall, evaluation was satisfactory since all the changes were detected with relatively small commission errors (Table 6) and the mapping accuracy was also satisfactory (Completeness 80.9%, Correctness 77.7% - Table 7). In the other two areas, rooftop shifting further affected the detection of the number of changes and the mapping accuracy.

Omission error occurred mainly when the area detected as change was not enough, or the shape of the change was not satisfying the shape restrictions defined in the ontology. To lessen the omission error, an optimization of the parameters related to the rooftop shape was attempted, however, this increased the commission error so it was not adopted. The commission error was mostly related with the commission of building sides to the result, or by confusing bare ground or road areas with similar spectral and geometric properties with the rooftops, as change. Improved results could be achieved by employing Digital Surface Model (DSM) data for the creation of true ortho-photos thus reducing the errors related to the geometry and position of the rooftops.

Possible future work might include some of the following. In previous approaches (e.g. Durand et al. 2007) performed automatic development of ontologies based on machine learning techniques. It is desirable to examine the potential of such approaches in building change detection, through multi-scale analysis, to determine optimal features for class definitions. SPOR could be extended by integrating additional supervised techniques such as the SVM and to be further developed to better support OWL 2 expressiveness (such as symmetrical or transitive properties etc.) or examine and deal with cases where undecidability might occur. Furthermore it would be desirable to examine the probability of integrating unsupervised machine learning with ontologies in GEOBIA. Regarding the change detection process, the involvement of DSM or advanced registration approaches can be examined to reduce the offset between the rooftops. Furthermore the approach can be generalized by examining additional cases, such as building change detection in a continuous urban environment.

4.7 Conclusions and Future Perspectives

Development of GEOBIA ontologies is important as it provides for critical review of the knowledge base. The knowledge base can be directly employed in GEOBIA processes to extract landscape components. Furthermore adoption of Semantic Web technologies for knowledge representation can provide for sharing, extension, and integration of the developed ontologies with others from the same or different disciplines by employing or

extending approaches such as the ones described in Kavouras et al. (2005) and Kavouras and Kokla (2007).

Machine learning is widely adopted in image analysis since it enables the classification of objects based on data-derived information. The integration of state-of-the-art machine learning methods, such as the DBN, with ontological reasoning could assist towards the automation of an ontology-based GEOBIA approach, since thresholds of spectral and geometric properties are not required to be determined by the designer, to classify objects in a designated class. However, complex thematic concepts require human interpretation knowledge to be explicitly represented. This was shown through the developed building change detection approach. AML reduced the spatial detail of the imagery and provided a simplified imagery representing smoothed building rooftops. DBN along with fuzzy ontological reasoning aided to satisfactorily determine areas of possible rooftop change, by employing spectral properties of the present rooftops. Interpretation knowledge related to geometric and spatial relations of the objects, represented within the ontology determined the building changed areas from noise or other areas unrelated to building changes. Qualitative and quantitative evaluation of results showed that the changes were detected satisfactorily. However, the developed method relies in a correct detection of areas of possible change on *Level 1* based mainly on the spectral properties of the present infrastructure. Thus, in cases where the rooftops have a large shift due to the acquisition angle, the detection of areas of possible change on *Level 1* will not be adequate to detect the change. Furthermore, the method should be extended to consider rooftops having different spectral and geometric properties from the ones examined. Finally, it would be interesting to examine the developed approach in dense urban areas where the complexity of the environment is higher than the one examined in this study.

5 GEOBIA-based Identification of Alluvial Fans and Bajadas through Geomorphometry, Image Analysis, and Fuzzy Ontology-Based Reasoning

5.1 Introduction

Mapping of alluvial fans and bajadas is important for practical and economic importance to society, especially in arid and semiarid climates where they may be the principal groundwater source for irrigation farming and the sustenance of life. However, the flash flooding and the shifting streams develop may develop issues on man-made objects. Cities, such as Los Angeles, have been developed on alluvial fan. Furthermore, it provides climatic information (Beratan and Anderson 1998, Miliaresis 2001, Britannica 2016).

Mapping of terrain elements such as alluvial fans and bajadas from remote sensing data is performed by manual interpretation through terrain analysis. In terrain analysis the landscape is composed by distinct terrain units called landforms. In United States, the landform-pattern element approach has been the most prominent terrain analysis approach (Way 1978, Mintzer and Messmore 1984). When a landform is developed under similar climate, weathering, and erosion conditions, it exhibits a distinct and predictable range of visual and physical properties. Any two landforms derived from the same soil and bedrock, or deposited by similar processes, and existing under the same climatic conditions, exhibit similar physical and visual features on satellite or airborne imagery, called *pattern elements.* The pattern elements examined in the landform-pattern element approach include topography, drainage pattern and texture, gully characteristics, soil spectral signature, landuse, and other special features that may be present (Mintzer and Messmore 1984, ASPRS 1997).

Alluvial fan development requires three necessary conditions: (a) a spatial/topologic organization where an upland catchment drains to a valley; (b) sufficient sediment production in the catchment to construct the fan, and (c) a process to transfer the upland sediments into the basin, which is usually sporadic high water discharge (Hunt 1975, Bull 1977, Harvey et al. 2005, Blair and McPherson 2009). The head of an alluvial fan is located right at the downstream end of the upland drainage network, where a stream pours abruptly into a basin at the startup of the creation of an alluvial fan (Figure 22). It has a semi-circular, fan-like shape. It has slopes from near 0°, rarely exceeding 10°-12° (Troeh 1965, Bull 1977, Rachocki 1981, Miliaresis and Argialas 2000). Smaller forms with slopes greater than 20° are rather alluvial cones (Bull 1977). Bissenbach (1954) stated that alluvial fans have three distinct morphological parts: i) the *fan-head*, which is the fan area closest to the apex with the largest slopes; ii) the *fan-toe*, which is the outermost and lowest zone of the fan having the lowest slopes usually grading into a zone of coalescence with other fans; iii) the *mid-fan* which is the area between the *fan-head* and the *fan-toe.*

Figure 22: Fan developed in front of a valley mouth at the adjacent basin floor. Image © 2017 Digital Globe.

An alluvial fan has a dichotomic drainage pattern (Way 1978, Mintzer and Messmore 1984). In this pattern, branches are diverging from the main stream. These branches may also have braiding, causing them to intersect (Fenneman 1931, Rachocki 1981, Pandey 1987, Drummond and Erkeling 2014). Individual fans may grow laterally to an extent that they coalesce to form bajadas (Hooke 1972, Bull 1977). Bajadas are created when a series of adjacent fans are coalescing and they form a continuous piedmont alluvial apron, in-between the mountain front and the basin floor.

Landform photo-interpretation it is carried out manually by expert photo-interpreters, thus it is a time consuming process and cost-deficient. Thus, investigation of automated landform mapping approaches is desirable for economy and efficiency. Automated approaches also aid in the standardization and objectiveness of the process, as books, often, do not describe explicitly the procedural framework for terrain interpretation problem-solving. Due to the complexity of the pattern elements involved in landform interpretation such as slope gradient, landform shape, drainage pattern, and context (Way 1978, Mintzer and Messmore 1984, Argialas and Miliaresis 2000) it is necessary to represent image primitives related to the shape and topological organization of the examined landforms, making object-based approaches (GEOBIA) appropriate (Argialas and Harlow 1990, Drăgut and Eisank 2011, Blaschke et al. 2014). In GEOBIA, segments corresponding to image patterns, are extracted and are later assigned into thematic categories through machine learning. However, in cases where the recognition process involves the investigation of complex relationships involving properties of the object itself and its spatial organization, it is required to express photo-interpretation knowledge derived from knowledge stored in books, field work, and personal experience into machine-readable formalization and employ it in the identification process. Knowledge formalization into a computer-conceivable form needs to address a semantic gap between the

complex high-level semantics employed by experts (e.g. an alluvial fan is a gently-sloping feature) and the low-level data-derived numerical information (specific value ranges of slope gradient, curvature etc), thus requiring a knowledge representation approach (Argialas and Harlow 1990, Arvor et al. 2013, Blaschke et al. 2014, Argyridis and Argialas 2015).

Knowledge representation in the Semantic Web is performed through ontologies (W3C 2012). Gruber (1995) defines the ontology as a formal, explicit specification of a shared conceptualization. Thus, Semantic Web ontologies were designed to be extensible, visible, support inference, and provide semantic interoperability (Ding et al. 2007, Janowicz 2010).

Ontologies can provide solution to the semantic gap issue by bridging the expert derived symbolic information and the numerical information extracted from the image (Arvor et al. 2013). Their applicability in GEOBIA has already been demonstrated in previous studies (e.g. Durand et al. 2007, Forestier et al. 2012, Belgiu et al. 2014, Argyridis and Argialas 2015).

Alluvial fans and bajadas have already been extracted from remote sensing data. Argialas and Miliaresis (2000) developed an expert system to aid human interpretation of physiographic regions through the landform-pattern element approach. Spatial terrain decomposition was achieved by partitioning each physiographic section into its component physiographic features, and each physiographic feature into its component topographic forms, and each topographic form into its component landforms. Miliaresis and Argialas (2000) developed a region growing segmentation method to extract alluvial fans from DTM and Landsat TM imagery. The process began with drainage network extraction through runoff simulation, thresholding, and skeletonisation to one-pixel wide lines. Afterwards the outflow points to the basin floor were detected. Through visual interpretation it was determined that all the outflow points were located on the piedmont slope and, in particular, on the alluvial fan regions. Region growing of the outflow points was performed on the basis of the gradient value of the surrounding pixels in the digital elevation model, and a set of fan polygons was derived. The final fans were extracted through spectral refinement on Landsat TM imagery. In Miliaresis (2001) bajadas were extracted from DTM and Landsat TM imagery through region growing segmentation, by considering the drainage that crossed the uplands and the bajadas, their slope, and their spectral signature in Landsat TM. Asselen and Seijmonsbergen (2006) extracted alluvial fans from 1m Laser DTM through multi-scale GEOBIA approach. On Level 1 potential incised channels were identified. This information, was used on Level 2 to separate incised channels from river terraces and to classify other geomorphological units. Alluvial fans were determined based on their elevation and slope gradient properties. Classification result was optimized on *Level 3* by merging adjacent objects classified in the same class, and by filtering out small misclassified ones. Argialas and Tzotsos (2006) extracted alluvial fans from ASTER L1 and 1º DTM through multi-scale analysis. At first, basins, piedmont slopes, and mountains were approximated (Level 1). These were refined, through classification-based

fusions (Level 2), spectral nearest neighbor (Level 2) and context-based, knowledge based classification (Level 2 - 4), to deliver the alluvial fans on the coarsest level. Crouvi et al. (2006) mapped alluvial fans from field spectrometer and hyperspectral remote sensing data. Roberts and Cunningham (2008) separated alluvial fans from SRTM data through slope thresholds and topographic roughness filter. Schneevoigt et al. (2008) classified various alpine landforms through multi-scale GEOBIA analysis from ASTER-derived spectral and DTM data. On Level 1 spectral classification was performed to define the boundaries of all objects. Level 4 displayed the strata mask, while on Level 3 hollow forms and crest regions were extracted. Alluvial fans were extracted based on their slopes on Level 2, along with all other landforms. Classification results were satisfactory, however for the alluvial fans it was mentioned that it was difficult to separate them from floodplains or vegetation-covered channels. Yong et al. (2008) developed a four-level segmentation approach to identify piedmonts, basin, and mountains. After experimentation the segmentation parameters were determined and the final product was delivered through Nearest Neighbor classification of the final level. Hardgrove et al. (2009) employed thermal imagery to extract geomorphic features and evidence of sedimentary processes on the surfaces of alluvial fans.

Previous studies employed spectral, slope, and elevation properties to determine alluvial fans and bajadas. Furthermore elements of the drainage network were considered in the identification process to identify their outflow points / apex points (e.g. Miliaresis and Argialas 2000, Miliaresis 2001). However still remains the need to employ additional landform-pattern elements such as the landform shape, and the drainage pattern type and texture. Thus in this study geomorphometric and image analysis techniques were investigated and integrated through a GEOBIA multi-scale approach, towards the automated identification of alluvial fans and bajadas. At first, the elements required for the identification process were specified. Drainage pattern identification requires the extraction of the drainage network, thus state-of-the-art DTM filtering, depression treatment, and drainage network extraction methods were investigated. Employment of topographic properties such as slope and shape required the investigation, enhancement and creation of DTM-derived indices. A fuzzy ontology was developed, based on the landform-pattern element approach, interweaving topographic-form, drainage pattern, and spatial properties to carry out the identification of alluvial fans and bajadas.

5.2   Materials and Methods

5.2.1   Area of study and Data used

The study area is part of the Great Basin section of the Basin and Range Physiographic Province in the Death Valley region in Nevada, USA. This region is characterized by large mountain ranges intervened by tectonic alluvial basins (Fenneman 1931, Peterson 1981). Eastward tilting of Death Valley has caused the west-side fans to be rather extensive, and the toes of

the east-side fans to be buried by playa deposits (Bull 1977). Numerous springs and wells are evident at the emergence of the alluvial landforms to the valley floor (Hunt 1975) and a seasonal shallow lake is formed occasionally in the Badwater Basin, in the northwest portion of the study area (Figure 23). Badwater Basin is confined by two mountain ranges the Panamint Range on the west side and the Black Mountains on the east side. It has the lowest elevation of any area in the United States.
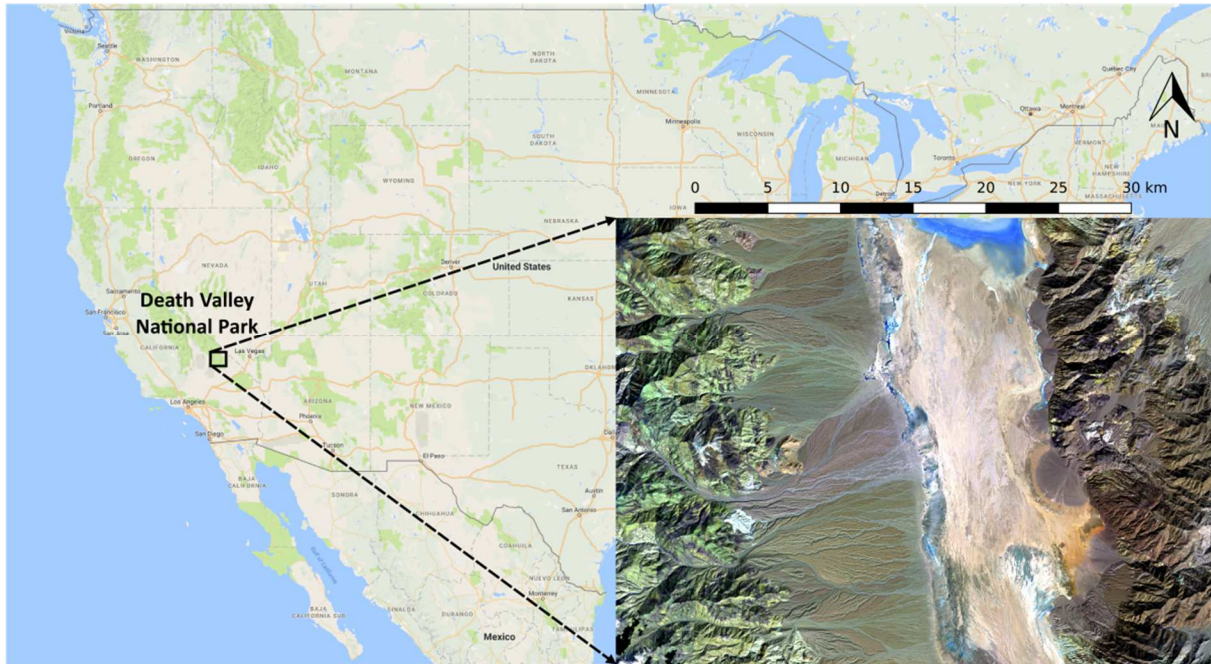
Figure 23: Overview of the study area (Landsat OLi imagery). Map data © 2017 Google, INEGI.

Data used included the NED DTM provided by USGS and Landsat OLi multispectral imagery taken in 2015. The NED assembly process involves edge matching and mosaicking elevation data into NED layers. The processing system for the NED Seamless Layers is designed to assemble a seamless dataset from multiple data sources, resolutions, and production methods. Procedures have been developed to maintain the database with continuous updates and to insure the integration of higher resolution elevation data as they become available (USGS 2016). In this study, the 10m spatial resolution NED was employed. The examined area covered around 1270 km^2.

5.2.2 DTM processing

An overview of the developed methodology is presented in Figure 24. DTM processing aimed to reduce noise and ensure the computation of continuous flowpaths from the uplands until the end of the drainage network through depression treatment.
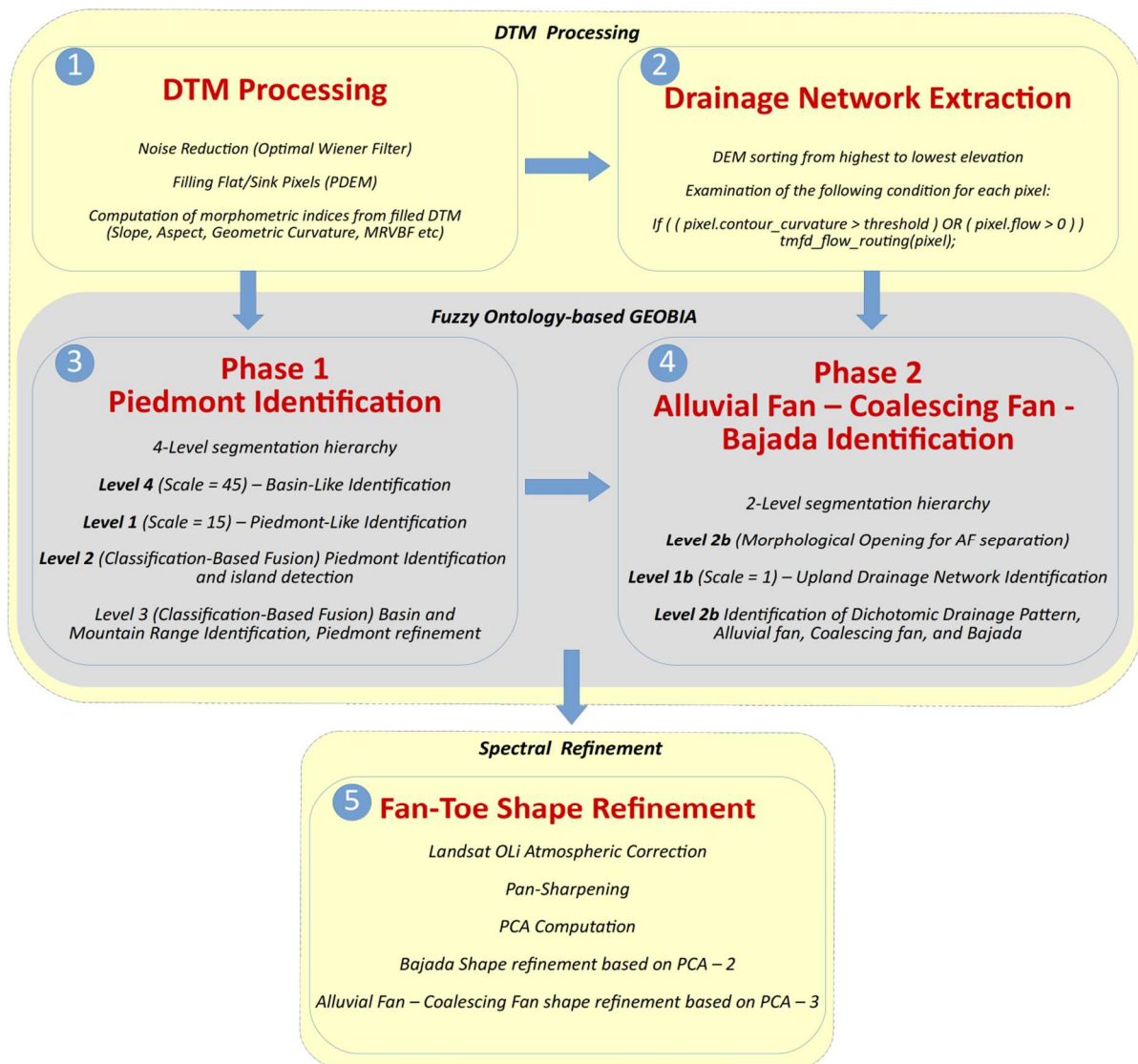
Figure 24: Overview of the developed method for alluvial fan and bajada identification.

Following Pelletier (2013), noise reduction was performed through optimal Wiener filtering, which removed microtopographic noise. Depression treatment was performed by an enhanced version of the PDEM algorithm which was stated in Feifei et al. (2012). PDEM performs depression treatment through linear interpolation. For each pixel, the downward elevation gradient (DEG) was computed in a 3x3 neighborhood. A Flat or Sink (FS) pixel was identified if its DEG was less or equal to zero. Afterwards, 8-connected FS pixels were grouped into Flat – or – Depression – Areas (FAD). For each FAD the bordering pixels were also determined. The border pixels with the minimum elevation were defined as *outlets*, while all the others were called *inflows*. Their coordinates were stored in arrays. Depression treatment began by setting the minimum border elevation to all FAD pixels. From an outlet a line was drawn towards a FS pixel (OF line) and extended until it intersected the border. The interpolation was performed if the OF was passing completely through the FAD. The OF line

was extended from the FS towards the border as follows. The maximum distance between the FS pixel and all inflow pixels was computed, rounded, and increased by 1. Iteratively, possible border coordinates were computed as shown in Equations (34)-(35).

$$X_m = int(FSx + m * 0.1 * cos (ang)) \tag{34}$$

$$Y_m = int (Fsy + m * 0.1 * sin (ang)), ang: direction angle, m = 1,....,M \tag{35}$$

X_m and Y_m were matched with all inflow coordinate pixels. If these coordinates matched the coordinates of an inflow pixel, linear interpolation was performed. A similar process was performed to extend the line from the outlet to the FS pixel. This process was performed for all outlet pixels. The final height was the minimum one computed from all interpolations. After experimentation, two special FAD occasions were identified. The first special occasion addressed the case where all border pixels had the same height. In this case, each border elevation was recomputed based on the height of the pixel it flowed into, determined by Single Flow Direction (SFD - O'Callaghan and Mark, 1984). The second special occasion addressed the case where all OF lines were connecting two outlet pixels. In this case each outlet elevation was recomputed based on the pixel it flowed into, determined by the SFD. After treatment of a single FAD, the algorithm reprocess the entire DTM to detect FADs and perform the above process.

To deal with possible errors and improve computation efficiency, this algorithm was modified as follows. To ignore large flat areas (such as the sea) the modified algorithm ignores pixels having a certain mask value. Considering that each FAD is treated independently, to avoid the identification of the same FADs in multiple iterations and thus reducing computations, all FADs were treated in one iteration. Computations during line extension from the FS pixel towards the border were reduced by employing a raster in which the border pixels for each FAD were flagged. During OF line extension, a pixel was verified as inflow if it was flagged as border pixel and had larger elevation than the outflow. Similarly, it was verified if the OF line was passing outside the FAD. To reduce the possibility of computing the same elevation for two neighboring pixels, a small random value (between 0 and 1 cm) was added to the interpolation-derived height. Finally, to ensure compatibility with current Open GIS raster standards, the Orfeo Toolbox (OTB Development Team 2016) was employed for its development.

5.2.3 Drainage Network Extraction
Pelletier (2013) extracted the drainage network as follows. After wiener filtering, depression treatment was performed through Pelletier (2008). Valley heads were identified by a user-defined contour-curvature threshold criterion. From each detected valley-head all down-slope pixels were flagged as non-valley-heads. Flow routing from each valley head was performed,

by the Multiple Flow Direction (MFD) as stated in Freeman (1991) and discontinuous reaches where the flow was divided into multiple paths were removed from the drainage network by applying a user-defined discharge-per-upstream-valley-head threshold criterion. The drainage network was derived by thinning the flow routing to a single pixel width (Rosenfeld and Kak 1982).

To investigate modern flow routing approaches since the MFD may produce artifacts (Freeman 1991) and reduce computation time, this algorithm was modified as follows. Flow routing was performed by the Triangular Multiple Flow Direction (TMFD) as stated in Seibert and Mcglynn (2007). The contour curvature was mapped by computing the geometric curvature (Passalacqua et al. 2010), defined in Equation (36) as follows:

$$\nabla \cdot (\nabla h / |\nabla h|) \text{ (h: input DTM)} \tag{36}$$

The DTM was searched in ranked order. Flow was routed if the examined pixel had contour curvature value greater than the specified threshold (thus the pixel was recognized as a valley head), or if it had accepted flow from TMFD routing (thus being downstream from the valley head). This reduces computations since valley heads are determined during flow routing and not in a separate process.

Drainage network extraction, aimed in the identification of the dichotomic drainage pattern, as it was specified by the landform-pattern element approach. Furthermore as it will be presented later, it was important to compute the Strahler order of the network. This however requires integrated stream network. Thus, the discharge-per-upstream-valley-head threshold was not applied in flow routing computation to ensure network continuity. Finally, single pixel width streams were computed through the Ehlschlaeger (1989) method, which is based on A^T search algorithm. The developed drainage network extraction method is presented as pseudocode in Equation (37) as follows:

```
filtered_dtm = optimal_wiener_filter( input_dtm );

treated_dtm = pdem( filtered_dtm );

sorted_dtm = sort( treated_dtm );

for_each ( pixel in sorted_dtm )

    if ( ( pixel.contour_curvature > threshold ) OR ( pixel.flow > 0 ) )

        accumulation = tmfd_flow_routing( pixel );

drainage_network =  ehlschlaeger( accumulation );                    (37)
```

After experimentation through trial and error, a geometric curvature threshold of 0.015 was found appropriate for stream extraction. Results were satisfactory in the upland areas (Figure 25). However, in the piedmont, streams appropriate for dichotomic drainage pattern identification were not extracted satisfactorily. Dichotomic drainage pattern has multiple branches diverging from the apex, however the extracted branches did not had such integration. In some cases a sufficient number of branches was not extracted (Figure 25 – Example A) while in other cases they had topological errors since they were not initiated from the main stream (Figure 25 – Example B). Furthermore braiding of the branches also complicated network integration.
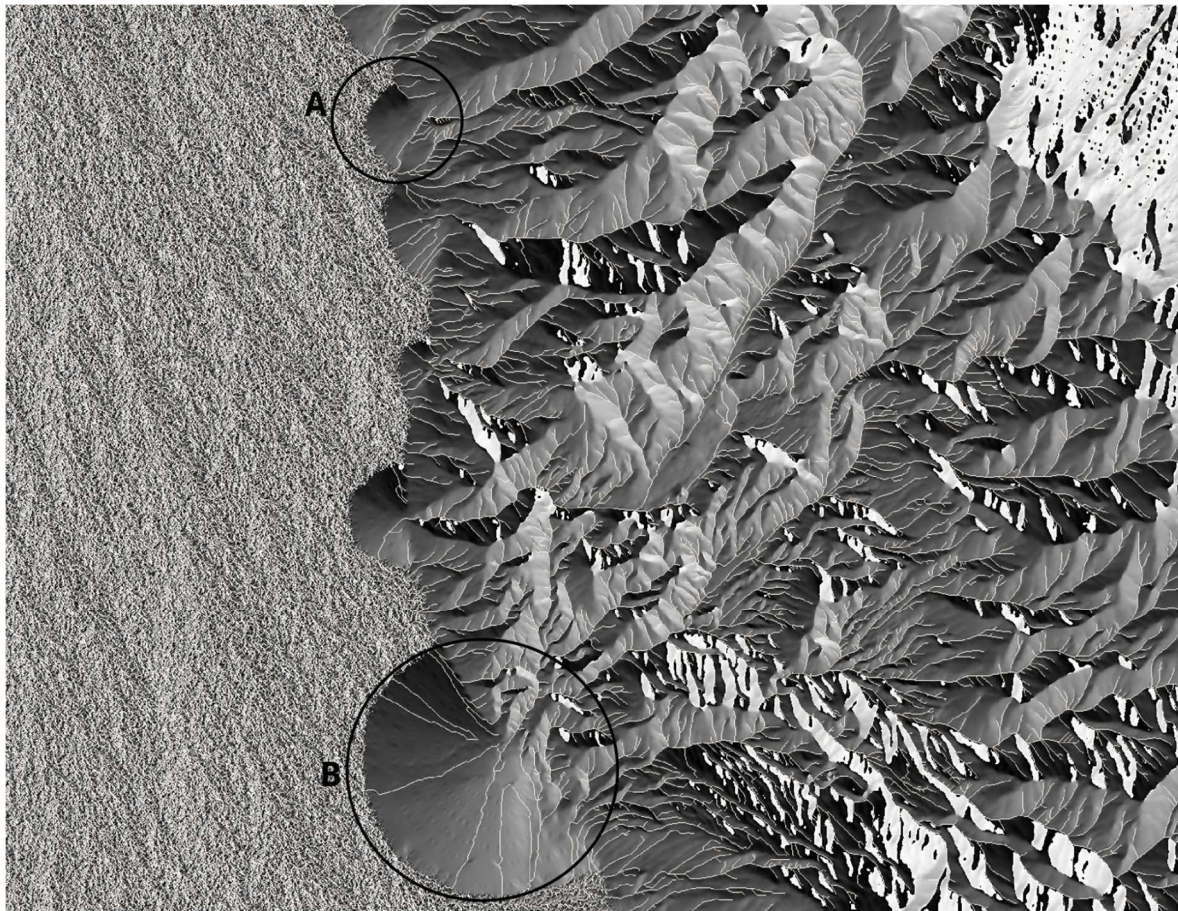
Figure 25: Detail of the extracted drainage network (appearing in white). In the upland areas, streams were extracted satisfactorily. Circle A denotes the small number of extracted streams in the alluvial fan. Circle B denotes topological errors in the extracted stream network.

5.2.4   Fuzzy Ontologies for GEOBIA

Alluvial fan and bajada identification was performed through the design and development of a GEOBIA multi-scale approach. Knowledge representation and reasoning was performed through the development of a fuzzy ontology. Aim of the ontology was the representation of domain knowledge such as topographic forms related to the spatial organization of alluvial fans and bajadas, and remote sensing knowledge related to the landform-pattern element approach required for the definition of each class. The final ontology was developed following

three phases: *specification*, *conceptualization*, and *formalization* (Paslaru et al. 2006, Brusa et al. 2006).

Reasoning was performed through the SPatial Ontology Reasoner SPOR (Argyridis and Argialas 2015). SPOR was designed to perform fuzzy and spatial reasoning through multi-scale analysis. Fuzzy operations were performed based on Zadeh semantics (Zadeh 1965). To formalize an ontology in SPOR, an enhanced version of OWL 2 with fuzzy representations was adapted (Bobillo and Straccia 2011). OWL 2 supports the development of *Classes, Data Properties* (to express numerical properties such as slope, or curvature), *Object Properties* (to express topological relationships) datatypes (to express value ranges), *Annotation Properties* (to encode metadata) and *Restrictions* (class definitions). As membership functions were employed the left shoulder (LS), right shoulder (RS), triangular (TR), and trapezoidal (TRP) functions (Bobillo and Straccia 2011). This allowed to involve *fuzzy data properties restrictions* in class definitions. For example the expression *slope some fuzzy_TRP_0_10_15_20* restricts the *slope* property with a TR function having borders 0, 10, 15, and 20 degrees. Furthermore the expression *fuzzy_RS_0.8_1.0_RelativeBorder some piedmont* restricts the spatial relationship *relative border* of the segments with the ones classified as *Piedmont* to have values determined by an RS function with borders 0.8 and 1.0. The general framework of the SPOR reasoning process is described in Argyridis and Argialas (2015).

5.3   Identification of Alluvial Fans and Bajadas

5.3.1   Ontology Specification

In the *specification* phase, the major thematic categories that will be defined in the ontology were determined. The developed classes considered the implicitly or explicitly mentioned landforms in alluvial fan and bajada definitions and the landform-pattern element approach. Given that alluvial fans and bajadas are residing on the piedmont, one first recognizes a piedmont which is a topographic form, then the alluvial feature (AF) as an intermediate conceptual and visual feature, before arriving at the final level of recognition where alluvial fans are distinguished from bajadas. Thus the term AF was introduced in the present conceptual scheme to represent both alluvial fans and bajadas.

Following Argialas and Miliaresis (2000) and Argialas and Tzotsos (2006), since the examined area is a part of a physiographic province (Figure 23), it is required to represent topographic forms related to the province spatial organization (*Basin*, *Piedmont*, *UplandMountainRange*) and the landforms (*AlluvialFan* and *Bajada*). However, due to the different size of the bajadas appearing on the Panamint Range and the ones appearing on the Black Mountains, it was determined that bajadas composed of two or three coalescing fans, having an area closer to an alluvial fan, should be represented with a different class, namely *CoalescingAlluvialFan.* Furthermore, in the landform-pattern element approach an important feature is the drainage pattern type and texture. Thus, the dichotomic drainage network

(*DichotomicDrainageNetwork*) and its texture should be identified. Finally, the AFs apex points formed by the upland drainage network should be identified. Thus, the upland drainage network (*UplandDrainageNetwork*) draining the *UplandMountainRange* should be identified.

5.3.2   Ontology Conceptualization

In the *Conceptualization phase*, the major categories determined in the *Specification phase* were represented in an initial taxonomy. For each class, properties which could be employed in their definition and identification were also examined. Following Argialas and Miliaresis (2000), It was determined that, at first, topographic forms should be identified (i.e. *Basin*, *Piedmont*, and *MountainRange*). Afterwards the *Piedmont* should be refined into the *AlluvialFan, Bajada*, and *CoalescingAlluvialFan* (Figure 26)*.
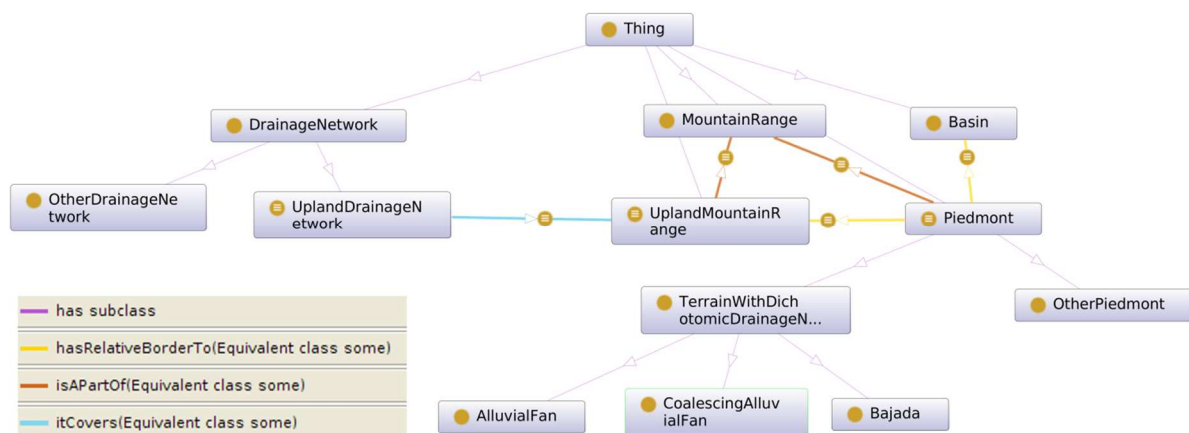
Figure 26: Conceptualization of the ontology.

At first the basin should be distinguished from the *MountainRange.* The *Basin* has large area extent and small slopes thus it can be identified based on its topography, through properties such as the MultiResolution index of Valley Bottom Flatness (MRVBF - Gallant and Dowling 2003). This index takes advantage of the slope and aspect of the present forms, and determines flat areas. The *MountainRange* should be separated into the *Piedmont* (where AFs reside) and *UplandMountainRange*. Considering the literature and after experimentation it was observed that alluvial fans (and thus bajadas as well) have slope gradient values from nearly 0°, and generally did not exceed 10°-12° and this should be involved in *Piedmont* identification. Furthermore, *Basin, MountainRange, and Piedmont* spatial organization can be implied from the definitions and thus is should be represented in the ontology. Since the *Piedmont* is part of the *MountainRange*, it has relative border with the *Basin.* Furthermore *Piedmont* has relative border with the *UplandMountainRange* which is eroded and the produced sediments are deposited on the *Piedmont.*

From the entire *DrainageNetwork*, *the UplandDrainageNetwork* and the *DichotomicDrainageNetwork* should be identified. *UplandDrainageNetwork* definition (which erodes the upland and carries the sediments) should correspond to the *DrainageNetwork*

covering the *UplandMountainRange*. Determination of the areas not drained by a dichotomic drainage pattern should aid in the elimination of piedmont areas which are not part of an AF. Thus, *DichotomicDrainagePattern* definition should encompass its geometry, topology, and texture. However, since the drainage network extraction did not represent network topology adequately, only its texture will be further quantified. Thus, *TerrainWithDichotomicDrainagePatternTexture* should represent objects having dichotomic drainage network texture. Pelletier (2013) employed low values of the *discharge-per-upstream-valley-head* ratio to eliminate from the drainage network areas where the flow was not confined. Since the dichotomic drainage network it is not integrated, the same heuristic can be employed in *TerrainWithDichotomicDrainagePatternTexture* definition. Furthermore, proper texture features such as the Haralick measures should be employed in its definition.

TerrainWithDichotomicDrainagePatternTexture should be refined into *AlluvialFan*, *CoalescingFan,* and *Bajada*. *AlluvialFan* definition should consider additional topographic properties related to its geometric signature which is close to a circular sector (CS). An index enhancing the *AlluvialFan* geometric signature was computed as follows. An ideal corresponding CS was determined for each AF (Figure 5). This required the computation of the CS angle and the direction of its bisector. CS center should be positioned on apex. An apex-like point was identified by intersecting *UplandDrainageNetwork* objects with each AF and selecting the stream-end closest to each AF centroid. CS angle bisector direction was defined as the line connecting the apex-like point and each AF centroid. The radius (R) of the CS sector was computed by extending the CS bisector until the end of each AF. The central angle was computed in Equation (38) as follows, while the final index value was computed as shown in Equation (39) as follows:

$$central angle = \frac{2AFArea}{R^2} \tag{38}$$

$$Fan-ShapeIndex = \frac{JointAFCSArea}{Joint\,AFCSArea + AFOnlyArea + CSOnlyArea} \tag{39}$$

In Equations (2-3) *AFArea* is the area of an AF, *JointAFCSArea* is the common area between an AF and its corresponding CS, *AFOnlyArea* is the area that belongs only to an AF and not its corresponding CS, and *CSOnlyArea* is the area that belongs only to the CS and not its corresponding AF.

From Figure 27 it is observed that alluvial fans were satisfactorily matched with a CS. In such cases, the fan-shape index had a value greater than 0.60-0.65. However, the CS is not coincident to the observed bajada/coalescing fan, since it is not clearly fan-shaped (although

it is composed of multiple fan-shaped objects). The Index value for the bajada was around 0.36.
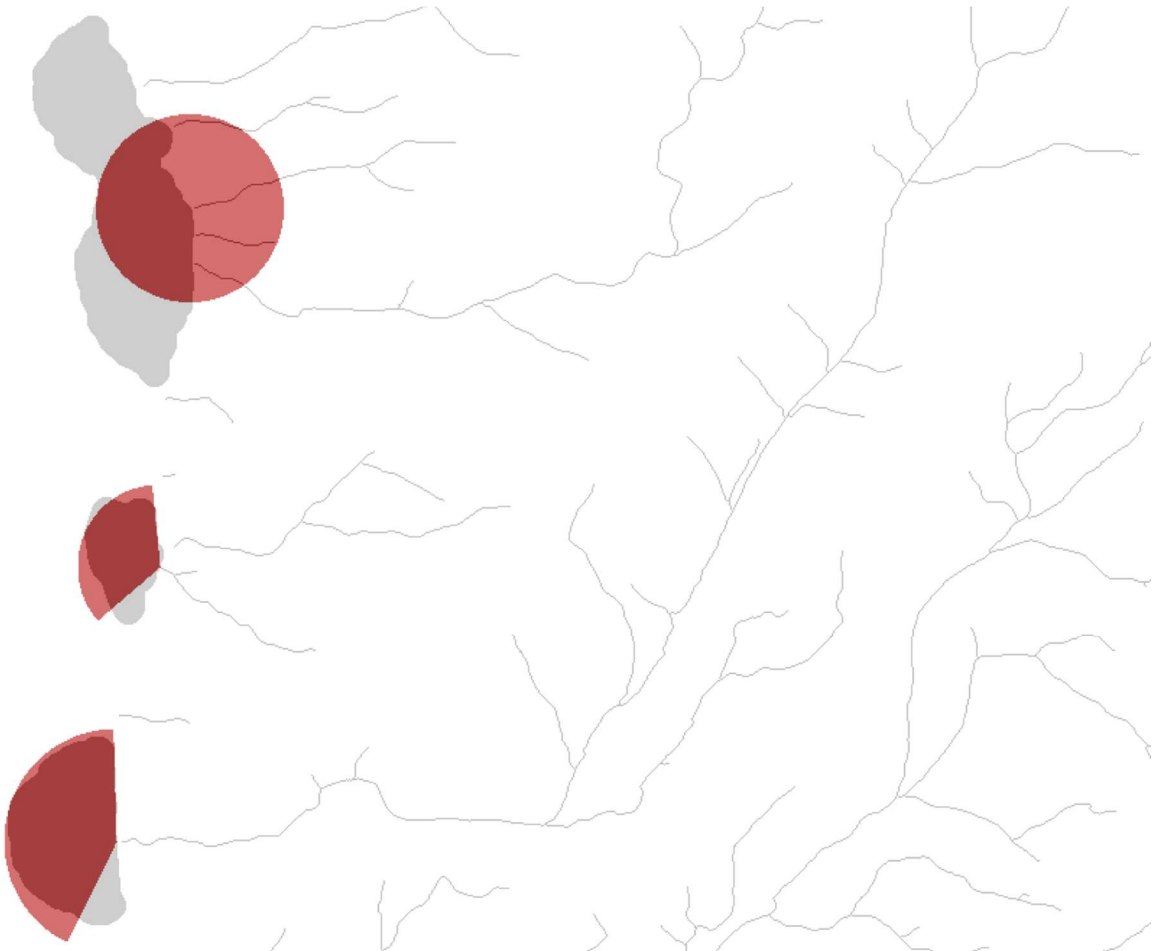
Figure 27: Example of fan-shape index computation. The *UplandDrainageNetwork* objects were intersected with AFs and apex-like points were defined as the stream edges closer to each AF centroid. The alluvial fans (middle and bottom) were satisfactorily matched with a circular sector. However, this was not true for the bajada/coalescing fan on the top.

5.3.3 Knowledge formalization for the Identification of Alluvial Fans and Bajadas

During *knowledge formalization*, the derived taxonomy from the *Conceptualization phase* was expanded into a fuzzy OWL 2 ontology. In the *conceptualization phase*, it was determined that *Basin, MountainRange,* and *Piedmont* areas need to be determined first (Figure 5 - Phase 1). Alluvial fans, bajadas, and coalescing fans should be detected afterwards, as sub-objects of *piedmont* (Figure 5 - Phase 2). Thus the developed formalization aimed at first to extract the *Basin* and the *Piedmont* areas. From the later, the fans and bajadas should be separated and identified. This was achieved after performing sufficient tests to determine through an iterative trial – and – error process the required number of segmentation levels, the exact taxonomy, classes, and properties for their definition.

Segments were derived by Definiens eCognition multiresolution segmentation (Baatz and Shäpe 2000, Trimble 2011) and were stored in PostgreSQL to be available to SPOR for the

reasoning process. In a multi-scale approach, larger objects were created on the higher levels of the hierarchy while finer-scaled objects on the lower. Figure 28 presents an overview of the classes developed and their interweaving, derived from the *knowledge formalization* stage. To represent the segmentation hierarchy within the classification hierarchy and ease the expression of spatial relationships between levels, each segmentation level was represented by a class. The class name indicated the level in the hierarchy and its purpose. Thus, for *Level 3* segmentation the class *Level3* was created. Details concerning the exact formalized classes, properties, and class definitions, can be found in the uploaded ontology in the following URL.

https://github.com/ArArgyridis/GEOBIA-Ontologies/blob/master/GEOBIA_alluvial_bajada.owl

5.3.3.1   Phase 1 - Identification of topographic forms
Level 4: Basin identification through topographic properties

Figure 29 presents magnifications of the major geomorphometric features employed in Phase 1. Based on the conceptualization scheme, classification began with the determination of Basin areas. Since it was difficult to determine a segmentation parameter to compute a single object for the entire Basin, it was decided to compute large objects representing parts of the Basin. Thus a large segmentation scale parameter should be employed.
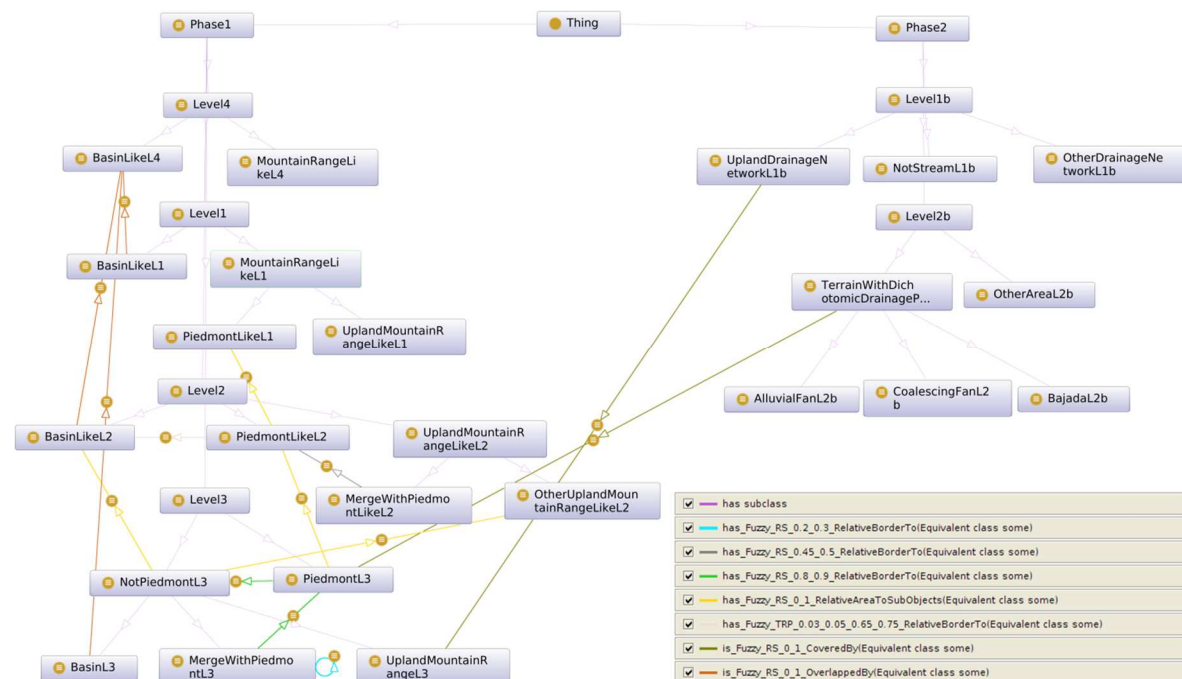
Figure 28: Final identification strategy. Phase 1 was designed to perform the identification of Basin, Mountain, and Piedmont areas. Phase 2 was designed to distinguish and identify each AF type.

After experimentation, a scale of 45 (shape 0.1, compactness 0.5) was found appropriate for the segmentation process and *Level 4* was designed as the highest in the hierarchy. Segmentation was performed on the slope gradient and the MRVBF index (Figure 29.f). Computation of the later requires a large number of parameters, however Gallant and

Dowling (2003) stated that adjustment of MRVBF slope gradient threshold, which is related to DTM resolution, should be sufficient to determine flat areas. The authors stated that a value of 32% was appropriate in the case of an 8m resolution DTM. Since NED has around 10m spatial resolution the 32% threshold was applied to compute the MRVBF. All other MRVBF parameters remained the same. Results were satisfactory since the basin had large values of the MRVBF index and was separated from the mountain range (Figure 29.f). The computation was performed on SAGA GIS (Condrad et al. 2015).
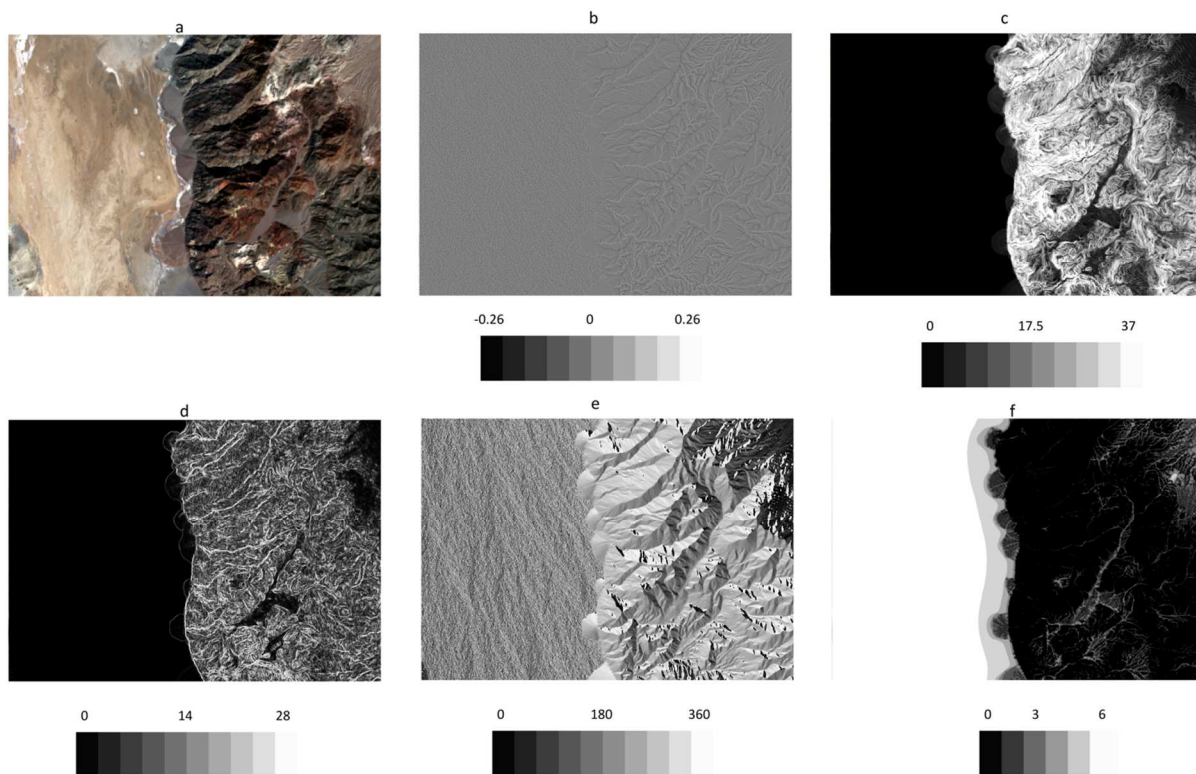
Figure 29: Subsets of the major geomorphometric features employed in Phase 1. a. Landsat OLi imagery. b. geometric curvature. AFs have medium values. c. slope gradient. AFs have slope values from near zero to 10-12 degrees. d. first order derivative of slope gradient. AFs have small values. e. aspect. Mountain range and AFs have small aspect variation. f. MRVBF index. Basin areas have medium to large values.

Based on the conceptualization scheme classification began with the declaration of *BasinLikeL4* and *MountainRangeLikeL4* as sub-classes of *Level4* (Figure 26, Figure 28). Definition of *BasinLikeL4* was based on the topography of the basin objects. Basin flatness was expressed through medium to large values of the *MRVBF* (Figure 29.f). Furthermore, it was observed that large values of the standard deviation of the *aspect* were also appropriate for *BasinLikeL4* definition, to properly separate the AFs from the basin, since their aspect is homogeneous compared to the basin (Figure 29.e). All other objects were classified as *MountainRangeLikeL4*. After classification the objects of each class were spatially merged.

Level 1: Identification of piedmont-like objects through topographic properties
To extract *Piedmont-Like* areas as sub-objects of the *MountainRangeLikeL4* objects, a new Level (*Level 1*) was created below *Level 4*. *Level 1* was designed to represent objects

completely included within the piedmont area. Thus, segmentation was performed on the slope gradient, with a smaller scale parameter (scale = 15, shape = 0.3, compactness = 0.5), on the objects classified as *MountainRangeLikeL4* (Figure 26, Figure 28). For *Level 1* classification, *BasinLikeL1* and *MountainRangeLikeL1* were created as sub-classes of *Level1*. *BasinLikeL1* was defined by projecting classification results from *Level 4* through the is_*Fuzzy_RS_0_1_OverlappedBy* spatial feature. All other objects were classified as *MountainRangeLikeL1.*

PiedmontLikeL1 and *UplandMountainRangeLikeL1* were created as sub-classes of the *MountainRangeLikeL1* (Figure 28). Since AFs reside on the Piedmont, properties representing AFs topography were added in *PiedmontLikeL1* definition*.* This involved slope gradient thresholds as they were depicted in the *Conceptualization* phase (Figure 29.c) which were represented through a fuzzy trapezoidal function as shown in Equation (40). The AFs gently-sloping property was represented through low values of the slope gradient first order derivative (Figure 29.d). Finally, to separate AF apex-like areas from the end of the upland drainage network, low to medium contour curvature values were also employed. Remaining *MountainRangeLikeL1* objects were classified as *UplandMountainRangeLikeL1*.

  Class: PiedmontLikeL1   EquivalentTo:

     MountainRangeLikeL1

      and (mCurvature some fuzzy_LS_0.011_0.013)

      and (mSlope some fuzzy_TRP_0.00_0.00001_10.0_20.0)

      and (mSlopeFirstOrderDerivative some fuzzy_LS_8.4_9.0)   (40)

This definition reads as follows: *MountainRangeLikeL1 objects having geometric curvature values smaller than 0.012, and slopes from nearly 0° to 10° but no more than 20°, and having values of the first order derivative of slope smaller than 8.7, were classified as objects of PiedmontLikeL1.*

Figure 30 presents subsets of *Level 1* classification result. It is observed that piedmont areas were satisfactorily identified. However, *MountainRange* areas were committed to *PiedmontLikeL1* objects and islands (gaps) were observed on the piedmont. To address these errors further refinement was necessary.
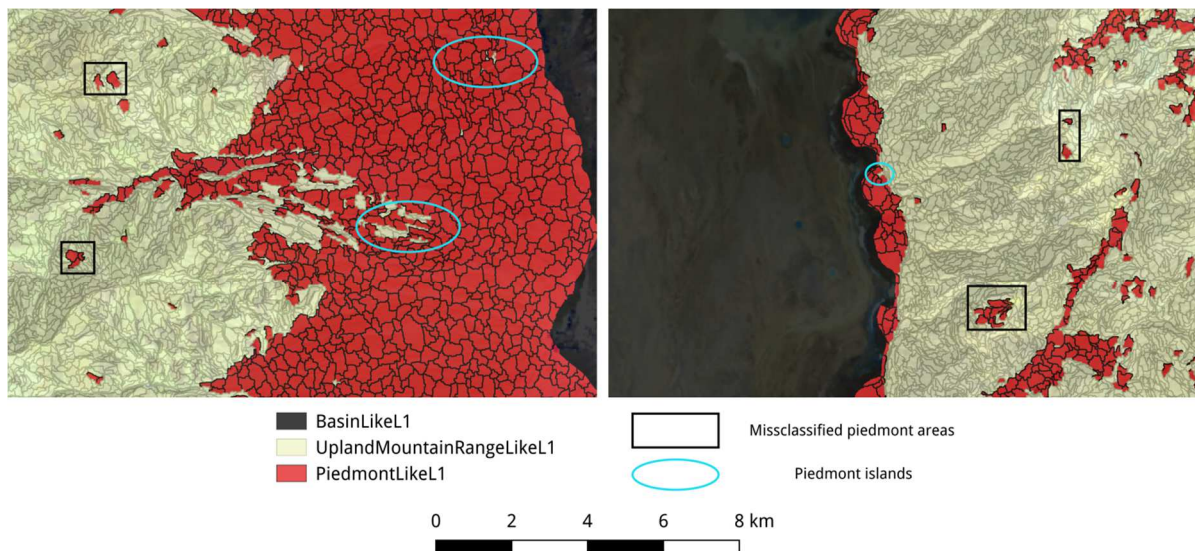
Figure 30: Subsets of Level 1 classification result.

Level 2: Piedmont identification through spatial reasoning

Upon identifying *Piedmont-Like* objects through topographic properties, now *Piedmont* spatial relationships should be expressed for its identification. Spatial reasoning was developed to identify the *Piedmont* as sub-object of the *MountainRangeLikeL4* objects having relative border with the *Basin* and to identify piedmont islands. To express piedmont spatial relationships, the piedmont area needed to be represented by a single object, thus *PiedmontLikeL1* objects were merged and *Level 2* was created above *Level 1*. *BasinLikeL2*, *PiedmontLikeL2*, and *UplandMountainRangeLikeL2* were created as sub-classes of *Level2* (Figure 28).

Level2 objects covered by objects classified as *BasinLikeL4* were classified as *BasinLikeL2*. *Level2* objects covering *PiedmontLikeL1* objects, with relative border with *BasinLikeL2* objects were identified as *PiedmontLikeL2*. All other *Level2* objects were classified as *UplandMountainRangeLikeL2*. To fill *PiedmontLikeL2* islands, *MergeWithPiedmontLikeL2* and *OtherUplandMountainRangeLikeL2* were created as sub-classes of *UplandMountainRangeLikeL2*. After trial-and-error as *MergeWithPiedmontLikeL2* were classified objects having at least 47.5% *relative border* with *PiedmontLikeL2* objects. All other objects were classified as *OtherUplandMountainRangeLikeL2*.

Level 3: Piedmont refinement through spatial reasoning

MergeWithPiedmontLikeL2 objects did not contain all *PiedmontLikeL2* islands, thus further piedmont refinement was necessary. To address this, a new level was created. *PiedmontLikeL2,* and *MergeWithPiedmontLikeL2* objects were merged together. Also *OtherUplandMountainRangeLikeL2* objects were merged and *Level 3*, was created between *Level 2* and *Level 4.* The classes *PiedmontL3*, and *NotPiedmontL3* were defined as sub-classes of *Level3* (Figure 28). *Level3* objects covering *BasinLikeL2* or *OtherUplandMountainRangeLike-*

L2 objects by at least 50% were classified as *NotPiedmontL3*. *Level3* objects, covering *PiedmontLikeL2* objects by at least 50%, having *relative border* with *NotPiedmontL3* objects greater than 85% were classified as *PiedmontL3*. As sub-classes of *NotPiedmontL3* the *BasinL3, MergeWithPiedmontL3*, and *UplandMountainRangeL3* were created. After experimentation, as *MergeWithPiedmontL3* were classified the objects having relative border greater than 85% with the objects classified as *PiedmontL3* or the objects having relative border greater than 25% with objects classified as *MergeWithPiedmontL3*.

NotPiedmontL3 objects, covered by *BasinLikeL4* objects, which were not classified as *MergeWithPiedmontL3* were classified as *BasinL3* (Figure 28)*. All other *NotPiedmontL3* objects were classified as *UplandMountainRangeL3*. The objects classified as *UplandMountainRangeL3*, *PiedmontL3,* and *MergeWithPiedmontL3* were merged after classification. Figure 31.a presents a detail of *Level 3* AF classification result in the Panamint Range region. It is observed that the piedmont and the remaining islands (*MergeWithPiedmontL3*) were satisfactorily identified. Furthermore Figure 31.b shows that in the Black Mountains region the piedmont was also satisfactorily identified, however the AFs are merged and further processing was required to separate them.

■ BasinL3
▨ UplandMountainRangeL3
■ PiedmontL3
■ MergeWithPiedmontL3
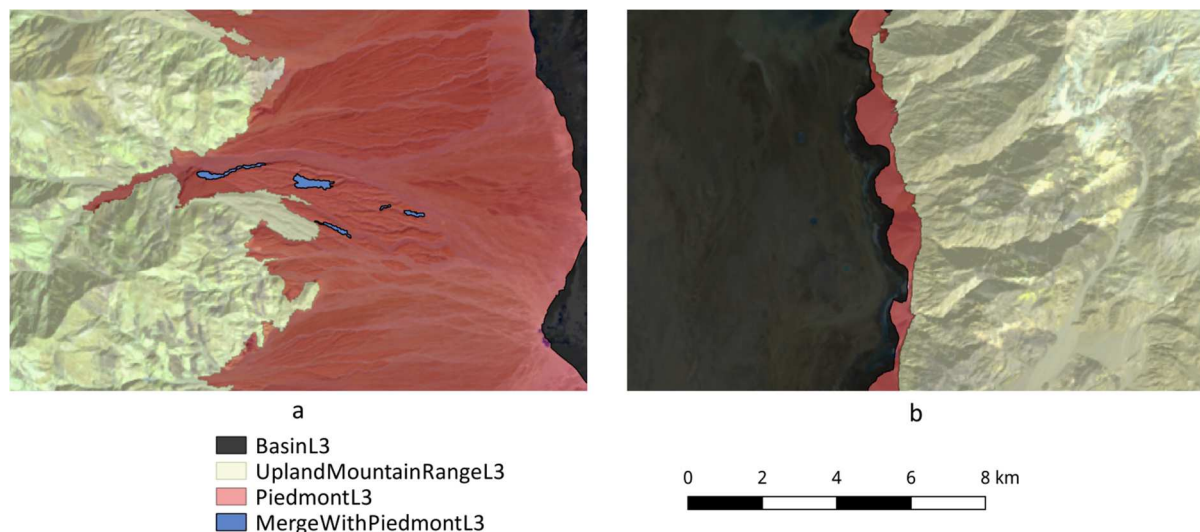
Figure 31: Classification result of Level 3. Background: Landsat OLi imagery. The piedmont was captured satisfactorily in both cases. a. The Panamint Range Piedmont islands were identified. b. Black Mountain AFs requires further processing to be separated.

5.3.3.2   Phase 2 - Identification of Alluvial Fans, Bajadas, and Coalescing Fans

Upon identifying the topographic forms related to AF spatial organization, now each AF form will be identified. Their identification will be based on drainage pattern texture, and geometric properties.

The *UplandDrainageNetwork* should be identified to determine apex-like points and compute the fan-shape index. To compute proper objects representing the *UplandDrainageNetwork* (Figure 26), these objects should not be covered by AFs. It was determined that at first the AF

objects should be created on an upper level and the drainage network should be created on the lower. After the determination of the *UplandDrainageNetwork,* the AFs could be separated into the *AlluvialFan, CoalescingFan*, and *Bajada* classes*.

Level 2b: Separation of each alluvial feature through morphological opening

Separation of each AF object was achieved through morphological opening on all *Level 3* objects. However, since this action would affect the hierarchical properties of the segmentation levels, it was decided that a new segmentation hierarchy should be developed. (Figure 26, Figure 28). The upper level was designed to represent each individual AF. Thus, at first, morphological opening on all *Level 3* objects with a 10 pixel radius structural element was performed and *Level 2b* was created. Classification of *Level 2b* objects was performed after *UplandDrainageNetwork* identification since the later is required for the computation of AF fan-shape index.

Level 1b: Upland Drainage Network Identification

To determine the upland drainage network (*UplandDrainageNetwork* – Figure 26), a new level (*Level 1b*) was developed on the lowest level of the second hierarchy. Since the drainage network had a single-pixel width, a scale parameter equal to 1 was employed in the segmentation process, resulting into pixel-sized objects. Segmentation was performed on the Strahler raster. As sub-classes of *Level1b,* the classes *UplandDrainageNetworkL1b*, *NotStreamL1b*, and *OtherStreamL1b* were created (Figure 26, Figure 28). Streams with sufficient sediment carrying capacity were considered these having Strahler order larger than 3. Furthermore, these streams should drain the upland mountain range in order to produce the required sediments. Thus, the class *UplandDrainageNetworkL1b* was defined in Equation (41) as follows:

  Class: UplandDrainageNetworkL1b   EquivalentTo:

    Level1b

    and (is_Fuzzy_RS_0_1_CoveredBy some UplandMountainRangeL3)

    and (mStrahler some fuzzy_TRP_2_3_254_255)   (41)

This definition reads as follows: Level1b objects covered by UplandMountainRangeL3 objec*ts, having Strahler order greater than 3, were classified as UplandDrainageNetworkL1b.*

Level 2b: Dichotomic drainage pattern texture and alluvial feature identification

On *Level 2b*, AFs were separated from other objects, based on heuristics representing dichotomic drainage pattern texture properties. Thus, the classes *TerrainWithDichotomicDrainagePatternTextureL2b* and *OtherAreaL2b* were developed (Figure 26, Figure 28). Figure 32 presents the main features employed for the final identification of *TerrainWithDichotomicDrainagePatternTextureL2b*.
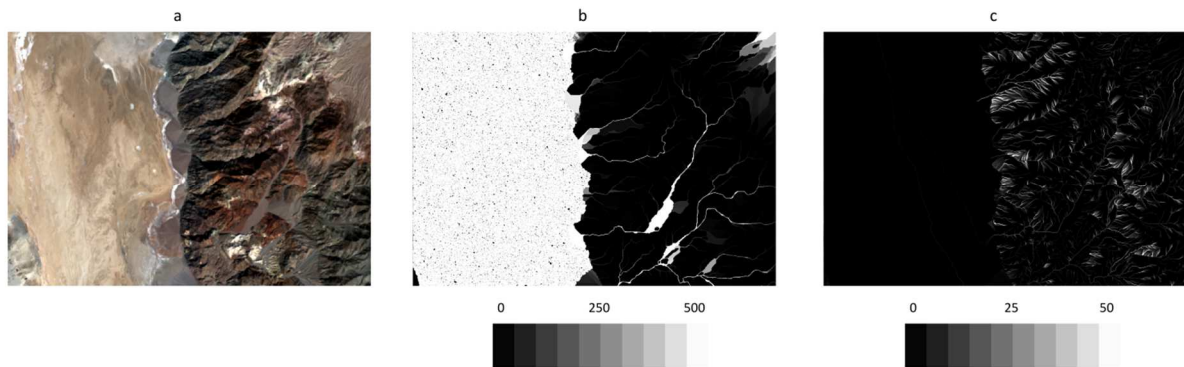
Figure 32: Major geomorphometric features employed in Phase 2. a. Landsat OLi imagery. b. number of valley head contribution for each pixel. AFs and basin have a large number of contributing valley heads per pixel c. discharge-per-upstream-valley-head ratio. AFs and basin have low values of this ratio.

TerrainWithDichotomicDrainagePatternTextureL2b was defined as follows. As shown in the conceptualization phase, these areas should be part of the piedmont, having low values of the discharge-per-upstream-valley-head (Figure 32.c). Furthermore, since in the AFs the flow is not confined but it is rather distributed on the entire area due to the dichotomic drainage pattern, the *discharge-per-upstream-valley-head* and *flow accumulation values* were low and were not deviating much. This heuristic was represented in the ontology through low values of the Grey-Level Co-occurrence Matrix (GLCM) Contrast and the GLCM Angular 2nd Moment Haralick features. These features have small values on areas with small local variation. Appropriate values for these features were determined by plotting their values in QGIS and testing appropriate thresholds. AF formation requires a considerable sediment quantity. Thus it was assumed that a considerable number of streams should contribute flow into the apex, thus an AF should receive flow from a large number of upstream valley-heads. However, since all streams end up in the basin, the basin has very large values of this feature (Figure 32.b). Thus, medium values of flow-contributing valley heads per pixel were included into *TerrainWithDichotomicDrainagePatternTextureL2b* definition. Finally small noise was eliminated by applying an area feature restriction. Definition of the class *TerrainWithDichotomicDrainagePatternTextureL2b* is presented in Equation (42) as follows.

Class: TerrainWithDichotomicDrainagePatternTextureL2b   EquivalentTo:

    Level2b

    and (is_Fuzzy_RS_0_1_CoveredBy some PiedmontL3)

    and (areaPxl some fuzzy_RS_330_350)

    and (glcmContrastAccumulation some fuzzy_LS_800_900)

    and (glcmAngular2ndMomentDischargePerValleyHead some fuzzy_LS_0.5_0.6)

    and (glcmContrastDischargePerValleyHead some fuzzy_LS_640_700)

    and (mDischargePerValleyHead some fuzzy_LS_8.0_8.5)

    and (mNumberOfValleyHeads some fuzzy_TRP_130_210_5000_6000)　　　　(42)

This definition reads as follows: *Level2b objects covered by PiedmontL3 objects, having area greater than 340 pixels, and GLCM contrast values (computed on the flow accumulation) smaller than 850, and GLCM Angular 2nd Moment values (computed on the discharge-per-upstream-valley-head) smaller than 0.55, and GLCM Contrast values (computed on the discharge-per-upstream-valley-head) smaller than 670, and discharge-per-upstream-valley-head values smaller than 8.25, accepting flow from 170 to 5500 valley heads, were classified as TerrainWithDichotomicDrainagePatternTextureL2b.*

Based on the conceptualization scheme, *TerrainWithDichotomicDrainagePatternTextureL2b* objects were further separated into *AlluvialFanL2b*, *BajadaL2b*, and *CoalescingFanL2b* (Figure 26, Figure 28)*.* As *AlluvialFanL2b* were classified *DichotomicDrainagePatternTextureL2b* objects having *fanShape* index values greater than 0.60. As *CoalescingFanL2b* were classified the small bajadas in the area. It was determined that these should be defined as areas which were not classified as *AlluvialFanL2b* (thus they could not be determined as fan-shaped) having a maximum area determined by a left shoulder function with left border equal to 80000 and right border equal to 140000 pixels. All other areas were classified as *BajadaL2b.* Evaluation of results was satisfactory since the AF entities were successfully identified. However, overlaying the results on Landsat OLi imagery indicated a systematic omission error on the fan-toe of the AFs. This error was corrected by considering the spectral signature of the soil composing each individual AF as it will be presented in the next section.

5.3.4   Fan-toe shape Refinement based on Soil Spectral Signature

To correct the fan-toe of the AFs, the soil spectral signature of each AF needed to be enhanced through proper spectral indices. It was determined that such indices should present each AF with a homogeneous spectral signature. After experimentation, the following approach was developed. PCA-2 was appropriate to enhance bajada spectral signature and PCA-3 was

appropriate for alluvial fans and coalescing fans. For each AF the mean and standard deviation of its respective index was computed. Afterwards to identify candidate pixels for addition to each AF and avoid merging the AFs between them, through experimentation, dilation was performed with a 30-pixel radius disk. If a pixel belonging to the dilated AF had a PCA-2(3) value in the range [mean – std, mean + std] and was classified as *BasinL3* it was added to the original AF. For shape optimization, gap filling, and morphological opening with a 9 kernel radius was performed on the result of this process. The result was vectorized and the objects overlapping the original DEM-derived AFs were retained. The effects of this process are presented in Figure 33. It is observed that the boundary of the AFs is extended within the basin, following the spectral signature of the material each AF is composed.
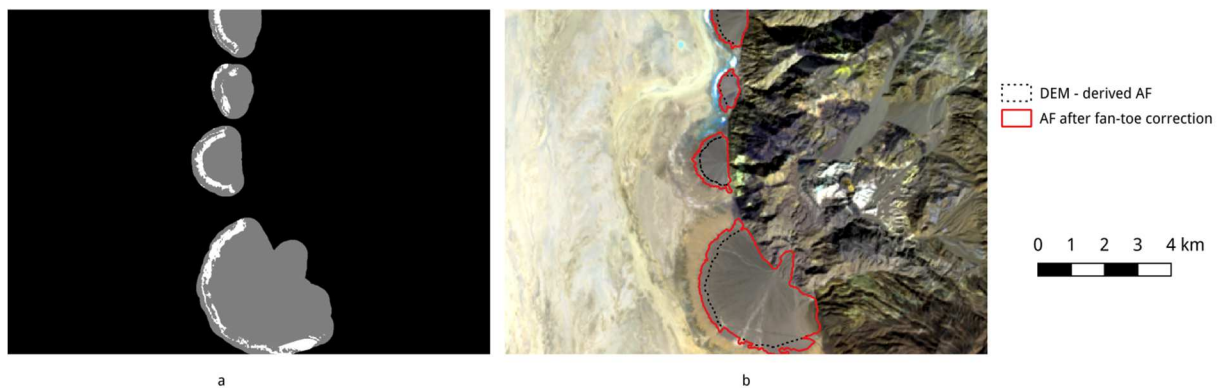
Figure 33: a. Each dilated AF is presented with grey color, while in white are denoted the criterion-determined, dilated, AF pixels. b. Final results after gap filling on Landsat OLi imagery.

The final classification result is presented in Figure 34. The major fan/coalescing fans and bajadas in the examined area were successfully identified. Furthermore, the majority of each AF omitted alluvial material was included to the final result through the spectral shape optimization.

5.4   Evaluation of Results and Discussion

Classification results were compared with reference data derived by human interpretation and evaluated as follows. At first the areas correctly detected (True Positive – TP), omitted (False Negative – FN) or committed (False Positive – FP) were computed by comparison to the reference data. Based on these areas, the Completeness, Correctness and Quality indices (Agouris et al. 2004) were computed as presented in Equations (4)-(6). The results are presented in Table 8.

Omission errors were observed on the northern parts of the bajadas, which were caused by the criteria involved in *PiedmontLikeL1* identification. Small commission errors were caused due to the existence of alluvial material with similar spectral signature with the AFs within the Badwater basin. Visual evaluation of the result was performed by comparing the existing road near the Black Mountains with the extracted alluvial/coalescing fan polygons. The comparison

99

is sound, since the roads are built on the same level as the alluvial fan surface because roads that are lower than the surface of the fan tend to be buried and roads that are higher may be destroyed by floods (Bull 1977). It was observed that the border of the road followed satisfactorily the fan border towards the playa. It should be noted that the objects classified as *AlluvialFanL2b* and *CoalescingFanL2b* did not contain the coalescing zone between fans, since the aim was to identify individual AFs. Extraction of this zone as a part of an alluvial/coalescing fan would result into their merging, which was undesirable. Small alluvial fans (Figure 12) were not identified by the developed method. Their size was too small and the geometry of the extracted objects were considerably affected by the morphological opening process. Thus, further investigation is required to identify them, or consider examining finer resolution data.
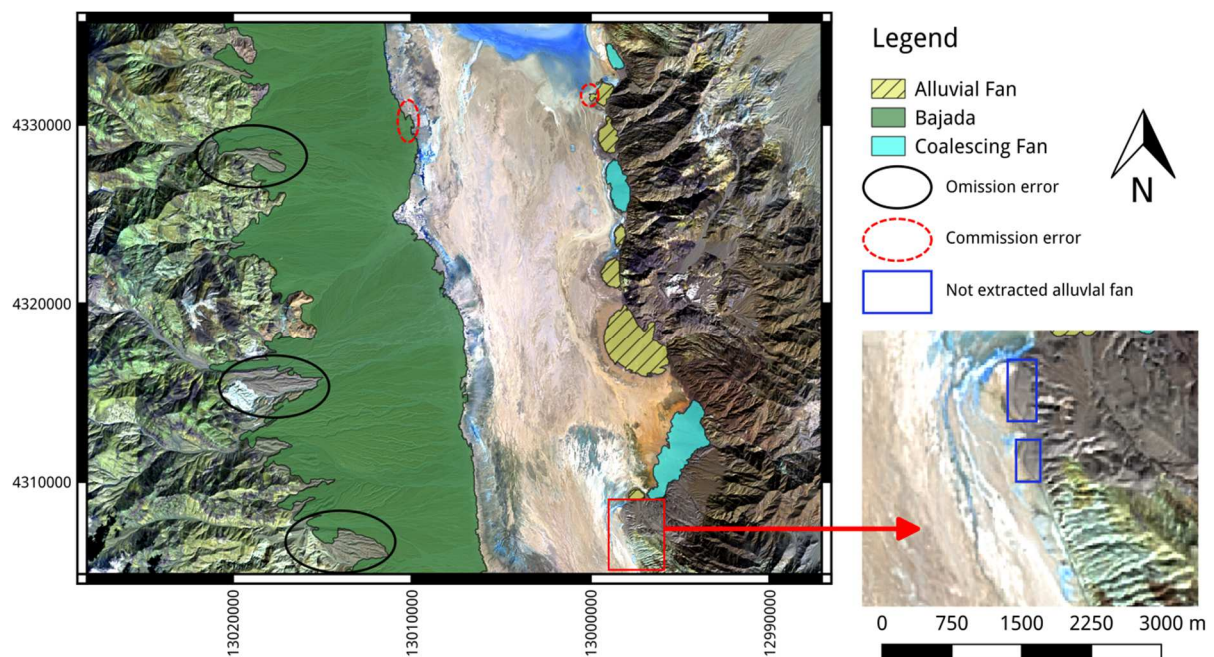
Figure 34: Areas identified as alluvial fan, coalescing fan, and bajada, shown on Landsat OLi 765 color composite. In the magnification small alluvial fans, not extracted, in the present study are presented. The coordinates are in WGS 84 Pseudo Mercator (EPSG: 3857).

Table 8: Comparison of the extracted alluvial fan, coalescing fan, and bajadas with reference data.

	Omission Error (%)	Commission Error (%)	Completeness (%)	Correctness (%)	Quality (%)
Alluvial Fans	11.9	4.1	88.1	95.5	84.6
Coalescing Fans	15.1	5.0	84.9	94.4	80.8
Bajadas	9.5	1.3	90.5	98.6	89.4
Total	**9.8**	**1.5**	**90.2**	**98.3**	**88.8**

Overall an omission and commission error of 9.7% and 1.8% was achieved. The largest omission error was computed for the coalescing fans (15.1%) while the largest commission

error was computed for the alluvial fans and (6.1%). The smallest errors were computed for both measures for the bajadas. Similar results were obtained through the evaluation with the Completeness, Correctness, and Quality indices. For coalescing fans the smallest quality was scored (82.4%) while for bajadas the largest (89.4%). These findings can be justified since the bajadas have very large area extent, and thus, the omission/commission errors observed on their border did not affect the evaluation significantly. It should be noted however that in the evaluation process as isolated alluvial fans were considered and old alluvial fans that may completely contain younger alluvial fans, since in such cases only the geometric signature of the old alluvial fans could be examined by the developed approach.

The developed GEOBIA approach for alluvial fan, coalescing fan, and bajada identification was based on the landform-pattern element approach. The semantic gap between the human-employed semantics in terrain analysis, the low-level numerical values, and medium level descriptors employed in an automated approach, was addressed through the design and development of a fuzzy ontology. This required the investigation, development and interweaving of numerical indices expressing the shape, topography and spatial organization of the examined landforms and their employment in landform class representation. To aid drainage network extraction, optimal wiener filtering reduced DTM noise, and flat and sink areas were treated through an enhanced version of PDEM algorithm. Drainage extraction results showed that the drainage was extracted satisfactorily in the upland areas (Figure 4). However, the extracted drainage network in each AF was not integrated (like it is in the dendritic or rectangular drainage pattern). The number of the branches composing the dichotomic drainage pattern were not sufficient, and they required topological correction. Thus, it was not possible to identify the dichotomic drainage pattern through geometric and topological relations of the extracted streams as in cases of integrated drainage networks (Argialas et al. 1988, Ichoku and Chorowicz 1994). Improper extraction could be also affected by the fact that dichotomic drainage pattern streams present braiding causing them to intersect. Furthermore, examination of the accumulation raster showed that most of the surface of each AF was accepting flow. This made difficult for the drainage extraction algorithm to initiate the dichotomic drainage pattern branches. Additionally the drainage network was not extracted satisfactorily in the basin area. A lot of streams were extracted, creating a rather complex drainage network system within the basin. This was caused by the fact that the basin is a rather flat area, with small slopes, thus the water is not confined in streams but in rain events it spreads within the entire basin area. However, since the drainage network in the basin was not a requirement in this study, it was not further examined.

Previous GEOBIA studies extracted alluvial fans by taking advantage on their slope gradient, curvature properties, elements of the upland drainage network, spectral, and spatial properties. The employed semantics examined mostly the topographic properties of the

alluvial fans, thus identifying the alluvial fans as a topographic form. Furthermore, in the event of multiple co-existing alluvial fans, each alluvial fan was not examined as a separate entity but rather the entirety of alluvial fans were examined as a unified polygon area. However, the landform-pattern element approach human interpretation descriptors examine landform properties as a single entity. Furthermore, additional properties referring to the shape and the landform specific drainage network pattern and texture are also examined. Thus, to properly investigate such properties, in this study proper descriptors were designed and implemented. The developed reasoning in the first GEOBIA phase aimed to take advantage of the topographic properties (slope gradient, curvature, spatial organization), similar to previous studies, to identify the piedmont areas. To examine each form separately, through morphological operations the piedmont polygons were refined and objects corresponding to single alluvial fan entities were created. Although distant alluvial fans, coalescing fans and bajadas were satisfactorily separated, this process could not separate alluvial fans in cases where an older alluvial fan may contain younger alluvial fans. Such refinement would require further processing which could examine indicators such as the upland drainage network related with an alluvial fan (e.g. the number of streams which touches an AF) and the extraction of strong and weak edges in order to identify the border of the younger alluvial fans within the older AF. Drainage network texture was approximated by developing the class *TerrainWithDichotomicDrainagePatternTextureL2b* which was defined by features such as the mean value of the discharge-per-upstream-valley-head ratio, its GLCM Contrast and 2nd Angular moment, and the number of contributing valley-heads per pixel. However, the drainage pattern approximation did not examined the topological relationships of the drainage network streams. Furthermore, the landform-pattern element approach examines the landform drainage network texture visually, by examining the density of the drainage network streams. Thus, investigation of methods for dichotomic drainage network pattern extraction should be performed towards the automatic identification of alluvial fans.

Since individual alluvial fans have a characteristic fan-shape geometric signature, while coalescing fans and large-extent bajadas do not, a fan-shape index was developed which examined the site, the relation with the upstream drainage network, and each AF orientation. Large scores were computed for isolated alluvial fans, and lower scores were computed for coalescing fans and bajadas. However, since an old alluvial fan could contain younger alluvial fans which could not be separated, during fan-shape index computation the geometric signature of the old alluvial fans was only examined. However, in the event that younger alluvial fans would be identified, their shape could be also examined in this approach.

5.5   Conclusions

Earlier GEOBIA studies, considered the slope, spectral, and spatial organization for alluvial fan or bajada identification. In this study these properties were examined and interweaved with

additional landform pattern elements which consider the landform shape (fan shaped) and the drainage network pattern (dichotomic) through the development of a fuzzy ontology. Heuristics were developed to express the drainage network texture. A fan-shape index was developed to examine each form shape. The developed approach should work satisfactorily in areas with similar conditions. However, towards the automation of alluvial fan mapping and the identification of specific types of alluvial fans further investigation is required. This can be aided by the developed algorithms and the developed ontology which are available online and can be examined by anyone who wants to investigate alluvial fan mapping and further enhance it.

Future work might include some of the following. The developed method can be extended to consider other, more complex cases, e.g. to examine cases when the bajada has covered the entire basin, examine fans and bajadas in humid climates, to examine coalescing fans in cases where younger fans are formed over older fans, examine cases where the alluvial materials are not exposed but are covered by vegetation or infrastructure, or determination of more appropriate indices to emphasize alluvial materials. It is also desirable to investigate the extraction of the dichotomic drainage pattern through topological properties, by either employing finer DTM data, or investigating other approaches for drainage network extraction.

6 Overall Conclusions and Prospect

In this research state-of-the-art image analysis, machine-learning, and knowledge representation methods were investigated towards the automatic identification of landscape components within the framework of GEOBIA.

Ontologies were developed for the following remote sensing problems: building extraction and change detection, foreshore extraction, and alluvial fan, coalescing fan, and bajada identification. In all cases, the required knowledge was satisfactorily represented with an ontology, based on the available axioms (Chapter 2). By assigning objects to the thematic categories defined in the developed ontologies, SPOR classified successfully single (Chapter 2, Chapter 3, Chapter 4) and multiple segmentation hierarchies (Chapter 5), thus addressing the first objective of this research. Furthermore both machine learning and fuzzy ontological reasoning was employed simultaneously within SPOR (Chapter 4). This qualifies SPOR as a satisfactory classifier for GEOBIA, and addresses the second research objective. The derived classification results were compared with reference data, with promising results, thus, addressing the third objective of this research. For the development of SPOR, DEM depression treatment, and drainage extraction algorithms, free (as in freedom) software such as LibXML2, Boost, PostgreSQL/PostGIS, OrfeoToolbox, QGIS, and GDAL was employed. For SPOR knowledge formalization the open standard OWL 2 was adopted. For all algorithms the coding was performed in C++ to gain in terms of computation performance. All developed algorithms and ontologies are available on the following GitHub repository under the terms of GPL v3, thus addressing the fourth and final objective of this research.

https://github.com/ArArgyridis/

Future work, might include some of the following. A significant amount of effort has been developed within the GEOBIA community to extract semantic information from images. The results of these efforts (knowledge bases, employed strategies, extraction processes) today exist only on paper or isolated and unrelated implementations. Thus, the generic knowledge base is available only to a limited number of individuals. Development of multiple GEOBIA ontologies for different remote sensing problems in this dissertation depicts their suitability for knowledge formalization. Furthermore adoption of Semantic Web technologies for knowledge representation can provide for sharing, extension, and integration of the developed ontologies with others from the same or different disciplines. Therefore, such efforts provide an opportunity for the development of a collaboration tool to allow exchanging and enhancing of the developed ontologies for image extraction by all GEOBIA community.

During GEOBIA analysis it is often desirable to perform pre-classification or post-classification processes on the objects belonging to a single or multiple classes (e.g. object merging or morphological operations). SPOR could be extended through its integration with image

analysis tools such as Orfeo Toolbox or vector processing tools such as QGIS in order to perform such actions. Encoding of such information within a GEOBIA ontology can be performed by designing and implementing proper metadata describing the exact processes and the order in which they should be executed on the objects of a class.

Integration of SPOR with technologies such as PostgreSQL, allows for sharing classification results through OGC Services such as Web Map Services (WMS) and Web Feature Services (WFS) over the Internet. By taking advantage of such protocols, a free and open source web application which can perform GEOBIA processing can be built. A web server integrating segmentation algorithms such as MSEG (Tzotsos and Argialas 2006) and SPOR for the classification process is required. A Graphical User Interface (GUI) which can allow to design GEOBIA processes (e.g. developing processing flows, optimizing segmentation parameters, developing classes for the classification process) can be built by taking advantage on W3C standards such as HTML5, CSS3, and Asynchronous Javascript and XML (AJAX) techniques. Exchange of information between the server and the GUI can be performed by developing Representational state transfer (REST) services. Javascript libraries such as OpenLayers or Leaflet can be employed to display web maps and classification results.

Bibliography

Agouris, P., Doucette, P., and Stefanidis, A., 2004. Automation and digital photogrammetric workstations. *In:* C. McGlone, E. Mikhail, and J. Bethel eds. *Manual of Photogrammetry (5th Edition)*. American Society of Photogrammetry and Remote Sensing, 949-981.

Argialas, D., and Harlow, C., 1990. Computational image interpretation models: an overview and a perspective, *Photogrammetric Engineering and Remote Sensing*, 56 (6), 871–886.

Argialas, D., and Tzotsos, A., 2006. Extraction of Physiographic Features and Alluvial Fans in Nevada, USA, from Digital Elevation Models and Satellite Imagery through Multiresolution Segmentation. *Proceedings of the ASPRS Annual Conference*, Reno, Nevada.

Argialas, D., Lyon, J., and Mintzer, O., 1988. Quantitative description and classification of drainage patterns. *Photogrammetric Engineering and Remote Sensing*, 54 (4), 505–509.

Argialas, D., Michailidou, S., and Tzotsos, A., 2013. Change detection of buildings in suburban areas from high resolution satellite data developed through object based image analysis. *Survey Review*, 45 (333), 441–450.

Argyridis, A. and Argialas, D.P., 2015. A fuzzy spatial reasoner for multi-scale geobia ontologies. *Photogrammetric Engineering and Remote Sensing*, 81 (6), 491–498.

Argyridis, A., Argialas, D.P., 2016. Building change detection through multi-scale GEOBIA approach by integrating deep belief networks with fuzzy ontologies. *International Journal of Image and Data Fusion*, 7 (2), 148 – 171

Argyridis, A., Argialas, D.P., 2017a. GEOBIA-based identification of alluvial fans and bajadas through geomorphometry, image analysis, and fuzzy ontology. *International Journal of Image and Data Fusion*. In minor revision.

Argyridis, A., Argialas, D.P., 2017b. Fuzzy ontology-based foreshore identification from digital terrain model and very high resolution airborne imagery through GEOBIA multi-scale analysis. In review.

Arvor, D., Durieux, L., Andrés, S., and Laporte, M.-A., 2013. Advances in Geographic Object-Based Image Analysis with ontologies: A review of main contributions and limitations from a remote sensing perspective. *ISPRS Journal of Photogrammetry and Remote Sensing*, 82, 125–137.

ASPRS, 1997. *Manual of Photographic Interpretation 2nd Edition.* Bethesda: ASPRS.

Asselen, S., and Seijmonsbergen, A.C., 2006. Expert-driven semi-automated geomorphological mapping for a mountainous area using a laser DTM, *Geomorphology*, 78 (3–4), 309–320. doi:10.1016/j.geomorph.2006.01.037.

Baatz, M., and Schäpe, A., 2000. Multiresolution segmentation: an optimization approach for high quality multi-scale image segmentation. In: J. Strobl, T. Blaschke, and G. Griesebner, eds. *Angewandte Geographische Informations - Verarbeitung XII*. Heindelberg: Wichmann-Verlag, 12–23.

Band, L., 1986. *Topographic partition of watersheds with digital elevation models. Water Resources Research*, 22 (1), 15-24.

Bannour, H., and Hudelot, C., 2014. Building and using fuzzy multimedia ontologies for semantic image annotation. *Multimedia Tools and Applications*, 72 (3), 2107–2141.

Baptist, E., 2009. *A multi-scale object-bases approach to mapping coastal Natura 2000 habitat types using high spatial resolution airborne imagery and LIDAR data*.

Belgiu M., T. Lampoltshammer, and B. Hofer, 2013. An Extension of an Ontology-Based Land Cover Designation Approach for Fuzzy Rules*, GI_Forum 2013: Creating the GISociety*, (T. Jekel, A. Car and G. Griesebner editors), Austrian Academy of Sciences Press, Vienna, Austria, pp. 59-70.

Belgiu, M., and Lampoltshammer, T., 2013. Ontology based interpretation of very high resolution imageries – grounding ontologies on visual interpretation keys. *Sixteenth AGILE International conference on geographic information science*. 14-17 May 2013, Leuven Belgium, 1-5.

Belgiu, M., Tomljenovic, I., Lampoltshammer, T., Blaschke, T., Höfle, B., 2014. Ontology-based classification of building types detected from airborne laser scanning data. *Remote Sensing*, 6 (2), 1347-1366.

Bengio, Y., Lamblin, P., Popovici, D., and Larochelle, H., 2007. Greedy layer-wise training of deep networks. *Advances in Neural Information Processing Systems* 19, 153-160.

Beratan, K., and Anderson, R., 1998. The use of Landsat thematic mapper data for mapping and correlation of quaternary geomorphic surfaces in the southern Whipple mountains, California, *International Journal of Remote Sensing*, 9 (12), 2359–2435.

Bertels, L., Houthuys, R., Deronde, B., Janssens, R., Verfaillie, E., and Van Lancker, V., 2012. Integration of Optical and Acoustic Remote Sensing Data over the Backshore-

Foreshore-Nearshore Continuum: A Case Study in Ostend (Belgium). *Journal of Coastal Research*, 28 (6), 1426–1436.

Bertrand de Beuvron, F., Marc-Zwecker, S., Puissant, A., Zanni-Merk, C., 2013. From expert knowledge to formal ontologies for semantic interpretation of the urban environment from satellite images. *International Journal of Knowledge-Based and Intelligent Engineering Systems*, 17 (1), 55–65.

Bishop, C.M., 2006. *Pattern Recognition and Machine Learning*. Berlin, Heidelberg: Springer, 738p.

Bissenbach, E., 1954. Geology of alluvial fans in semi-arid regions. *Bulletin of the Geological Society of America*, 65, 175-190.

Blair, T., and McPherson, J., 2009. Processes and forms of alluvial fans. In A. Parsons and A. Abrahams eds. *Geomorphology of Desert Environments*. Dordrecht: Springer, 413–467. doi:10.1007/978-1-4020-5719-9_14.

Blaschke, T., and Strobl, J., 2010. Geographic information science developments. *GIS Science - Zeitschrift für Geoinformatik*, 23(1), 9-15.

Blaschke, T., Hay, G.J., Kelly, M., Lang, S., Hofmann, P., Addink, E., Queiroz Feitosa, R., van der Meer, F., van der Werff, H., van Coillie, F., and Tiede, D., 2014. Geographic Object-Based Image Analysis - Towards a new paradigm. *ISPRS Journal of Photogrammetry and Remote Sensing*, 87, 180–191.

Blaschke, T., S. Lang, and G. Hay, 2008. *Object-Based Image Analysis - Spatial concepts for knowledge-driven remote sensing applications*. Springer, New York, 818 p.

Bobillo, F. and Straccia, U., 2011. Fuzzy ontology representation using OWL 2. *International Journal of Approximate Reasoning*, 52 (7), 1073–1094.

Bouziani, M., Kalifa, G., and Dong-Chen, H., 2010. Automatic change detection of buildings in urban environment from very high spatial resolution images using existing geodatabase and prior knowledge. *ISPRS Journal of Photogrammetry and Remote Sensing,* 65 (1), 143–153.

Braga, F., Tosi, L., Prati, C., and Alberotanza, L., 2013. Shoreline detection: Capability of COSMO-SkyMed and high-resolution multispectral images. *European Journal of Remote Sensing*, 46 (1), 837–853.

Brunner, D., Lemoine, G., and Bruzzone, L., 2010. Earthquake damage assessment of buildings using VHR optical and SAR imagery. *Geoscience and Remote Sensing IEEE Transactions* 48 (5), 2403-2420.

Brusa, G., Caliusco, M., and Chiotti, O., 2006. A process for building a domain ontology: an experience in developing a government budgetary ontology. *Proceedings of the AOW*

Second Australasian Workshop on Advances in Ontologies. 5 December 2006, Hobalt, Australia, 72, pp. 7-15.

Bull, W., 1977. The alluvial fan environment. *Progress in Physical Geography*, 1, 222–270.

Burnett, C., and Blaschke, T., 2003. A multi-scale segmentation / object relationship modelling methodology for landscape analysis. *Ecological Modelling*, 168(3), 233-249.

Deng, L., and Yu, D., 2014. Deep learning: methods and applications. *Foundations and Trends in Signal Processing,* 7 (3–4), 197-387.

Department of Water, 2012. *Operational policy 4.3: identifying and establishing waterways foreshore areas*. Australia: *Department of Water, Perth*.

Ding, L., Kolari, P., Ding, Z., and Avancha, S., 2007. Using Ontologies in the Semantic Web: A Survey. *Integrated Series in Information Systems*, 14, 79-113.

Doulaverakis C., Tzotsos, A., Tsampoulatidis, I., Gerontidis, N., Argyridis, A., Karantzalos, K., Kompatsiaris, I., and Argialas, D., 2014. Gnorasi: a modular knowledge-based platform for object-based image analysis, Proceedings of 5th GEOBIA, Advancements, Trends and Challenges, Thessaloniki, Greece, 3(2S), pp. 473-476.

Doxani, G., Karantzalos, K., and Tsakiri, M., 2012. Monitoring urban changes based on scale-space filtering and object-oriented classification. *International Journal of Applied Earth Observation and Geoinformation*, 15, 38–48.

Drăgut, L., and Eisank, C., 2011. Object representations at multiple scales from digital elevation models. *Geomorphology*, 129 (3-4), 183-189.

Drummond, A., and Erkeling, G., 2014. Drainage pattern. In: J. Hargital, and A. Kerezturi eds. *Encyclopedia of Planetary Landforms*. 1-15.

Durand, N., Derivaux, S., Forestier, G., Wemmert, C., Gançarski, P., Boussaid, O., Puissant, A., 2007. Ontology-based object recognition for remote sensing image interpretation. *19th IEEE International Conference on Tools with Artificial Intelligence*, ICTAI 2007. 29-31 October, Patras, 1, 472-479.

Ehlschlaeger, C., 1989. Using the A^T search algorithm to develop hydrologic models from digital elevation data. *Proceedings of International Geographic Information Systems (IGIS) Symposium*, Baltimore, MD, 275-281.

Feifei, P., Stieglitz, M., and McKane, R., 2012. An algorithm for treating flat areas and depressions in digital elevation models using linear interpolation. *Water Resources Research,* 48 (2), 1–13.

Fenneman, N., 1931. *Physiography of Western United States*. New York: McGraw-Hill.

FM 5-33, 1992. *Terrain Analysis*. Headquarters Departments of the Army, Washington, DC, 8 September 1992.

Forestier, G., Puissant, A., Wemmert, C., and Gançarski, P., 2012. Knowledge-based region labeling for remote sensing image interpretation, Computers, Environment and Urban Systems, 36(5), 470–480.

Forestier, G., Wemmert, C., and Puissant, A., 2013. Coastal image interpretation using background knowledge and semantics. *Computers and Geosciences*, 54, 88–96.

Free Software Foundation, 2007. GNU general public license (version 3) [online]. Available from: http://www.gnu.org/licenses/gpl.html (last date accessed: 20 November 2014).

Freeman, G., 1991. Calculating catchment area with divergent flow based on a rectangular grid. *Computers and Geosciences*, 17, 413–422.

Gallant, J., and Dowling, T., 2003. A multiresolution index of valley bottom flatness for mapping depositional areas. *Water Resources Research*, 39 (12), 1347. doi:10.1029/2002WR001426.

Ghosh, M.K., Kumar, L., and Roy, C., 2015. Monitoring the coastline change of Hatiya Island in Bangladesh using remote sensing techniques. *ISPRS Journal of Photogrammetry and Remote Sensing*, 101, 137–144.

Gong, M., Li, Y., Jiao, L., Jia, M., and Su, L., 2014. SAR change detection based on intensity and texture changes. *ISPRS Journal of Photogrammetry and Remote Sensing*, 93, 123–135.

Gruber, T.R., 1995. Toward principles for the design of ontologies used for knowledge sharing? *International Journal of Human-Computer Studies*, 43, 907–928.

Guarino, N., 1997. Semantic matching: formal ontological distinctions for information organization, extraction, and integration. *In*: M. Pazienza, ed. *Information Extraction: A Multidisciplinary Approach to an Emerging Information Technology.* Berlin, Heidelberg: Springer, 1299, 139–170.

Hannv, Z., Qigang, J., and Jiang, X., 2013. Coastline extraction using support vector machine from remote sensing image. *Journal of Multimedia*, 8 (2), 175–182.

Hay, G., and Castilla, G., 2008. Geographic Object-Based Image Analysis (GEOBIA): A new name for a new discipline, Object-Based Image Analysis. In: T. Blaschke, S. Lang and G. Hay, eds: *Spatial Concepts for Knowledge-driven Remote Sensing Applications*. Berlin, Springer, 75-89.

Hebel, M., Arens, M., and Stilla, U., 2013. Change detection in urban areas by object-based analysis and on-the-fly comparison of multi-view ALS data. *ISPRS Journal of*

Photogrammetry and Remote Sensing, 86, 52-64.

Hinton, G.E., 2009. Deep belief networks [online]. Geoffrey E. Hinton. Available from: http://www.scholarpedia.org/article/Deep_belief_networks [last date accessed: 8 July 2015].

Hinton, G.E., and Salakhutdinov, R.R., 2006. Reducing the dimensionality of data with neural networks. *Science*, 313 (5786), 504–507.

Hinton, G.E., Osindero, S., and Teh, Y., 2006. A fast learning algorithm for deep belief nets. *Neural Computation*, 18, 1527-1554.

Hofmann, P., Lettmayer, P., Blaschke, T., Belgiu, M., Wegenkittl, S., Graf, R., Lampoltshammer, T.J., and Andrejchenko, V., 2015. Towards a framework for agent-based image analysis of remote-sensing data. *International Journal of Image and Data Fusion*, 6 (2), 115–137.

Hooke, R., 1972. Geomorphic evidence for late-Wisconsin and Holocene tectonic deformation, Death Valley, California. *Geological Society of America Bulletin*, 83, 2073–2098.

Hudelot, C., Atif, J., and Bloch, I., 2008. Fuzzy spatial relation ontology for image interpretation. *Fuzzy Sets and Systems,* 159 (15), 929–1951.

Hunt, B. 1975. *Death Valley: Geology, Ecology, and Archaeology*. Berkeley: University of California Press.

Ichoku, C., and Chorowicz, J., 1994. A numerical approach to the analysis and classification of channel network patterns. *Water Resources Research*, 30 (2), 161–174. doi:10.1029/93WR02279.

Ioannidis, C., Psaltis, C., and Potsiou, C., 2009. Towards a strategy for suburban informal building control through automatic change detection. *Computers, Environment and Urban Systems,* 33 (1), 64-74.

Janowicz, K., 2010. Semantic Interoperability. *In:* B. Warf ed. *Encyclopedia of Geography*. SAGE Publications.

Karantzalos, K. and Argialas, D., 2006. Improving edge detection and watershed segmentation with anisotropic diffusion and morphological levellings. *International Journal of Remote Sensing*, 27 (24), 5427–5434.

Karantzalos, K., 2015. Recent advances on 2D and 3D change detection in urban environments from remote sensing data. *In*: M. Heibich, J. Arsanjiani, and M. Leitner, eds. *Computational Approaches for Urban Environments*, Berlin, Heidelberg: Springer, 237–272.

Karantzalos, K., and Argialas, D., 2006. Improving edge and watershed segmentation with anisotropic diffusion and morphological levelings. *International Journal of Remote Sensing,* 27 (24), 5427–5434.

Karantzalos, K., Argialas, D., and Paragios, N., 2007. Comparing morphological levelings constrained by different markers. *In*: C. Hendriks, G. Borgefors, R. Strand, eds. *Mathematical Morphology and Its Applications to Signal and Image Processing.* Berlin, Heidelberg: Springer, 113-124.

Kavouras, M., Kokla, M., 2007. *Theories of Geographic Concepts: Ontological Approaches to Semantic Integration*. CRC Press.

Kavouras, M., Kokla, M., Tomai, E., 2005. Comparing categories among geographic ontologies. *Computers and Geosciences*, 31(2), 145 – 154.

Kohli, D., Sliuzas, R., Kerle, N., Stein, A., 2012. An ontology of slums for image-based classification. *Computers, Environment and Urban Systems*, 36 (2), 154–163.

Ktimatologio, S.A., 2006. Technical Specifications for the production of proper orthomosaic and DTM for foreshore delineation. February 2006, Ktimatologio S.A. Athens, (In Greek).

Lipakis, M., Chrysoulakis, N., and Kamarianakis, Y., 2008. Shoreline extraction using satellite imagery. *BEACHMED-e/OpTIMAL - Beach Erosion Monitoring*, 81–95.

Liu, H., Sherman, D., and Gu, S., 2007. Automated Extraction of Shorelines from Airborne Light Detection and Ranging Data and Accuracy Assessment Based on Monte Carlo Simulation. *Journal of Coastal Research*, 236, 1359–1369.

Lüscher, P., Weibel, R., and Burghardt, D., 2009. Integrating ontological modelling and bayesian inference for pattern classification in topographic vector data. *Computers, Environment and Urban Systems*, 33(5), 363–374.

Lutz, M., and Klien, E., 2006. Ontology-based retrieval of geographic information, International Journal of Geographical Information Science, 20(3), 233–260.

Mallinis, G., Gitas, I., Giannakopoulos, V., Maris, F., and Strati, M., 2013. An object-based approach for flood area delineation in a transboundary area using ENVISAT ASAR and LANDSAT TM data. *International Journal of Digital Earth*, 6(2), 124-136.

Meyer, F., 2004. Levelings, Image Simplification Filters for Segmentation. *Journal of Mathematical Imaging and Vision*, 20 (1–2), 59–72.

Meyer, F., and Maragos, P., 2000. Nonlinear scale-space representation with morphological levelings*. Journal of Visual Communication and Image Representation*, 11 (2), 245–265.

Miliaresis, G., 2001. Extraction of bajadas from digital elevation models and satellite imagery. *Computers and Geosciences*, 27 (10), 1157–1167. doi:10.1016/S0098-3004(01)00032-2.

Miliaresis, G., and Argialas, D., 2000. Extraction and delineation of alluvial fans from digital elevation models and Landsat thematic mapper images. *Photogrammetric Engineering and Remote Sensing*, 66 (9), 1093–1101.

Mintzer, O., and Messmore, J., 1984. Terrain Analysis Procedural Guide for Surface Configuration. Technical Report ETL-0352, U.S. Army Corps of Engineer, Engineer Topographic Laboratory, Fort Belvoir, Virginia.

Mnih, V., and Hinton, G.E., 2010. Learning to detect roads in high-resolution aerial images. *In*: K. Daniilidis, P. Maragos, and N. Paragios, eds. *Lecture Notes in Computer Science*. Berlin, Heidelberg: Springer, 6316, 210-223.

Moore, T., Morris, K., Blackwell, G., Gibson, S., and Stebbing, A., 1999. An Expert System for Integrated Coastal Zone Management: A Geomorphological Case Study. *Marine Pollution Bulletin*, 37 (3–7), 361–370.

Niya, A.K., Alesheikh, A.A., Soltanpor, M., Kheirkhahzarkesh, M.M., 2013. Shoreline Change Mapping Using Remote Sensing and GIS. *International Journal of Remote Sensing Applications*, 3 (3), 102–107.

O'Callaghan, J., and Mark, D., 1984. The extraction of drainage networks from digital elevating data. *Computer Vision, Graphics, Image Processing*, 28 (3), 323–344.

Open Geospatial Consortium 2014. OGC standards. Available from: http://www.opengeospatial.org /standards/ [last date accessed: 20 November 2014].

OTB Development Team, 2016. "The ORFEO Tool Box Software Guide Updated for OTB-5.6.0." Available from: https://www.orfeo-toolbox.org/SoftwareGuide/ [last date accessed: 14 October 2016].

Paslaru, E., Simprel, B., and Temprich, C., 2006. Ontology engineering: a reality check, on the move to meaningful internet systems 2006. *In*: R. Meersman, and Z. Tari, eds. *CoopIS, DOA, GADA, and ODBASE*. Berlin, Heidelberg: Springer, 4275, 836-854.

Passalacqua, P., et al. 2010. A geometric framework for channel network extraction from lidar: nonlinear diffusion and geodesic paths. *Journal of Geophysical Research*, 115 (F1), 1–18. doi:10.1029/2009JF001254.

Pelletier, J., 2013. A robust, two-Parameter method for the extraction of drainage networks from high-resolution digital elevation models (DEMs): evaluation using synthetic and real-world DEMs. *Water Resources Research*, 49 (1), 75–89. doi:10.1029/2012WR012452.

Peterson, F., 1981. Landforms of the Basin & Range province defined for soil survey. Technical Bulletin 28, Nevada Agricultural Experiment Station Reno: University of Nevada.

PostgreSQL Global Development Group, 2014. PostgreSQL 9.3.0 documentation. PostgreSQL Global Development Group [online]. Available from: http://www.postgresql.org/docs [last date accessed: 19 December 2015].

QGIS Development Team, 2014. QGIS 2.6, geographic information system user guide. Open Source Geospatial Foundation Project [online]. Available from: http://www.qgis.org/en/docs/index [last date accessed: 19 December 2015].

Rachocki, A., 1981. *Alluvial Fans*. New York: John Wiley and Sons.

Schneevoigt, N., et al. 2008. Detecting alpine landforms from remotely sensed imagery. A pilot study in the Bavarian alps. *Geomorphology*, 93 (1–2), 104–119. doi:10.1016/j.geomorph.2006.12.034.

Seibert, J., and McGlynn, B., 2007. A new triangular multiple flow direction algorithm for computing upslope areas from gridded digital elevation models. *Water Resources Research*, 43 (4), 1–8. doi:10.1029/2006WR005128.

Smeulders, W. M. A., et al., 2000. Content-based image retrieval at the end of the early years. *IEEE Transaction on Pattern Analysis and machine Intelligence*, 22 (12), 1349-1380.

Tieleman, T., 2008. Training restricted boltzmann machines using approximations to the likelihood gradient. *Machine Learning, Proceedings of the 21st International Conference ACM*.

Torres, M., Quintero, R., Moreno, M., and Fonseca, F., 2005. Ontology-Driven Description of Spatial Data for Their Semantic Processing. *In*: M. Rodríguez, I. Cruz, S. Levashkin and M. Egenhofer, eds. *GeoSpatial Semantics*, 3799, 242–249.

Trimble, 2011. *eCognition Developer 8.64.0 Reference Book*. Trimble München, Germany.

Troeh, F., 1965. Landform equations fitted to topographic maps. *American Journal of Science* 263, 616-627.

Tzotsos A., and Argialas, D., 2006. MSEG: A generic region-based multi-scale image segmentation algorithm for remote sensing imagery, *Proceedings of ASPRS 2006 Annual Conference.* Reno, Nevada, May 1-5, unpaginated CD-ROM.

Tzotsos, A., and Argialas, D., 2008. Support vector machine classification for object-based image analysis. *In*: T. Blaschke, S. Lang, and G. Hay, eds. *Object-Based Image Analysis, Lecture Notes in Geoinformation and Cartography.* Berlin, Heidelberg: Springer, 663-677.

Urbanski, J., 2010. The extraction of coastline using OBIA and GIS. *GEOBIA 2010 proceedings*, 29 June – 2 July, Ghent, Belgium.

USGS, 2016. National Elevation Dataset (NED) Seamless Layers ReadmeTable of Contents.

W3C, 2012. OWL 2 Web Ontology Language Document Overview (Second Edition). [online]. Available from: http://www.w3.org/TR/owl2-overview/ [last date accessed: 14 October 2016].

Wang, H., Cai, Y., Chen, L., 2014. A vehicle detection algorithm based on deep belief network. *Scientific World Journal* [online]. Available from: http://www.ncbi.nlm.nih.gov/pmc/articles/PMC4052056/#B11 [last date accessed: 19 December 2015].

Wang, H., Liu, S., and Chia, L., 2006. Does ontology help in image retrieval? — a comparison between keyword, text ontology and multi-modality ontology approaches. *14th annual ACM international conference on Multimedia*, 23-27 October 2006, Santa Barbara, CA USA. 109–112.

Water and Rivers Commission 2001. *Determining foreshore reserves*. Australia: Water & Rivers Commission Report No. RR16.

Way, D. 1978. *Terrain Analysis.* New York: McGraw-Hill.

Wurm, M., Taubenböck, H., Schardt, M., Esch, T., and Dech, S., 2011. Object-based image information fusion using multisensor earth observation data over urban areas. *International Journal of Image and Data Fusion*, 2 (2), 121–147.

Yong, A., Hough, S.E., Abrams, M.J., Cox, H.M., Wills, C.J., and Simila, G.W., 2008. Site characterization using integrated imaging analysis methods on satellite data of the Islamabad, Pakistan, region. *Bulletin of the Seismological Society of America*, 98 (6), 2679–2693. doi:10.1785/0120080930.

Zadeh, L., 1965. Fuzzy sets. *Information and Control*, 8(3), 338–353.

Zhan, Q., Zhang, X., and Li, D., 2008. Ontology-based semantic description model for discovery and retrieval of geospatial information. *The International Archives of the Photogrammetry, Remote Sensing and Spatial Information Sciences*, 37(B4), 141-146.